Chapter 1

Theory of Normal Vibrations

1.1. ORIGIN OF MOLECULAR SPECTRA

As a first approximation, the energy of the molecule can be separated into three additive components associated with (1) the motion of the electrons in the molecule,* (2) the vibrations of the constituent atoms, and (3) the rotation of the molecule as a whole:

$$E_{\text{total}} = E_{\text{el}} + E_{\text{vib}} + E_{\text{rot}} \tag{1.1}$$

The basis for this separation lies in the fact that electronic transitions occur on a much shorter timescale, and rotational transitions occur on a much longer timescale, than 10 vibrational transitions. The translational energy of the molecule may be ignored in this discussion because it is essentially not quantized.

If a molecule is placed in an electromagnetic field (e.g., light), a transfer of energy from the field to the molecule will occur when Bohr's frequency condition is satisfied:

$$\Delta E = h\nu \tag{1.2}$$

*Hereafter the word *molecule* may also represent an *ion*.

Infrared and Raman Spectra of Inorganic and Coordination Compounds, Sixth Edition, Part A: Theory and Applications in Inorganic Chemistry, by Kazuo Nakamoto

where ΔE is the difference in energy between two quantized states, h is Planck's constant (6.625×10^{-27} erg s), and ν is the frequency of the light. Here, the frequency is the number of electromagnetic waves in the distance that light travels in one second:

$$\nu = \frac{c}{\lambda} \tag{1.3}$$

where c is the velocity of light ($3 \times 10^{10}\,\mathrm{cm\,s^{-1}}$) and λ is the wavelength of the electromagnetic wave. If λ has the units of cm, ν has dimensions of $(\mathrm{cm\,s^{-1}})/\mathrm{cm} = \mathrm{s^{-1}}$, which is also called "Hertz (Hz)."

The wavenumber ($\tilde{\nu}$) defined by

$$\tilde{\nu} = \frac{1}{\lambda} \tag{1.4}$$

is most commonly used in vibrational spectroscopy. It has the dimension of $\mathrm{cm^{-1}}$. By combining Eqs. 1.3 and 1.4, we obtain

$$\tilde{\nu} = \frac{1}{\lambda} = \frac{\nu}{c} \quad \text{or} \quad \nu = \frac{c}{\lambda} = c\tilde{\nu} \tag{1.5}$$

Although the dimensions of ν and $\tilde{\nu}$ differ from one another, it is convenient to use them interchangeably. Thus, an expression such as "a frequency shift of $5\,\mathrm{cm^{-1}}$" is used throughout this book.

Using Eq. 1.5, Bohr's condition (Eq. 1.2) is written as

$$\Delta E = hc\tilde{\nu} \tag{1.6}$$

Since h and c are known constants, ΔE can be expressed in units such as*

$$\begin{aligned} 1(\mathrm{cm^{-1}}) &= 1.99 \times 10^{-16}(\mathrm{erg \cdot molecule^{-1}}) \\ &= 2.86\ (\mathrm{cal \cdot mol^{-1}}) \\ &= 1.24 \times 10^{-4}(\mathrm{eV \cdot molecule^{-1}}) \end{aligned}$$

Suppose that

$$\Delta E = E_2 - E_1 \tag{1.7}$$

where E_2 and E_1 are the energies of the excited and ground states, respectively.

Then, the molecule "absorbs" ΔE when it is excited from E_1 to E_2 and "emits" ΔE when it reverts from E_2 to E_1. Figure 1.1 shows the regions of the electromagnetic spectrum where ΔE is indicated in $\tilde{\nu}$, λ, and ν. In this book, we are concerned mainly with vibrational transitions which are observed in infrared (IR) or Raman (R) spectra.

---

*Use conversion factors such as

$$\begin{aligned} \text{Avogadro's number } N_0 &= 6.023 \times 10^{23}(\mathrm{mol^{-1}}) \\ 1\ (\mathrm{cal}) &= 4.1846 \times 10^{7}(\mathrm{erg}) \\ 1\ (\mathrm{eV}) &= 1.6021 \times 10^{-12}(\mathrm{erg \cdot molecule^{-1}}) \end{aligned}$$

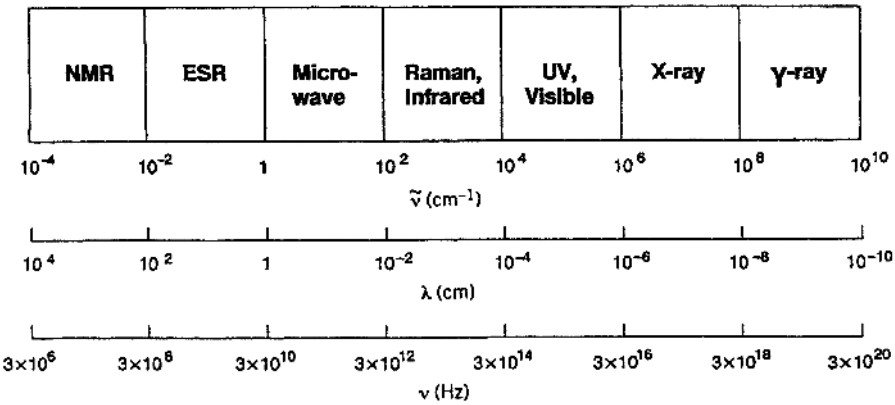

Fig. 1.1. *Regions of the electromagnetic spectrum and energy units.*

These transitions appear in the $10^2 \sim 10^4\,\mathrm{cm}^{-1}$ region, and originate from vibrations of nuclei constituting the molecule. Rotational transitions occur in the $1\text{–}10^2\,\mathrm{cm}^{-1}$ region (microwave region) because rotational levels are relatively close to each other, whereas electronic transitions are observed in the $10^4\text{–}10^6\,\mathrm{cm}^{-1}$ region (UV–visible region) because their energy levels are far apart. However, such division is somewhat arbitrary, for pure rotational spectra may appear in the far-infrared region if transitions to higher excited states are involved, and pure electronic transitions may appear in the near-infrared region if electronic levels are closely spaced.

Figure 1.2 illustrates transitions of the three types mentioned for a diatomic molecule. As the figure shows, rotational intervals tend to increase as the rotational quantum number J increases, whereas vibrational intervals tend to decrease as the vibrational quantum number v increases. The dashed line below each electronic level indicates the "zero-point energy" that must exist even at a temperature of absolute zero as a result of Heisenberg's uncertainty principle:

$$E_0 = \frac{1}{2}hv \tag{1.8}$$

It should be emphasized that not all transitions between these levels are possible. To see whether the transition is "allowed" or "forbidden," the relevant selection rule must be examined. This, in turn, is determined by the symmetry of the molecule.

As expected from Fig. 1.2, electronic spectra are very complicated because they are accompanied by vibrational as well as rotational fine structure. The rotational fine structure in the electronic spectrum can be observed if a molecule is simple and the spectrum is measured in the gaseous state under high resolution. The vibrational fine structure of the electronic spectrum is easier to observe than the rotational fine structure, and can provide structural and bonding information about molecules in electronic excited states.

Vibrational spectra are accompanied by rotational transitions. Figure 1.3 shows the rotational fine structure observed for the gaseous ammonia molecule. In most polyatomic molecules, however, such a rotational fine structure is not observed

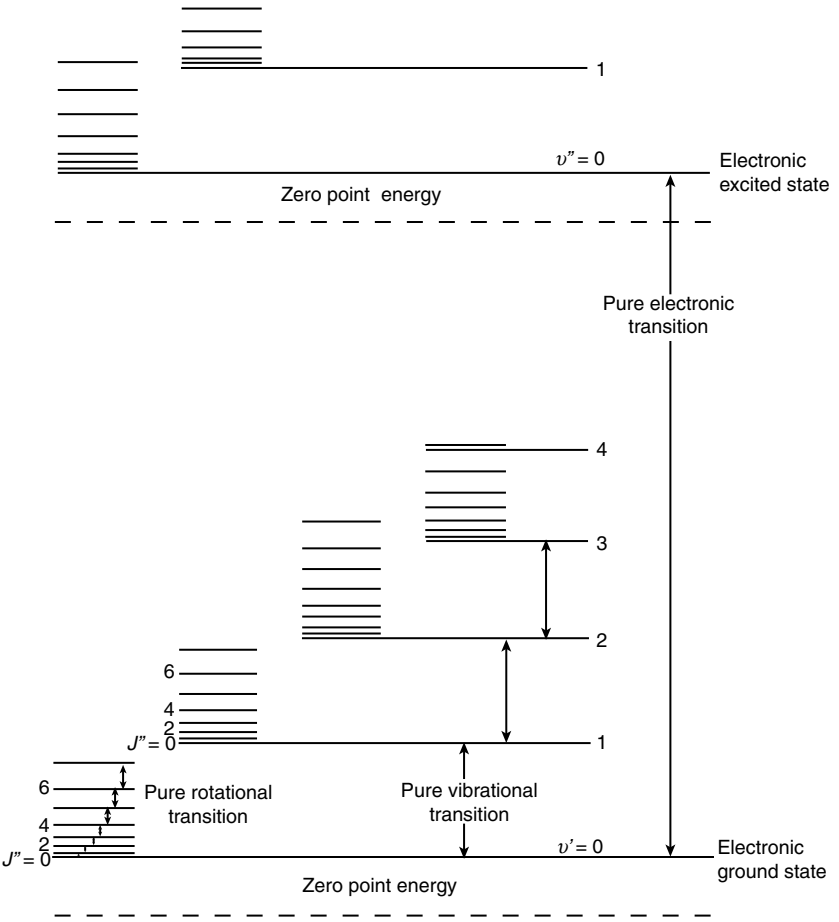

Fig. 1.2. *Energy level of a diatomic molecule (the actual spacings of electronic levels are much larger, and those of rotational levels are much smaller, than that shown in the figure).*

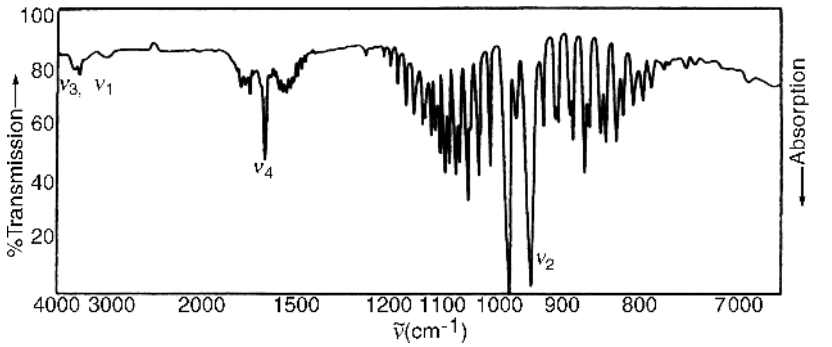

Fig. 1.3. *Rotational fine structure of gaseous NH_3.*

because the rotational levels are closely spaced as a result of relatively large moments of inertia. Vibrational spectra obtained in solution do not exhibit rotational fine structure, since molecular collisions occur before a rotation is completed and the levels of the individual molecules are perturbed differently.

The selection rule allows any transitions corresponding to $\Delta v = \pm 1$ if the molecule is assumed to be a harmonic oscillator (Sec. 1.3), Under ordinary conditions, however, only the *fundamentals* that originate in the transition from $v = 0$ to $v = 1$ in the electronic ground state can be observed. This is because the Maxwell–Boltzmann distribution law requires that the ratio of population at $v = 0$ and $v = 1$ states is given by

$$R = \frac{P(v = 1)}{P(v = 0)} = e^{-\Delta E_v / kT} \tag{1.9}$$

where ΔE_v is the vibrational frequency (cm^{-1}) and $kT = 208$ (cm^{-1}) at room temperature. In the case of H_2, $\Delta E_v = 4160\,cm^{-1}$ and $R = 2.16 \times 10^{-9}$. Thus, almost all molecules are at $v = 0$. However, the population at $v = 1$ increases as ΔE_v becomes small. For example, $R = 0.36$ for I_2 ($\Delta E_v = 213\,cm^{-1}$) Then, about 27% of the molecules are at $v = 1$ state, and the transition from $v = 1$ to $v = 2$ can be observed as a "hot band."

In addition to the harmonic oscillator selection rule, another restriction results from the symmetry of the molecule (Sec. 1.10). Thus, the number of allowed transitions in polyatomic molecules is greatly reduced. *Overtones and combination bands*[*] of these fundamentals are forbidden by the selection rule. However, they are weakly observed in the spectrum because of the anharmonicity of the vibration (Sec. 1.3). Since they are less important than the fundamentals, they will be discussed only when necessary.

1.2. ORIGIN OF INFRARED AND RAMAN SPECTRA

As stated previously, vibrational transitions can be observed as infrared (IR) or Raman spectra.[†] However, the physical origins of these two spectra are markedly different. Infrared (absorption) spectra originate in photons in the infrared region that are absorbed by transitions between two vibrational levels of the molecule in the electronic ground state. On the other hand, Raman spectra have their origin in the electronic polarization caused by ultraviolet, visible, and near-IR light. If a molecule is irradiated by monochromatic light of frequency v (laser), then, because of electronic polarization induced in the molecule by this incident beam, the light of frequency v ("Rayleigh scattering") as well as that of frequency $v \pm v_i$ ("Raman scattering") is scattered where v_i represents a vibrational frequency of the molecule. Thus, Raman spectra are presented as *shifts* from the incident frequency in the ultraviolet, visible, and near-IR region. Figure 1.4 illustrates the difference between IR and Raman techniques.

[*]Overtones represent some multiples of the fundamental, whereas combination bands arise from the sum or difference of two or more fundamentals.

[†]Raman spectra were first observed by C. V. Raman [*Indian J. Phys.* **2**, 387 (1928)] and C. V. Raman and K. S. Krishnan [*Nature* **121**, 501 (1928)].

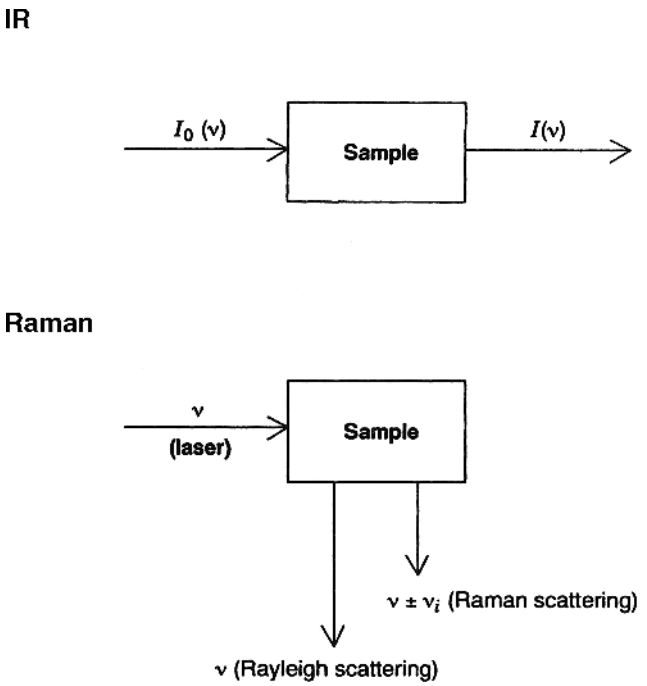

Fig. 1.4. *Mechanisms of infrared absorption and Raman scattering.*

Although Raman scattering is much weaker than Rayleigh scattering (by a factor of 10^{-3}–10^{-5}), it is still possible to observe the former by using a strong exciting source. In the past, the mercury lines at 435.8 nm (22.938 cm^{-1}) and 404.7 nm (24,705 cm^{-1}) from a low-pressure mercury arc were used to observe Raman scattering. However, the advent of lasers revolutionized Raman spectroscopy. Lasers provide strong, coherent monochromatic light in a wide range of wavelengths, as listed in Table 1.1. In the case of resonance Raman spectroscopy (Sec. 1.22), the exciting frequency is chosen so as to fall inside the electronic absorption band. The degree of resonance enhancement varies as a function of the exciting frequency and reaches a maximum when the exciting frequency coincides with that of the electronic absorption maximum. It is possible to change the exciting frequency continuously by pumping dye lasers with powerful gas or pulsed lasers.

The origin of Raman spectra can be explained by an elementary classical theory. Consider a light wave of frequency v with an electric field strength E. Since E fluctuates at frequency v, we can write

$$E = E_0 \cos 2\pi v t \tag{1.10}$$

where E_0 is the amplitude and t the time. If a diatomic molecule is irradiated by this light, the dipole moment P given by

$$P = \alpha E = \alpha E_0 \cos 2\pi v t \tag{1.11}$$

TABLE 1.1. Some Representative Laser Lines for Raman Spectroscopy

Laser[a]	Mode	Wavelength (nm)	$\tilde{\nu}$ (cm^{-1})
Gas lasers			
Ar–ion	CW	488.0 (blue)	20491.8
		514.5 (green)	19436.3
Kr–ion	CW	413.1 (violet)	24207.2
		530.9 (green/yellow)	18835.9
		647.1 (red)	15453.6
He–Ne	CW	632.8 (red)	15802.8
He–Cd	CW	441.6 (blue/violet)	22644.9
Nitrogen	Pulsed	337.1 (UV)	29664.7
Excimer (XeCl)		308 (UV)	32467.5
Solid-state lasers			
Nd:YAG[b]	CW or pulsed	1064 (near-IR)	9398.4
Liquid lasers			
A variety of dye solutions are pumped by strong CW or pulsed-laser sources; a wide range (440–800 nm) can be covered continuously by choosing proper organic dyes			

[a]Acronym of *light amplification by stimulated emission of radiation.*
[b]Acronym of *neodymium-doped yttrium aluminum garnet.*
Source: For more information, see Nakamoto and collegues [21,26].

is induced. Here α is a proportionality constant and is called the *polarizability.* If the molecule is vibrating with frequency v_i, the nuclear displacement q is written as

$$q = q_0 \cos 2\pi v_i t \tag{1.12}$$

where q_0 is the vibrational amplitude. For small amplitudes of vibration, α is a linear function of q. Thus, we can write

$$\alpha = \alpha_0 + \left(\frac{\partial \alpha}{\partial q}\right)_0 q \tag{1.13}$$

Here, α_0 is the polarizability at the equilibrium position, and $(\partial\alpha/\partial q)_0$ is the rate of change of α with respect to the change in q, evaluated at the equilibrium position. If we combine Eqs. 1.11–1.13, we have

$$\begin{aligned} P &= \alpha E_0 \cos 2\pi v t \\ &= \alpha_0 E_0 \cos 2\pi v t + \left(\frac{\partial \alpha}{\partial q}\right)_0 q_0 E_0 \cos 2\pi v t \cos 2\pi v_i t \\ &= \alpha_0 E_0 \cos 2\pi v t \\ &\quad + \frac{1}{2}\left(\frac{\partial \alpha}{\partial q}\right)_0 q_0 E_0 \{\cos[2\pi(v + v_i)t] + \cos[2\pi(v - v_i)t]\} \end{aligned} \tag{1.14}$$

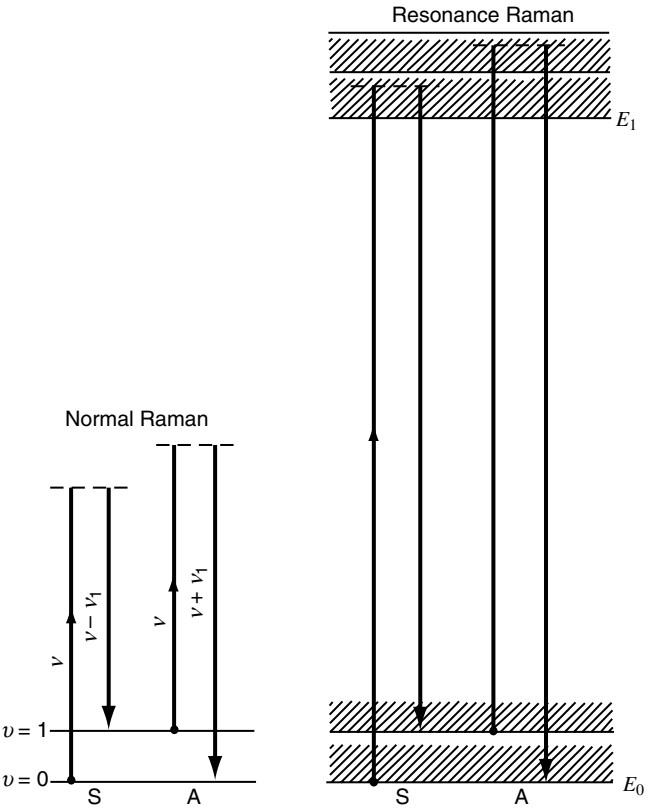

Fig. 1.5. *Mechanisms of normal and resonance Raman scattering. S and A denote Stokes and anti-Stokes scattering, respectively. The shaded areas indicate the broadening of rotational-vibrational levels in the liquid and solid states (Sec. 1.22).*

According to classical theory, the first term describes an oscillating dipole that radiates light of frequency ν (Rayleigh scattering). The second term gives the Raman scattering of frequencies $\nu + \nu_i$ (*anti-Stokes*) and $\nu - \nu_i$ (*Stokes*). If $(\partial\alpha/\partial q)_0$ is zero, the second term vanishes. Thus, the vibration is not Raman-active unless the polarizability changes during the vibration.

Figure 1.5 illustrates the mechanisms of *normal* and *resonance Raman* (*RR*) *scattering*. In the former, the energy of the exciting line falls far below that required to excite the first electronic transition. In the latter, the energy of the exciting line coincides with that of an electronic transition.* If the photon is absorbed and then emitted during the process, it is called *resonance fluorescence* (RF). Although the conceptual difference between resonance Raman scattering and resonance fluorescence is subtle, there are several experimental differences which can be used to

*If the exciting line is close to but not inside an electronic absorption band, the process is called *preresonance Raman scattering*.

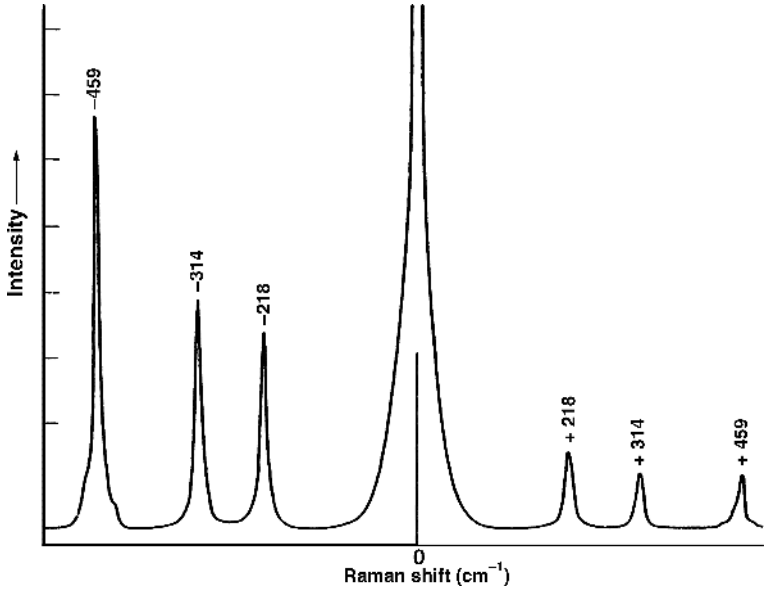

Fig. 1.6. *Raman spectrum of CCl_4 (488.0 nm excitation).*

distinguish between these two phenomena. For example, in RF spectra all lines are depolarized, whereas in RR spectra some are polarized and others are depolarized. Additionally, RR bands tend to be broad and weak compared with RF bands [66,67].

In the case of Stokes lines, the molecule at $v = 0$ is excited to the $v = 1$ state by scattering light of frequency $\nu - \nu_i$. Anti-Stokes lines arise when the molecule initially in the $v = 1$ state scatters radiation of frequency $\nu + \nu_1$ and reverts to the $v = 0$ state. Since the population of molecules is larger at $v = 0$ than at $v = 1$ (*Maxwell–Bottzmann distribution law*), the Stokes lines are always stronger than the anti-Stokes lines. Thus, it is customary to measure Stokes lines in Raman spectroscopy. Figure 1.6 illustrates the Raman spectrum (below 500 cm^{-1}) of CCl_4 excited by the blue line (488.0 nm) of an argon ion laser.

1.3. VIBRATION OF A DIATOMIC MOLECULE

Through quantum mechanical considerations [2,7], the vibration of two nuclei in a diatomic molecule can be reduced to the motion of a single particle of mass μ, whose displacement q from its equilibrium position is equal to the change of the internuclear distance. The mass μ is called the *reduced mass* and is represented by

$$\frac{1}{\mu} = \frac{1}{m_1} + \frac{1}{m_2} \tag{1.15}$$

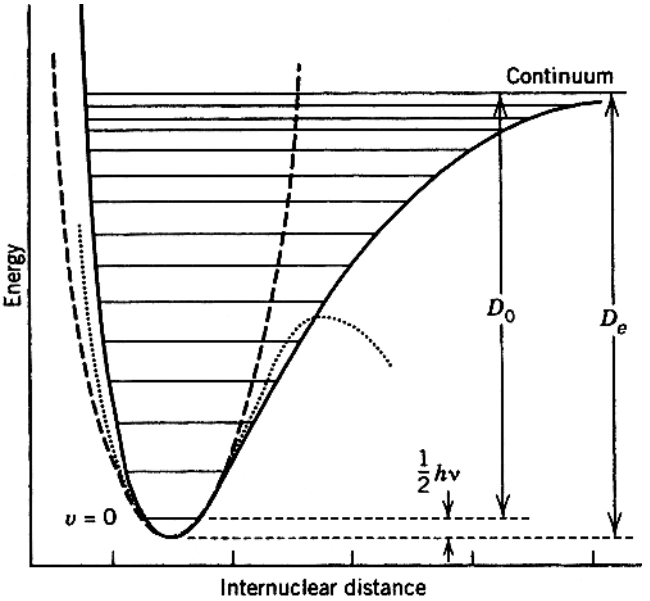

Fig. 1.7. *Potential energy curves for a diatomic molecule: actual potential (solid line), parabolic potential (dashed line), and cubic potential (dotted line).*

where m_1 and m_2 are the masses of the two nuclei. The kinetic energy is then

$$T = \frac{1}{2}\mu\dot{q}^2 = \frac{1}{2\mu}p^2 \tag{1.16}$$

where p is the conjugate momentum $\mu\dot{q}$. If a simple parabolic potential function such as that shown in Fig. 1.7 is assumed, the system represents a *harmonic oscillator*, and the potential energy is simply given by.

$$V = \frac{1}{2}Kq^2 \tag{1.17}$$

Here K is the force constant for the vibration. Then the Schrödinger wave equation becomes

$$\frac{d^2\psi}{dq^2} + \frac{8\pi^2\mu}{h^2}\left(E - \frac{1}{2}Kq^2\right)\psi = 0 \tag{1.18}$$

If this equation is solved with the condition that ψ must be single-valued, finite, and continuous, the eigenvalues are

$$E_v = h\nu\left(v + \frac{1}{2}\right) = hc\tilde{\nu}\left(v + \frac{1}{2}\right) \tag{1.19}$$

with the frequency of vibration

$$\nu = \frac{1}{2\pi}\sqrt{\frac{K}{\mu}} \quad \text{or} \quad \tilde{\nu} = \frac{1}{2\pi c}\sqrt{\frac{K}{\mu}} \tag{1.20}$$

Here v is the vibrational quantum number, and it can have the values 0, 1, 2, 3, and so on.

The corresponding eigenfunctions are

$$\psi_v = \frac{(\alpha/\pi)^{1/4}}{\sqrt{2^v v!}} e^{-\alpha q^2/2} H_v(\sqrt{\alpha} q) \tag{1.21}$$

where $\alpha = 2\pi\sqrt{\mu K}/h = 4\pi^2 \mu \nu / h$, and $H_v(\sqrt{\alpha} q)$ is a Hermite polynomial of the vth degree. Thus the eigenvalues and the corresponding eigenfunctions are

$$\begin{aligned} E_0 &= \frac{1}{2}h\nu, \quad \psi_0 = (\alpha/\pi)^{1/4} e^{-\alpha q^2/2} \\ E_1 &= \frac{3}{2}h\nu, \quad \psi_1 = (\alpha/\pi)^{1/4} 2^{1/2} q e^{-\alpha q^2/2} \\ &\vdots \qquad\qquad\qquad \vdots \end{aligned} \tag{1.22}$$

As Fig. 1.7 shows, actual potential curves can be approximated more exactly by adding a cubic term [2]:

$$V = \frac{1}{2}Kq^2 - Gq^3 \quad (K \gg G) \tag{1.23}$$

Then, the eigenvalues become

$$E_v = hc\omega_e\left(v + \frac{1}{2}\right) - hcx_e\omega_e\left(v + \frac{1}{2}\right)^2 + \cdots \tag{1.24}$$

where ω_e is the wavenumber corrected for *anharmonicity* and $x_e\omega_e$ indicates the magnitude of anharmonicity. Table 2.1a (in Chapter 2) lists ω_e and $x_e\omega_e$ for a number of diatomic molecules. Equation 1.24 shows that the energy levels of the anharmonic oscillator are not equidistant, and the separation decreases slowly as v increases. This anharmonicity is responsible for the appearance of overtones and combination vibrations, which are forbidden in the harmonic oscillator.

The values of x_e and $x_e\omega_e$ can be determined by observing a series of overtone bands in IR and Raman spectra. From Eq. 1.24, we obtain

$$\frac{E_v - E_0}{hc} = v\omega_e - x_e\omega_e(v^2 + v) + \cdots$$

Then

$$\begin{aligned} \text{Fundamental:} \quad & \tilde{\nu}_1 = \omega_e - 2x_e\omega_e \\ \text{First overtone:} \quad & \tilde{\nu}_2 = 2\omega_e - 6x_e\omega_e \\ \text{Second overtone:} \quad & \tilde{\nu}_3 = 3\omega_e - 12x_e\omega_e \end{aligned}$$

For $H^{35}C1$, these transitions are observed at 2885.9, 5668.1, and 8347.0 cm^{-1}, respectively, in IR spectrum [2]. Using these values, we find that

$$\omega_e = 2988.9\ \text{cm}^{-1} \quad \text{and} \quad x_e\omega_e = 52.05\ \text{cm}^{-1}$$

As will be shown in Sec. 1.23, a long series of overtone bands can be observed when Raman spectra of small molecules such as I_2 and TiI_4 are measured under rigorous resonance conditions. Anharmonicity constants can also be determined from the analysis of rotational fine structures of vibrational transitions [2].

Since the anharmonicity correction has not been made for most polyatomic molecules, in large part because of the complexity of the calculation, the frequencies given in Chapter 2 are not corrected for anharmonicity (except those given in Table 2.1a).

According to Eq. 1.20, the wavenumber of the vibration in a diatomic molecule is given by

$$\tilde{\nu} = \frac{1}{2\pi c}\sqrt{\frac{K}{\mu}} \tag{1.20}$$

A more exact expression is given by using the wavenumber corrected for anharmonicity:

$$\omega_e = \frac{1}{2\pi c}\sqrt{\frac{K}{\mu}} \tag{1.25}$$

or

$$K = 4\pi^2 c^2 \omega_e^2 \mu \tag{1.26}$$

For HC1, $\omega_e = 2989\ \text{cm}^{-1}$ and $\mu = 0.9799$ awu (where awu is the atomic weight unit). Thus, we obtain*

$$\begin{aligned} K &= \frac{4(3.14)^2(3\times 10^{10})^2}{6.025\times 10^{23}}\omega_e^2\mu \\ &= (5.8883\times 10^{-2})\omega_e^2\mu \\ &= (5.8883\times 10^{-2})(2989)^2(0.9799) \\ &= 5.16\times 10^5\,(\text{dyn/cm}) \\ &= 5.16\ (\text{mdyn/Å})^* \end{aligned}$$

Table 1.2 lists the observed frequencies $(\tilde{\nu})$, wavenumbers corrected for anharmonicity (ω_e), reduced masses (μ), and force constants (K) for several series of diatomic

*10^5 (dynes/cm) = 10^5 (10^3 millidynes/10^8 Å) = 1 (mdyn/Å) = 10^2 N/m (SI unit).

TABLE 1.2. Relationships between Vibrational Frequency, Reduced Mass, and Force Constant

Molecule	Obs. $\tilde{\nu}$ (cm^{-1})	ω_e (cm^{-1})	μ (awu)	K (mdyn/Å)
H_2	4160	4395	0.5041	5.73
HD	3632	3817	0.6719	5.77
D_2	2994	3118	1.0074	5.77
HF	3962	4139	0.9573	9.65
HCl	2886	2989	0.9799	5.16
HBr	2558	2650	0.9956	4.12
HI	2233	2310	1.002	3.12
F_2	892	—	9.5023	4.45
Cl_2	564	565	17.4814	3.19
Br_2	319	323	39.958	2.46
I_2	213	215	63.466	1.76
N_2	2331	2360	7.004	22.9
CO	2145	2170	6.8584	19.0
NO	1877	1904	7.4688	15.8
O_2	1555	1580	8.000	11.8

molecules. In the first series, ω_e decreases in the order $H_2 > HD > D_2$, because μ increases in the same order, while K is almost constant (*mass effect*). In the second series, ω_e decreses in the order $HF > HC1 > HBr > HI$, because K decreases in the same order, while μ shows little change (*force constant effect*). In the third series, ω_e decreases in the order $F_2 > Cl_2 > Br_2 > I_2$, because μ increases and K decreases in the same order. In this case, both mass effect and force constant effect are operative. In the last series, ω_e decreases in the order $N_2 > CO > NO > O_2$, mainly owing to the force constant effect. This may be attributed to the differences in bond order:

$$N{\equiv}N > C^{-}{\equiv}O^{+} \leftrightarrow C{=}O > N{=}O \leftrightarrow N^{-}{=}O^{+} > O{=}O \leftrightarrow O^{-}{-}O^{+}$$

More examples of similar series in diatomic molecules are found in Sec. 2.1. These simple rules, obtained for a diatomic molecule, are helpful in understanding the vibrational spectra of polyatomic molecules.

Figure 1.8 indicates the relationship between the force constant and the dissociation energy for the three series listed in Table 1.2. In the series of hydrogen halides, the dissociation energy decreases almost linearly as the force constant decreases. Thus, the force constant may be used as a measure of the bond strength in this case. However, such a monotonic relationship does not hold for the other two series. This is not unexpected, because the force constant is a measure of the curvature of the potential well near the equilibrium position

$$K = \left(\frac{d^2V}{dq^2}\right)_{q\to 0} \tag{1.27}$$

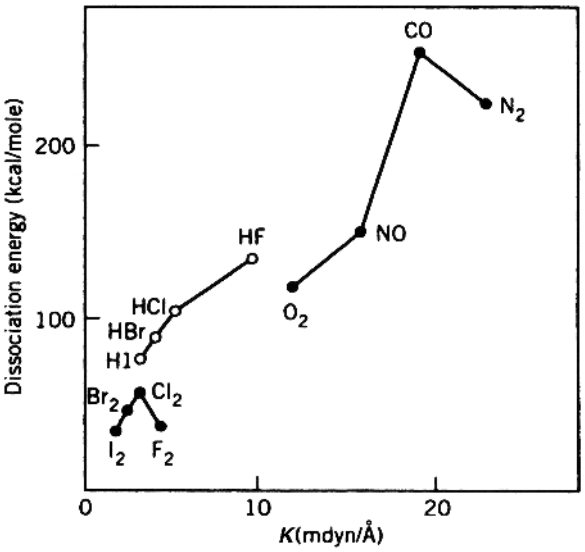

Fig. 1.8. *Relationships between force constants and dissociation energies in diatomic molecules.*

whereas the dissociation energy D_e is given by the depth of the potential energy curve (Fig. 1.7). Thus, a large force constant means sharp curvature of the potential well near the bottom, but does not necessarily indicate a deep potential well. Usually, however, a larger force constant is an indication of a stronger bond if the nature of the bond is similar in a series.

It is difficult to derive a general theoretical relationship between the force constant and the dissociation energy even for diatomic molecules.

In the case of small molecules, attempts have been made to calculate the force constants by quantum mechanical methods. The principle of the method is to express the total electronic energy of a molecule as a function of nuclear displacements near the equilibrium position and to calculate its second derivatives, $\partial^2 V/\partial q_i^2$, and so on for each displacement coordinate q_i. In the past, *ab initio* calculations of force constants were made for small molecules such as HF, H_2O, and NH_3. The force constants thus obtained are in good agreement with those calculated from the analysis of vibrational spectra. More recent progress in computer technology has made it possible to extend this approach to more complex molecules (Sec. 1.24).

There are several empirical relationships which relate the force constant to the bond distance. Badger's rule [68] is given by

$$K = 1.86(r - d_{ij})^{-3} \tag{1.28}$$

where r is the bond distance and d_{ij} has a fixed value for bonds between atoms of row i and j in the periodic table. Gordy's rule [69] is expressed as

$$K = aN\left(\frac{\chi_A \chi_B}{d^2}\right)^{3/4} + b \tag{1.29}$$

where χ_A and χ_B are the electronegativities of atoms A and B constituting the bond, d is the bond distance, N is the bond order, and a and b are constants for certain broad classes of compounds. Herschbach and Laurie [70] modified Badger's rule in the form

$$r = d_{ij} + (a_{ij} - d_{ij})K^{-1/3} \tag{1.30}$$

Here, a_{ij} and d_{ij} are constants for atoms of rows i and j in the periodic table.

Another empirical relationship is found by plotting stretching frequencies against bond distances for a series of compounds having common bonds. Such plots are highly important in estimating the bond distance from the observed frequency. Typical examples are found in the OH···O hydrogen-bonded compounds [71], carbon–oxygen and carbon–nitrogen bonded compounds [72], and molybdenum–oxygen [73] and vanadium–oxygen bonded compounds [74]. More examples are given in Sec. 2.2.

1.4. NORMAL COORDINATES AND NORMAL VIBRATIONS

In diatomic molecules, the vibration of the nuclei occurs only along the line connecting two nuclei. In polyatomic molecules, however, the situation is much more complicated because all the nuclei perform their own harmonic oscillations. It can be shown, however, that any of these extremely complicated vibrations of the molecule may be represented as a superposition of a number of *normal vibrations*.

Let the displacement of each nucleus be expressed in terms of rectangular coordinate systems with the origin of each system at the equilibrium position of each nucleus. Then the kinetic energy of an N-atom molecule would be expressed as

$$T = \frac{1}{2}\sum_N m_N \left[\left(\frac{d\Delta x_N}{dt} \right)^2 + \left(\frac{d\Delta y_N}{dt} \right)^2 + \left(\frac{d\Delta z_N}{dt} \right)^2 \right] \tag{1.31}$$

If generalized coordinates such as

$$q_1 = \sqrt{m_1}\Delta x_1, \quad q_2 = \sqrt{m_1}\Delta y_1, \quad q_3 = \sqrt{m_1}\Delta z_1 \quad q_4 = \sqrt{m_2}\Delta x_2, \ldots \tag{1.32}$$

are used, the kinetic energy is simply written as

$$T = \frac{1}{2}\sum_i^{3N} \dot{q}_i^2 \tag{1.33}$$

The potential energy of the system is a complex function of all the coordinates involved. For small values of the displacements, it may be expanded in a Taylor's series as

$$V(q_1, q_2, \ldots, q_{3N}) = V_0 + \sum_{i}^{3N} \left(\frac{\partial V}{\partial q_i}\right)_0 q_i + \frac{1}{2}\sum_{i,j}^{3N} \left(\frac{\partial^2 V}{\partial q_i\, \partial q_j}\right)_0 q_i q_j + \cdots \tag{1.34}$$

where the derivatives are evaluated at $q_i = 0$, the equilibrium position. The constant term V_0 can be taken as zero if the potential energy at $q_i = 0$ is taken as a standard. The $(\partial V/\partial q_i)_0$ terms also become zero, since V must be a minimum at $q_i = 0$. Thus, V may be represented by

$$V = \frac{1}{2}\sum_{i,j}^{3N} \left(\frac{\partial^2 V}{\partial q_i\, \partial q_j}\right)_0 q_i q_j = \frac{1}{2}\sum_{i,j}^{3N} b_{ij} q_i q_j \tag{1.35}$$

neglecting higher-order terms.

If the potential energy given by Eq. 1.35 did not include any cross-products such as $q_i q_j$, the problem could be solved directly by using Lagrange's equation:

$$\frac{d}{dt}\left(\frac{\partial T}{\partial \dot{q}_i}\right) + \frac{\partial V}{\partial q_i} = 0, \quad i = 1, 2, \ldots, 3N \tag{1.36}$$

From Eqs. 1.33 and 1.35, Eq. 1.36 is written as

$$\ddot{q}_i + \sum_{j} b_{ij} q_j = 0, \quad j = 1, 2, \ldots, 3N \tag{1.37}$$

If $b_{ij} = 0$ for $i \neq j$, Eq. 1.37 becomes

$$\ddot{q}_i + b_{ii} q_i = 0 \tag{1.38}$$

and the solution is given by

$$q_i = q_i^0 \sin\left(\sqrt{b_{ii}}t + \delta_i\right) \tag{1.39}$$

where q_i^0 and δ_i are the amplitude and the phase constant, respectively.

Since, in general, this simplification is not applicable, the coordinates q_i must be transformed into a set of new coordinates Q_i through the relations

$$\begin{aligned} q_1 &= \sum_i B_{1i} Q_i \\ q_2 &= \sum_i B_{2i} Q_i \\ &\vdots \\ q_k &= \sum_i B_{ki} Q_i \end{aligned} \tag{1.40}$$

The Q_i are called *normal coordinates* for the system. By appropriate choice of the coefficients B_{ki}, both the potential and the kinetic energies can be written as

$$T = \frac{1}{2}\sum_i \dot{Q}_i^2 \tag{1.41}$$

$$V = \frac{1}{2}\sum_i \lambda_i Q_i^2 \tag{1.42}$$

without any cross-products.

If Eqs. 1.41 and 1.42 are combined with Lagrange's equation (Eq. 1.36), there results

$$\ddot{Q}_i + \lambda_i Q_i = 0 \tag{1.43}$$

The solution of this equation is given by

$$Q_i = Q_i^0 \sin\left(\sqrt{\lambda_i}t + \delta_i\right) \tag{1.44}$$

and the frequency is

$$\nu_i = \frac{1}{2\pi}\sqrt{\lambda_i} \tag{1.45}$$

Such a vibration is called a *normal vibration*.

For the general N-atom molecule, it is obvious that the number of the normal vibrations is only $3N-6$, since six coordinates are required to describe the translational and rotational motion of the molecule as a whole. Linear molecules have $3N-5$ normal vibrations, as no rotational freedom exists around the molecular axis. Thus, the general form of the molecular vibration is a superposition of the $3N-6$ (or $3N-5$) normal vibrations given by Eq. 1.44.

The physical meaning of the normal vibration may be demonstrated in the following way. As shown in Eq. 1.40, the original displacement coordinate is related to the normal coordinate by

$$q_k = \sum_i B_{ki} Q_i \tag{1.40}$$

Since all the normal vibrations are independent of each other, consideration may be limited to a special case in which only one normal vibration, subscripted by 1, is excited (i.e., $Q_1^0 \neq 0, Q_2^0 = Q_3^0 = \cdots = 0$). Then, it follows from Eqs. 1.40 and 1.44 that

$$\begin{aligned} q_k = B_{k1}Q_1 &= B_{k1}Q_1^0 \sin(\sqrt{\lambda_1}t + \delta_1) \\ &= A_{k1}\sin(\sqrt{\lambda_1}t + \delta_1) \end{aligned} \tag{1.46}$$

This relation holds for all k. Thus, it is seen that the excitation of one normal vibration of the system causes vibrations, given by Eq. 1.46, of all the nuclei in the system. In other words, in the normal vibration, all the nuclei move with the same frequency and in phase.

This is true for any other normal vibration. Thus Eq. 1.46 may be written in the more general form

$$q_k = A_k \sin(\sqrt{\lambda}t + \delta) \tag{1.47}$$

If Eq. 1.47 is combined with Eq. 1.37, there results

$$-\lambda A_k + \sum_j b_{kj} A_j = 0 \tag{1.48}$$

This is a system of first-order simultaneous equations with respect to A. In order for all the As to be nonzero, we must solve

$$\begin{vmatrix} b_{11}-\lambda & b_{12} & b_{13} & \dots \\ b_{21} & b_{22}-\lambda & b_{23} & \dots \\ b_{31} & b_{32} & b_{33}-\lambda & \dots \\ \vdots & \vdots & \vdots & \end{vmatrix} = 0 \tag{1.49}$$

The order of this secular equation is equal to $3N$. Suppose that one root, λ_1, is found for Eq. 1.49. If it is inserted in Eq. 1.48, $A_{k1}, A_{k2}, \dots$ are obtained for all the nuclei. The same is true for the other roots of Eq. 1.49. Thus, the most general solution may be written as a superposition of all the normal vibrations:

$$q_k = \sum_l B_{kl} Q_l^0 \sin\left(\sqrt{\lambda_l}\, t + \delta_l\right) \tag{1.50}$$

The general discussion developed above may be understood more easily if we apply it to a simple molecule such as CO_2, which is constrained to move in only one direction. If the mass and the displacement of each atom are defined as follows:

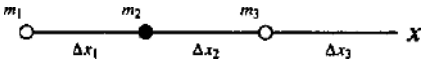

the potential energy is given by

$$V = \frac{1}{2}\, k\left[(\Delta x_1 - \Delta x_2)^2 + (\Delta x_2 - \Delta x_3)^2\right] \tag{1.51}$$

Considering that $m_1 = m_3$, we find that the kinetic energy is written as

$$T = \frac{1}{2}\, m_1(\Delta \dot{x}_1^2 + \Delta \dot{x}_3^2) + \frac{1}{2}\, m_2 \Delta \dot{x}_2^2 \tag{1.52}$$

Using the generalized coordinates defined by Eq. 1.32, we may rewrite these energies as

$$2V = k\left[\left(\frac{q_1}{\sqrt{m_1}} - \frac{q_2}{\sqrt{m_2}}\right)^2 + \left(\frac{q_2}{\sqrt{m_2}} - \frac{q_3}{\sqrt{m_1}}\right)^2\right] \tag{1.53}$$

$$2T = \sum \dot{q}_i^2 \tag{1.54}$$

From comparison of Eq. 1.53 with Eq. 1.35, we obtain

$$b_{11} = \frac{k}{m_1}, \qquad b_{22} = \frac{2k}{m_2}$$

$$b_{12} = b_{21} = -\frac{k}{\sqrt{m_1 m_2}}, \quad b_{23} = b_{32} = -\frac{k}{\sqrt{m_1 m_2}}$$

$$b_{13} = b_{31} = 0, \qquad b_{33} = \frac{k}{m_1}$$

If these terms are inserted in Eq. 1.49, we obtain the following result:

$$\begin{vmatrix} \frac{k}{m_1} - \lambda & -\frac{k}{\sqrt{m_1 m_2}} & 0 \\ -\frac{k}{\sqrt{m_1 m_2}} & \frac{2k}{m_2} - \lambda & -\frac{k}{\sqrt{m_1 m_2}} \\ 0 & -\frac{k}{\sqrt{m_1 m_2}} & \frac{k}{m_1} - \lambda \end{vmatrix} = 0 \tag{1.55}$$

By solving this secular equation, we obtain three roots:

$$\lambda_1 = \frac{k}{m_1}, \quad \lambda_2 = k\mu, \quad \lambda_3 = 0$$

where

$$\mu = \frac{2m_1 + m_2}{m_1 m_2}$$

Equation 1.48 gives the following three equations:

$$-\lambda A_1 + b_{11}A_1 + b_{12}A_2 + b_{13}A_3 = 0$$
$$-\lambda A_2 + b_{21}A_1 + b_{22}A_2 + b_{23}A_3 = 0$$
$$-\lambda A_3 + b_{31}A_1 + b_{32}A_2 + b_{33}A_3 = 0$$

Using Eq. 1.47, we rewrite these as

$$\begin{aligned}(b_{11}-\lambda)q_1+b_{12}q_2+b_{13}q_3&=0\\ b_{21}q_1+(b_{22}-\lambda)q_2+b_{23}q_3&=0\\ b_{31}q_1+b_{32}q_2+(b_{33}-\lambda)q_3&=0\end{aligned}$$

If $\lambda_1 = k/m_1$ is inserted in the simultaneous equations above, we obtain

$$q_1 = -q_3, \quad q_2 = 0$$

Similar calculations give

$$q_1 = q_3, \quad q_2 = -2\sqrt{\frac{m_1}{m_2}}q_1 \quad \text{for} \quad \lambda_2 = k\mu$$

$$q_1 = q_3, \quad q_2 = \sqrt{\frac{m_2}{m_1}}q_1 \quad \text{for} \quad \lambda_3 = 0$$

The relative displacements are depicted in the following figure:

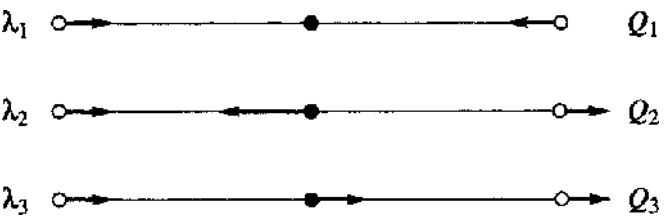

It is easy to see that λ_3 corresponds to the translational mode ($\Delta x_1 = \Delta x_2 = \Delta x_3$). The inclusion of λ_3 could be avoided if we consider the restriction that the center of gravity does not move; $m_1(\Delta x_1 + \Delta x_3) + m_2\Delta x_2 = 0$.

The relationships between the generalized coordinates and the normal coordinates are given by Eq. 1.40. In the present case, we have

$$\begin{aligned}q_1 &= B_{11}Q_1 + B_{12}Q_2 + B_{13}Q_3\\ q_2 &= B_{21}Q_1 + B_{22}Q_2 + B_{23}Q_3\\ q_3 &= B_{31}Q_1 + B_{32}Q_2 + B_{33}Q_3\end{aligned}$$

In the normal vibration whose normal coordinate is Q_1, B_{11}: B_{21}: B_{31} gives the ratio of the displacements. From the previous calculation, it is obvious that B_{11}: B_{21}: B_{31} = 1:0:−1. Similarly, $B_{12} : B_{22} : B_{32} = 1 : -2\sqrt{m_1/m_2} : 1$ gives the ratio of the displacements in the normal vibration whose normal coordinate is Q_2. Thus the mode

of a normal vibration can be drawn if the normal coordinate is translated into a set of rectangular coordinates, as is shown above.

So far, we have discussed only the vibrations whose displacements occur along the molecular axis. There are, however, two other normal vibrations in which the displacements occur in the direction perpendicular to the molecular axis. They are not treated here, since the calculation is not simple. It is clear that the method described above will become more complicated as a molecule becomes larger. In this respect, the **GF** matrix method described in Sec. 1.12 is important in the vibrational analysis of complex molecules.

By using the normal coordinates, the Schrödinger wave equation for the system can be written as

$$\sum_i \frac{\partial^2 \psi_n}{\partial Q_i^2} + \frac{8\pi^2}{h^2}\left(E - \frac{1}{2}\sum_i \lambda_i Q_i^2\right)\psi_n = 0 \tag{1.56}$$

Since the normal coordinates are independent of each other, it is possible to write

$$\psi_n = \psi_1(Q_1)\psi_2(Q_2)\cdots \tag{1.57}$$

and solve the simpler one-dimensional problem.

If Eq. 1.57 is substituted in Eq. 1.56, there results

$$\frac{d^2\psi_i}{dQ_i^2} + \frac{8\pi^2}{h^2}\left(E_i - \frac{1}{2}\lambda_i Q_i^2\right)\psi_i = 0 \tag{1.58}$$

where

$$E = E_1 + E_2 + \cdots$$

with

$$E_i = h\nu_i\left(\upsilon_i + \frac{1}{2}\right)$$
$$\nu_i = \frac{1}{2\pi}\sqrt{\lambda_i} \tag{1.59}$$

1.5. SYMMETRY ELEMENTS AND POINT GROUPS [9–14]

As noted before, polyatomic molecules have $3N-6$ or, if linear, $3N-5$ normal vibrations. For any given molecule, however, only vibrations that are permitted by

the selection rule for that molecule appear in the infrared and Raman spectra. Since the selection rule is determined by the symmetry of the molecule, this must first be studied.

The spatial geometric arrangement of the nuclei constituting the molecule determines its symmetry. If a coordinate transformation (a reflection or a rotation or a combination of both) produces a configuration of the nuclei indistinguishable from the original one, this transformation is called a *symmetry operation*, and the molecule is said to have a corresponding *symmetry element*. Molecules may have the following symmetry elements.

1.5.1. Identity *I*

This symmetry element is possessed by every molecule no matter how unsymmetric it is; the corresponding operation is to leave the molecule unchanged. The inclusion of this element is necessitated by mathematical reasons that will be discussed in Sec. 1.7.

1.5.2. A Plane of Symmetry σ

If reflection of a molecule with respect to some plane produces a configuration indistinguishable from the original one, the plane is called a *plane of symmetry.*

1.5.3. A Center of Symmetry *i*

If reflection at the center, that is, inversion, produces a configuration indistinguishable from the original one, the center is called a *center of symmetry.* This operation changes the signs of all the coordinates involved: $x_i \rightarrow -x_i,\ y_i \rightarrow -y_i,\ z_i \rightarrow -z_i$.

1.5.4. A *p*-Fold Axis of Symmetry C_p*

If rotation through an angle $360°/p$ about an axis produces a configuration indistinguishable from the original one, the axis is called a p-fold axis of symmetry C_p. For example, a twofold axis C_2 implies that a rotation of 180° about the axis reproduces the original configuration. A molecule may have a two-, three-, four-, five-, or sixfold, or higher axis. A linear molecule has an infinite-fold (denoted by ∞-fold) axis of symmetry C_∞ since a rotation of $360°/\infty$, that is, an infinitely small angle, transforms the molecule into one indistinguishable from the original.

1.5.5. A *p*-Fold Rotation–Reflection Axis S_p*

If rotation by $360°/p$ about the axis, followed by reflection at a plane perpendicular to the axis, produces a configuration indistinguishable from the original one, the axis is called a p-fold rotation–reflection axis. A molecule may have a two-, three-, four-,

* The notation C_p^n (or S_p^n) is used to indicate that the C_p (or S_p) operation is carried out successively n times.

five-, or sixfold, or higher, rotation–reflection axis. A symmetrical linear molecule has an S_∞ axis. It is easily seen that the presence of S_p always means the presence of C_p as well as σ when p is odd.

1.5.6. Point Group

A molecule may have more than one of these symmetry elements. Combination of more and more of these elements produces systems of higher and higher symmetry. Not all combinations of symmetry elements, however, are possible. For example, it is highly improbable that a molecule will have a C_3 and C_4 axis in the same direction because this requires the existence of a 12-fold axis in the molecule. It should also be noted that the presence of some symmetry elements often implies the presence of other elements. For example, if a molecule has two σ planes at right angles to each other, the line of intersection of these two planes must be a C_2 axis. A possible combination of symmetry operations whose axes intersect at a point is called a *point group*.*

Theoretically, an infinite number of point groups exist, since there is no restriction on the order (p) of rotation axes that may exist in an isolated molecule. Practically, however, there are few molecules and ions that possess a rotation axis higher than C_6. Thus most of the compounds discussed in this book belong to the following point groups:

(1) $\mathbf{C}_p$. Molecules having only a C_p and no other elements of symmetry: $\mathbf{C}_1$, $\mathbf{C}_2$, $\mathbf{C}_3$, and so on.

(2) $\mathbf{C}_{ph}$. Molecules having a C_p and a σ_h perpendicular to it: $C_{1h} \equiv C_s$, C_{2h}, C_{3h}, and so on.

(3) $\mathbf{C}_{pv}$. Molecules having a C_p and $p\sigma_v$ through it: $\mathbf{C}_{1v} \equiv \mathbf{C}_s, \mathbf{C}_{2v}, \mathbf{C}_{3v}, \mathbf{C}_{4v}, \ldots, \mathbf{C}_{\infty v}$.

(4) $\mathbf{D}_p$. Molecules having a C_p and pC_2 perpendicular to the C_p and at equal angles to one another: $\mathbf{D}_1 \equiv \mathbf{C}_2$, $\mathbf{D}_2 \equiv \mathbf{V}$, $\mathbf{D}_3$, $\mathbf{D}_4$, and so on.

(5) $\mathbf{D}_{ph}$. Molecules having a C_p, $p\sigma_v$ through it at angles of $360^\circ/2p$ to one another, and a σ_h perpendicular to the C_p: $\mathbf{D}_{1h} \equiv \mathbf{C}_{2v}, \mathbf{D}_{2h} \equiv \mathbf{V}_h, \mathbf{D}_{3h}, \mathbf{D}_{4h}, \mathbf{D}_{5h}, \mathbf{D}_{6h}, \ldots, \mathbf{D}_{\infty h}$.

(6) $\mathbf{D}_{pd}$. Molecules having a C_p, pC_2 perpendicular to it, and $p\sigma_d$ which go through the C_p and bisect the angles between two successive C_2 axes: $\mathbf{D}_{2d} \equiv \mathbf{V}_d$, $\mathbf{D}_{3d}$, $\mathbf{D}_{4d}$, $\mathbf{D}_{5d}$, and so on.

(7) $\mathbf{S}_p$. Molecules having only a S_p (p even). For p odd, S_p is equivalent to $C_p \times \sigma_h$, for which other notations such as $\mathbf{C}_{3h}$ are used: $\mathbf{S}_2 \equiv \mathbf{C}_i$, $\mathbf{S}_4$, $\mathbf{S}_6$, and so on.

(8) $\mathbf{T}_d$. Molecules having three mutually perpendicular C_2 axes, four C_3 axes, and a σ_d through each pair of C_3 axes: regular tetrahedral molecules.

*In this respect, point groups differ from space groups, which involve translations and rotations about nonintersecting axes (see Sec. 1.27).

(9) $\mathbf{O}_h$. Molecules having three mutually perpendicular C_4 axes, four C_3 axes, and a center of symmetry, i: regular octahedral and cubic molecules.

(10) $\mathbf{I}_h$. Molecules having 6 C_5 axes, 10 C_3 axes, 15 C_2 axes, 15 σ planes, and a center of symmetry. In total, such molecules possess 120 symmetry elements. One example is an icosahedron having 20 equilateral triangular faces, which is found in the B_{12} skeleton of the $B_{12}H_{21}^{2-}$ ion (Sec. 2.13). Another example is a regular dodecahedron having 12 regular pentagonal faces. Buckminsterfullerene, $\mathbf{C}_{60}$ (Sec. 2.14), also belongs to the $\mathbf{I}_h$ point group. It is a truncated icosahedron with 20 hexagonal and 12 pentagonal faces.

Figure 1.9 illustrates the symmetry elements present in the point group, $\mathbf{D}_{4h}$. Complete listings of the symmetry elements for common point groups are found in the character tables included in Appendix I. Figure 1.10 illustrates examples of molecules belonging to some of these point groups. From the symmetry perspective, molecules

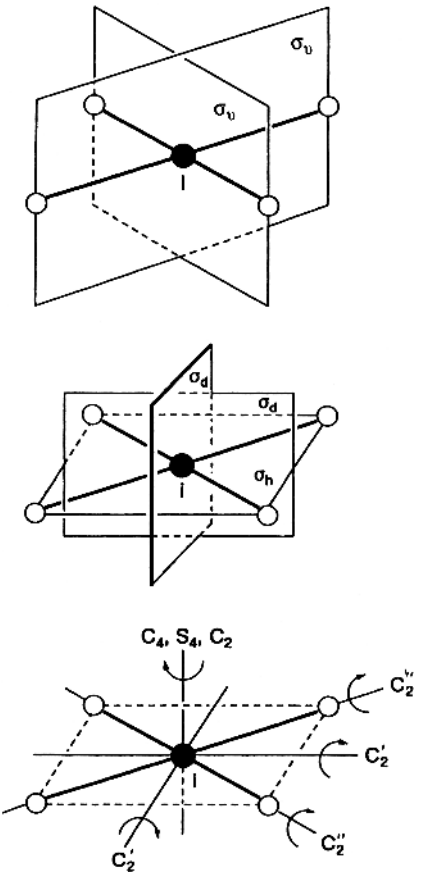

Fig. 1.9. *Symmetry elements in* $\boldsymbol{D}_{4h}$ point group.

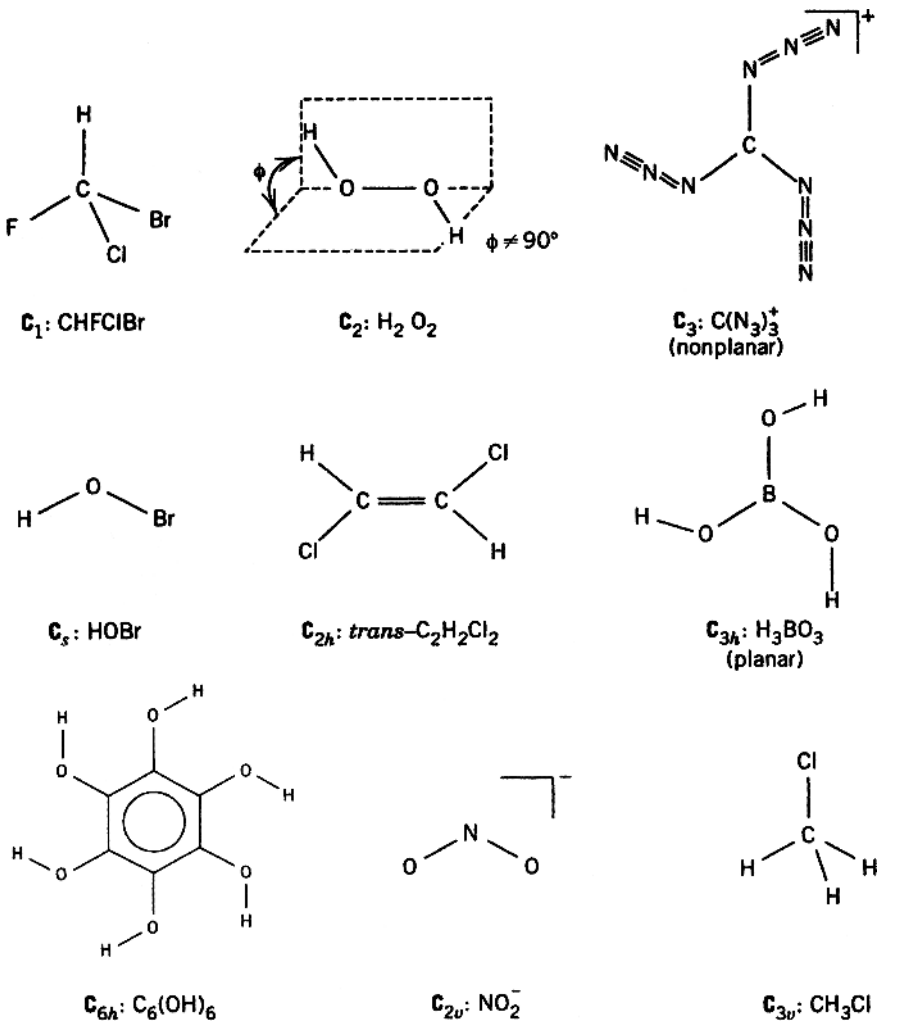

Fig. 1.10. *Examples of molecules belonging to some point groups.*

belonging to the $\mathbf{C}_1$, $\mathbf{C}_2$, $\mathbf{C}_3$, $\mathbf{D}_2 \equiv \mathbf{V}$, and $\mathbf{D}_3$ groups possess only C_p axes, and are thus optically active.

1.6. SYMMETRY OF NORMAL VIBRATIONS AND SELECTION RULES

Figures 1.11 and 1.12 illustrate the normal modes of vibration of CO_2 and H_2O molecules, respectively. In each normal vibration, the individual nuclei carry out a simple harmonic motion in the direction indicated by the arrow, and all the nuclei have

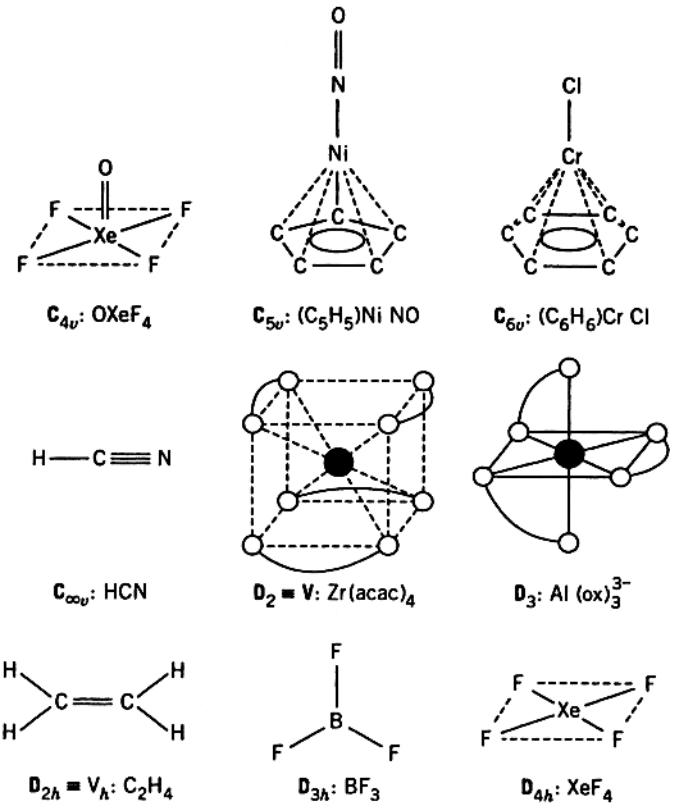

Fig. 1.10. *(Continued)*

the same frequency of oscillation (i.e., the frequency of the normal vibration) and are moving in the same phase. Furthermore, the relative lengths of the arrows indicate the relative velocities and the amplitudes for each nucleus.* The v_2 vibrations in CO_2 are worth comment, since they differ from the others in that two vibrations (v_{2a} and v_{2b}) have exactly the same frequency. Apparently, there are an infinite number of normal vibrations of this type, which differ only in their directions perpendicular to the molecular axis. Any of them, however, can be resolved into two vibrations such as v_{2a} and v_{2b}, which are perpendicular to each other. In this respect, the v_2 vibrations in CO_2 are called *doubly degenerate vibrations*. Doubly degenerate vibrations occur only when a molecule has an axis higher than twofold. *Triply degenerate vibrations* also occur in molecules having more than one C_3 axis.

To determine the symmetry of a normal vibration, it is necessary to begin by considering the kinetic and potential energies of the system. These were discussed in Sec. 1.4:

*In this respect, all the normal modes of vibration shown in this book are only approximate.

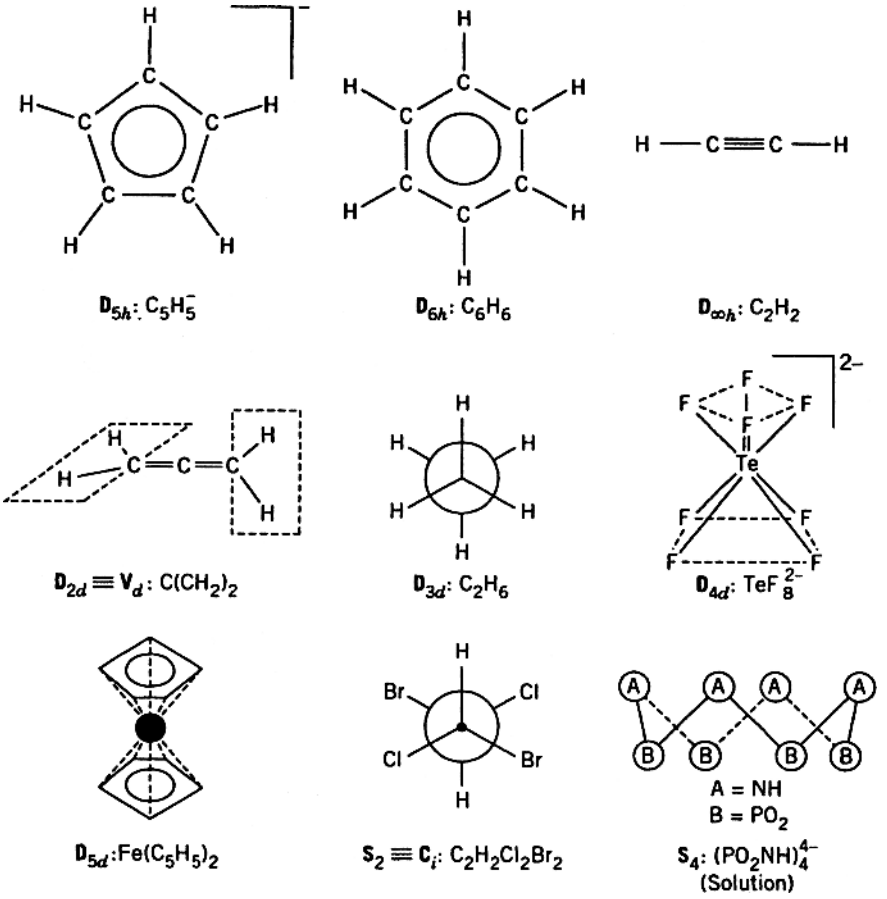

Fig. 1.10. *(Continued)*

$$T = \frac{1}{2}\sum_i \dot{Q}_i^2 \tag{1.60}$$

$$V = \frac{1}{2}\sum_i \lambda_i Q_i^2 \tag{1.61}$$

Consider a case in which a molecule performs only one normal vibration, Q_i. Then, $T = \frac{1}{2}\dot{Q}_i^2$ and $V = \frac{1}{2}\lambda_i Q_i^2$. These energies must be invariant when a symmetry operation, R, changes Q_i to RQ_i. Thus, we obtain

$$T = \frac{1}{2}\dot{Q}_i^2 = \frac{1}{2}(R\dot{Q}_i)^2$$

$$V = \frac{1}{2}\lambda_i Q_i^2 = \frac{1}{2}\lambda_i (RQ_i)^2$$

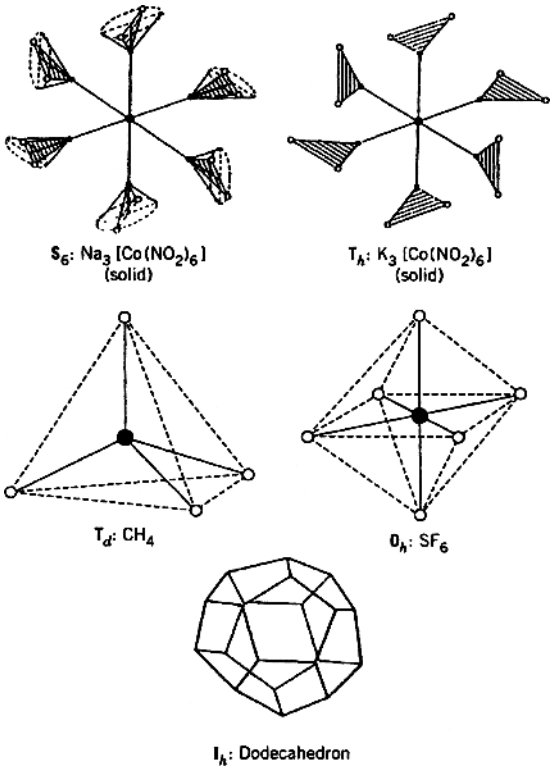

Fig. 1.10. *(Continued)*

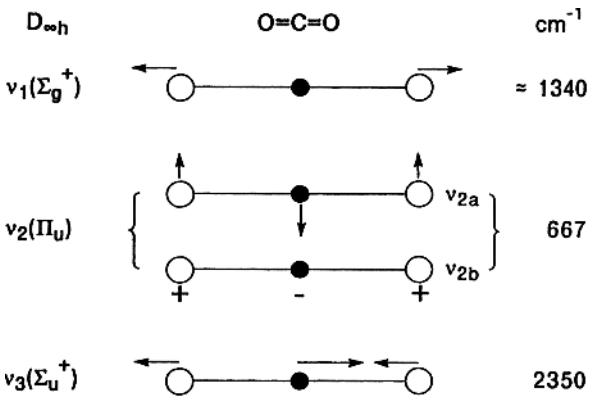

Fig. 1.11. *Normal modes of vibration in CO_2 (+ and – denote vibrations going upward and downward, respectively, in the direction perpendicular to the paper plane).*

For these relations to hold, it is necessary that

$$(RQ_i)^2 = Q_i^2 \quad \text{or} \quad RQ_i = \pm Q_i \tag{1.62}$$

Thus, the normal coordinate must change either into itself or into its negative. If $Q_i = RQ_i$, the vibration is said to be *symmetric*. If $Q_i = -RQ_i$, it is said to be *antisymmetric*.

If the vibration is doubly degenerate, we have

$$T = \frac{1}{2}\dot{Q}_{ia}^2 + \frac{1}{2}\dot{Q}_{ib}^2$$

$$V = \frac{1}{2}\lambda_i(Q_{ia})^2 + \frac{1}{2}\lambda_i(Q_{ib})^2$$

In this case, a relation such as

$$(RQ_{ia})^2 + (RQ_{ib})^2 = Q_{ia}^2 + Q_{ib}^2 \tag{1.63}$$

must hold. As will be shown later, such a relationship is expressed more conveniently by using a matrix form:*

$$R\begin{bmatrix} Q_{ia} \\ Q_{ib} \end{bmatrix} = \begin{bmatrix} A & B \\ C & D \end{bmatrix}\begin{bmatrix} Q_{ia} \\ Q_{ib} \end{bmatrix}$$

where the values of A, B, C, and D depend on the symmetry operation, R. In any case, the normal vibration must be either symmetric or antisymmetric or degenerate for each symmetry operation.

The symmetry properties of the normal vibrations of the H_2O molecule shown in Fig. 1.12 are classified as indicated in Table 1.3. Here, $+1$ and -1 denote symmetric and antisymmetric, respectively. In the ν_1 and ν_2 vibrations, all the symmetry properties are preserved during the vibration. Therefore they are *symmetric vibrations* and are called, in particular, *totally symmetric vibrations*. In the ν_3 vibration, however, symmetry elements such as C_2 and σ_v (xz) are lost. Thus, it is called a *nonsymmetric vibration*. If a molecule has a number of symmetry elements, the normal vibrations are classified according to the number and the kind of symmetry elements preserved during the vibration.

To determine the activity of the vibrations in the infrared and Raman spectra, the selection rule must be applied to each normal vibration. As will be shown in Sec. 1.10, rigorous selection rules can be derived quantum mechanically, and applied to individual molecules using group theory.

For small molecules, however, the IR and Raman activities may be determined by simple inspection of their normal modes. First, we consider the general rule which states that *the vibration is IR-active if the dipole moment is changed during the vibration*. It is obvious that the vibration of a homopolar diatomic molecule is

*For matrix algebra, see Appendix II.

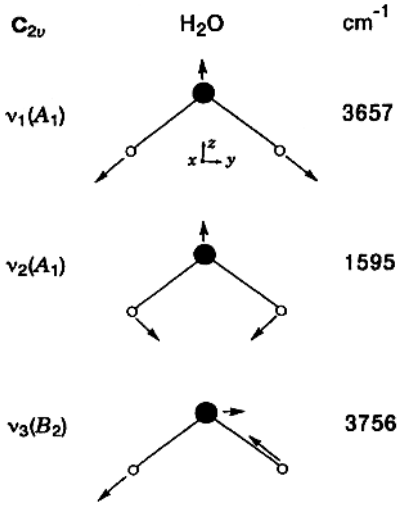

Fig. 1.12. *Normal modes of vibration in H_2O.*

TABLE 1.3.

C_{2v}	I	$C_2(z)$	$\sigma_v(xz)$[a]	$\sigma_v(xz)$[a]
Q_1, Q_2	+1	+1	+1	+1
Q_3	+1	−1	−1	+1

[a] σ_v = vertical plane of symmetry.

not IR-active, whereas that of a heteropolar diatomic molecule is IR-active. In the case of CO_2, shown in Fig. 1.11, it is readily seen that the ν_1 is not IR-active, whereas the ν_2 and ν_3 are IR-active. Figure 1.13 illustrates the changes in dipole moment during the three normal vibrations of H_2O. It is readily seen that all the vibrations are IR-active because the magnitude or direction of the dipole moment is changed as indicated.

To discuss Raman activity, we must consider the nature of polarizability introduced in Sec. 1.2. When a molecule interacts with the electric field of a laser beam, its electron cloud is distorted because the positively charged nuclei are attracted toward the negative pole, and the electrons toward the positive pole, as shown in Fig. 1.14. The charge separation produces an induced dipole moment (P) given by*

$$P = \alpha E^* \tag{1.64}$$

*A more complete form of this equation is $P = \alpha E + \frac{1}{2}\beta E^2 \ldots$. Here, $\beta \ll \alpha$ and β is called the *hyperpolarizability*. The second term becomes significant only when E is large ($\sim 10^9$ V cm^{-1}). In this case, we observe novel spectroscopic phenomena such as the hyper Raman effect, stimulated Raman effect, inverse Raman effect, and coherent anti-Stokes Raman scattering (CARS). For a discussion of nonlinear Raman spectroscopy, see Refs. 25 and 26.

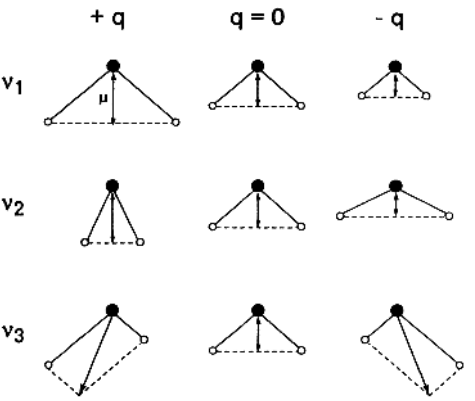

Fig. 1.13. *Changes in dipole moment for H_2O during each normal vibration.*

where E is the strength of the electric field and α is the polarizability. By resolving P, α, and E in the x, y, and z directions, we can write.

$$P_x = \alpha_x E_x, \quad P_y = \alpha_y E_y, \quad P_z = \alpha_z E_z \tag{1.65}$$

However, the actual relationship is more complicated since the direction of polarization may not coincide with the direction of the applied field. This is so because the direction of chemical bonds in the molecule also affects the direction of polarization. Thus, instead of Eq. 1.65, we have the relationship

$$\begin{aligned} P_x &= \alpha_{xx}E_x + \alpha_{xy}E_y + \alpha_{xz}E_z \\ P_y &= \alpha_{yx}E_x + \alpha_{yy}E_y + \alpha_{yz}E_z \\ P_z &= \alpha_{zx}E_x + \alpha_{zy}E_y + \alpha_{zz}E_z \end{aligned} \tag{1.66}$$

In matrix form, Eq. 1.66 is written as

$$\begin{bmatrix} P_x \\ P_y \\ P_z \end{bmatrix} = \begin{bmatrix} \alpha_{xx} & \alpha_{xy} & \alpha_{xz} \\ \alpha_{yx} & \alpha_{yy} & \alpha_{yz} \\ \alpha_{zx} & \alpha_{zy} & \alpha_{zz} \end{bmatrix} \begin{bmatrix} E_x \\ E_y \\ E_z \end{bmatrix} \tag{1.67}$$

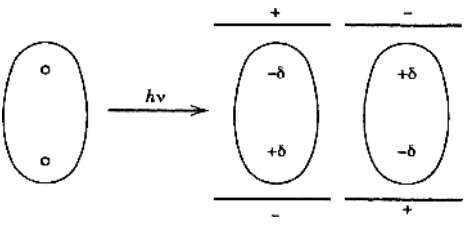

Fig. 1.14. *Polarization of a diatomic molecule in an electric field.*

and the first matrix on the right-hand side is called the *polarizability tensor*. In normal Raman scattering, the tensor is symmetric; $\alpha_{xy} = \alpha_{yx}$, $\alpha_{yz} = \alpha_{zy}$, and $\alpha_{xz} = \alpha_{zx}$. This is not so, however, in the case of resonance Raman scattering (Sec. 1.22).

According to quantum mechanics, *the vibration is Raman-active if one of these six components of the polarizability changes during the vibration*. Thus, it is obvious that the vibration of a homopolar diatomic molecule is Raman-active but not IR-active, whereas the vibration of a heteropolar diatomic molecule is both IR- and Raman-active.

Changes in the polarizability tensor can be visualized if we draw a *polarizability ellipsoid* by plotting $1/\sqrt{\alpha}$ in every direction from the origin. This gives a three-dimensional surface such as shown below:

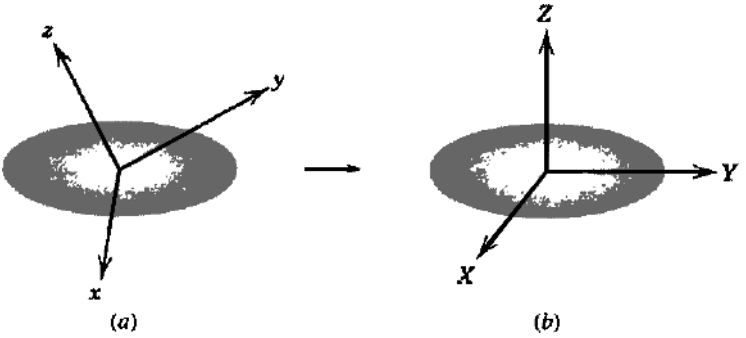

If we rotate such an ellipsoid so that its principal axes coincide with the molecular axes (X, Y, and Z), Eq. 1.67 is simplified to

$$\begin{bmatrix} P_X \\ P_Y \\ P_Z \end{bmatrix} = \begin{bmatrix} \alpha_{XX} & 0 & 0 \\ 0 & \alpha_{YY} & 0 \\ 0 & 0 & \alpha_{ZZ} \end{bmatrix} \begin{bmatrix} E_X \\ E_Y \\ E_Z \end{bmatrix} \tag{1.68}$$

Such axes are called *principal axes of polarizability*. In terms of the polarizability ellipsoid, *the vibration is Raman-active if the polarizability ellipsoid changes in size, shape, or orientation during the vibration*.

As an example, Fig. 1.15 illustrates the polarizability ellipsoids for the three normal vibrations of H_2O at the equilibrium ($q = 0$) and two extreme configurations ($q = \pm q$). It is readily seen that both ν_1 and ν_2 are Raman-active because the size and the shape of the ellipsoid (α_{xx}, α_{yy}, and α_{zz}) change during these vibrations. The ν_3 is also Raman-active because the orientation of the ellipsoid (α_{yz}) changes during the vibration. Thus, all three normal vibrations of H_2O are Raman-active. Figure 1.16 illustrates the changes in polarizability ellipsoids during the normal vibrations of CO_2. It is readily seen that ν_1 is Raman-active because the size of the ellipsoid

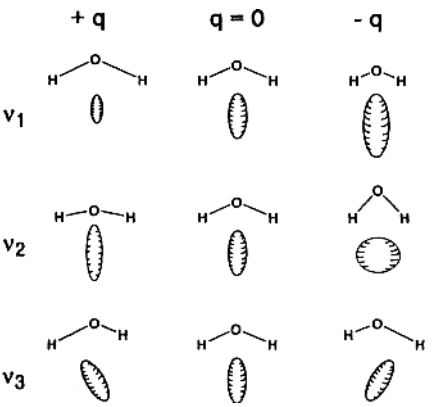

Fig. 1.15. *Changes in polarizability ellipsoid during normal vibrations of H_2O.*

changes during the vibration (α_{xx}, α_{yy}, and α_{zz} change proportionately). Although the size and/or shape of the ellipsoid change during the v_2 and v_3 vibrations, they are identical in two extreme positions, as seen in Fig. 1.16. If we consider a limiting case where the nuclei undergo very small displacements, there is effectively no change in the polarizability. This is illustrated in Fig. 1.17. Thus, these two vibrations are not Raman-active.

It should be noted that in CO_2 the vibration symmetric with respect to the center of symmetry (v_1) is Raman-active and not IR-active, whereas the vibrations antisymmetric with respect to the center of symmetry (v_2 and v_3) are IR-active but not Raman-active. In a polyatomic molecule having a center of symmetry, the vibrations symmetric with respect to the center of symmetry (g vibrations*) are Raman-active

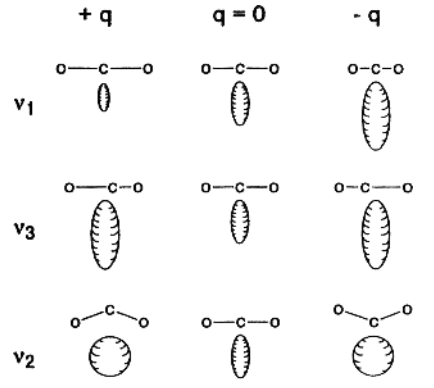

Fig. 1.16. *Changes in polarizability ellipsoid during normal vibrations of CO_2.*

*The symbols g and u stand for *gerade* and *ungerade* (German), respectively.

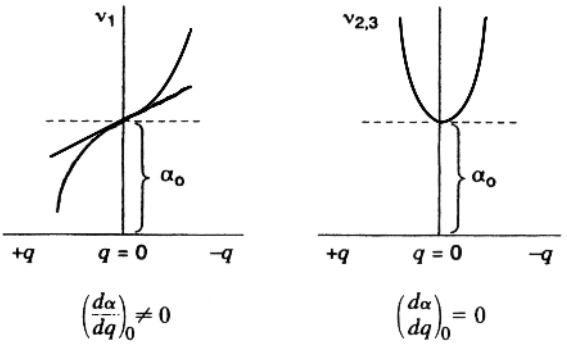

Fig. 1.17. *Changes in polarizability with respect to displacement coordinate during the ν_1 and $\nu_{2,3}$ vibrations in CO_2.*

and not IR-active, but the vibrations antisymmetric with respect to the center of symmetry (*u* vibrations*) are IR-active and not Raman-active. This rule is called the "mutual exclusion rule." It should be noted, however, that in polyatomic molecules having several symmetry elements in addition to the center of symmetry, the vibrations that should be active according to this rule may not necessarily be active, because of the presence of other symmetry elements. An example is seen in a square–planar XY_4-type molecule of $\mathbf{D}_{4h}$ symmetry, where the A_{2g} vibrations are not Raman-active and the A_{1u}, B_{1u}, and B_{2u} vibrations are not IR-active (see Sec. 2.6).

1.7. INTRODUCTION TO GROUP THEORY [9–14]

In Sec. 1.5, the symmetry and the point group allocation of a given molecule were discussed. To understand the symmetry and selection rules of normal vibrations in polyatomic molecules, however, a knowledge of group theory is required. The minimum amount of group theory needed for this purpose is given here.

Consider a pyramidal XY_3 molecule (Fig. 1.18) for which the symmetry operations I, C_3^+, C_3^-, σ_1, σ_2, and σ_3 are applicable. Here, C_3^+ and C_3^- denote rotation through 120° in the clockwise and counterclockwise directions, respectively; and σ_1, σ_2, and σ_3 indicate the symmetry planes that pass through X and Y_1, X and Y_2, and X and Y_3, respectively. For simplicity, let these symmetry operations be denoted by I, A, B, C, D, and E, respectively. Other symmetry operations are possible, but each is equivalent to some one of the operations mentioned. For instance, a clockwise rotation through 240° is identical with operation B. It may also be shown that two successive applications of any one of these operations is equivalent to some single operation of the group mentioned. Let operation C be applied to the original figure. This interchanges Y_2 and Y_3. If operation A is applied to the resulting figure, the net result is the same as

*The symbols *g* and *u* stand for *gerade* and *ungerade* (German), respectively.

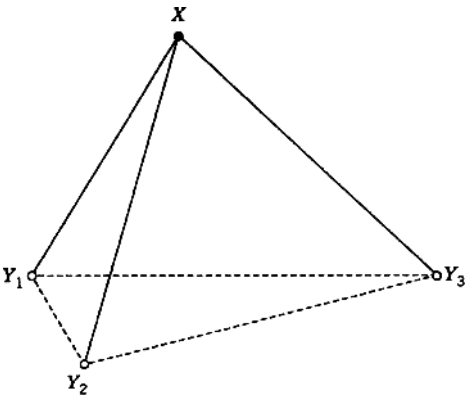

Fig. 1.18. *Pyramidal XY_3 molecule.*

application of the single operation D to the original figure. This is written as $CA = D$. If all the possible multiplicative combinations are made, then a tabular display such as Table 1.4, in which the operation applied first is written across the top, is obtained. This is called the *multiplication table* of the group.

It is seen that a group consisting of the mathematical elements (symmetry operations) I, A, B, C, D, and E satisfies the following conditions:

(1) The product of any two elements in the set is another element in the set.
(2) The set contains the identity operation that satisfies the relation $IP = PI = P$, where P is any element in the set.
(3) The associative law holds for all the elements in the set, that is, $(CB)A = C(BA)$, for example.
(4) Every element in the set has its reciprocal, X, which satisfies the relation $XP = PX = I$, where P is any element in the set. This reciprocal is usually denoted by P^{-1}.

These are necessary and sufficient conditions for a set of elements to form a *group*. It is evident that operations I, A, B, C, D, and E form a group in this sense. It should be noted

TABLE 1.4.

	I	*A*	*B*	*C*	*D*	*E*
I	*I*	*A*	*B*	*C*	*D*	*E*
A	*A*	*B*	*I*	*D*	*E*	*C*
B	*B*	*I*	*A*	*E*	*C*	*D*
C	*C*	*E*	*D*	*I*	*B*	*A*
D	*D*	*C*	*E*	*A*	*I*	*B*
E	*E*	*D*	*C*	*B*	*A*	*I*

that the commutative law of multiplication does not necessarily hold. For example, Table 1.4 shows that $CD \neq DC$.

The six elements can be classified into three types of operation: the identity operation I, the rotations C_3^+ and C_3^-, and the reflections σ_1, σ_2, and σ_3. Each of these sets of operations is said to form a *class*. More precisely, two operations, P and Q, which satisfy the relation $X^{-1}PX = P$ or Q, where X is any operation of the group and X^{-1} is its reciprocal, are said to belong to the same class. It can easily be shown that C_3^+ and C_3^-, for example, satisfy the relation. Thus the six elements of the point group $\mathbf{C}_{3v}$ are usually abbreviated as I, $2C_3$, and $3\sigma_v$.

The relations between the elements of the group are shown in the multiplication table (Table 1.4). Such a tabulation of a group is, however, awkward to handle. The essential features of the table may be abstracted by replacing the elements by some analytical function that reproduces the multiplication table. Such an analytical expression may be composed of a simple integer, an exponential function, or a matrix. Any set of such expressions that satisfies the relations given by the multiplication table is called a *representation* of the group and is designated by Γ. The representations of the point group $\mathbf{C}_{3v}$ discussed above are indicated in Table 1.5. It can easily be proved that each representation in the table satisfies the multiplication table.

In addition to the three representations in Table 1.5, it is possible to write an infinite number of other representations of the group. If a set of six matrices of the type $S^{-1}R(K)S$ is chosen, where $R(K)$ is a representation of the element K given in Table 1.5, $S(|S| \neq 0)$ is any matrix of the same order as R, and S^{-1} is the reciprocal of S, this set also satisfies the relations given by the multiplication table. The reason is obvious from the relation

$$S^{-1}R(K)SS^{-1}R(L)S = S^{-1}R(K)R(L)S = S^{-1}R(KL)S$$

Such a transformation is called a *similarity transformation*. Thus, it is possible to make an infinite number of representations by means of similarity transformations.

On the other hand, this statement suggests that a given representation may possibly be broken into simpler ones. If each representation of the symmetry element K is

TABLE 1.5.

C_{3v}	I	A	B	C	D	E
$A_1(\Gamma_1)$	1	1	1	1	1	1
$A_2(\Gamma_2)$	1	1	1	−1	−1	−1
$E(\Gamma_3)$	$\begin{pmatrix} 1 & 0 \\ 0 & 1 \end{pmatrix}$	$\begin{pmatrix} -\frac{1}{2} & \frac{\sqrt{3}}{2} \\ -\frac{\sqrt{3}}{2} & -\frac{1}{2} \end{pmatrix}$	$\begin{pmatrix} -\frac{1}{2} & -\frac{\sqrt{3}}{2} \\ \frac{\sqrt{3}}{2} & -\frac{1}{2} \end{pmatrix}$	$\begin{pmatrix} -1 & 0 \\ 0 & 1 \end{pmatrix}$	$\begin{pmatrix} \frac{1}{2} & -\frac{\sqrt{3}}{2} \\ -\frac{\sqrt{3}}{2} & -\frac{1}{2} \end{pmatrix}$	$\begin{pmatrix} \frac{1}{2} & \frac{\sqrt{3}}{2} \\ \frac{\sqrt{3}}{2} & -\frac{1}{2} \end{pmatrix}$

transformed into the form

$$R(K) = \left|\begin{array}{c|c|c|c} Q_1(K) & 0 & 0 & 0 \\ \hline 0 & Q_2(K) & 0 & 0 \\ \hline 0 & 0 & Q_3(K) & 0 \\ \hline 0 & 0 & 0 & Q_3(K) \end{array}\right| \tag{1.69}$$

by a similarity transformation, $Q_1(K), Q_2(K), \ldots$ are simpler representations. In such a case, $R(K)$ is called *reducible*. If a representation cannot be simplified any further, it is said to be *irreducible*. The representations Γ_1, Γ_2, and Γ_3 in Table 1.5 are all irreducible representations. It can be shown generally that the number of irreducible representations is equal to the number of classes. Thus, only three irreducible representations exist for the point group $\mathbf{C}_{3v}$. These representations are entirely independent of each other. Furthermore, the sum of the squares of the dimensions (l) of the irreducible representations of a group is always equal to the total number of the symmetry elements, namely, the *order of the group* (h). Thus

$$\sum l_i^2 = l_1^2 + l_2^2 + \cdots = h \tag{1.70}$$

In the point group $\mathbf{C}_{3v}$, it is seen that

$$1^2 + 1^2 + 2^2 = 6$$

A point group is classified into *species* according to its irreducible representations. In the point group C_{3v}, the species having the irreducible representations Γ_1, Γ_2, and Γ_3 are called the A_1, A_2, and E species, respectively.*

The sum of the diagonal elements of a matrix is called the *character* of the matrix and is denoted by χ. It is to be noted in Table 1.5 that the character of each of the elements belonging to the same class is the same. Thus, using the character, Table 1.5 can be simplified to Table 1.6. Such a table is called the *character table* of the point group $\mathbf{C}_{3v}$.

That the *character* of a matrix is not changed by a similarity transformation can be proved as follows. If a similarity transformation is expressed by $T = S^{-1}RS$, then

$$\begin{aligned} \chi T &= \sum_i (S^{-1}RS)_{ii} = \sum_{i,j,k} (S^{-1})_{ij} R_{jk} S_{ki} = \sum_{j,k,i} S_{ki} (S^{-1})_{ij} R_{jk} \\ &= \sum_{j,k} \delta_{kj} R_{jk} = \sum_k R_{kk} = \chi R \end{aligned}$$

*For labeling of the irreducible representations (species), see Appendix I.

TABLE 1.6. Character Table of the Point Group C_{3v}

C_{3v}	I	$2C_3(z)$	$3\sigma_v$
A_1 (χ_1)	1	1	1
A_2 (χ_2)	1	1	−1
E (χ_3)	2	−1	0

where δ_{kj} is Krönecker's delta (0 for $k \neq j$ and 1 for $k = j$). Thus, any reducible representation can be reduced to its irreducible representations by a similarity transformation that leaves the character unchanged. Therefore, the character of the reducible representation, $\chi(K)$, is written as

$$\chi(K) = \sum_m a_m \chi_m(K) \tag{1.71}$$

where $\chi_m(K)$ is the character of $Q_m(K)$, and a_m is a positive integer that indicates the number of times that $Q_m(K)$ appears in the matrix of Eq. 1.69. Hereafter the character will be used rather than the corresponding representation because a 1 : 1 correspondence exists between these two, and the former is sufficient for vibrational problems.

It is important to note that the following relation holds in Table 1.6:

$$\sum_K \chi_i(K)\chi_j(K) = h\delta_{ij} \tag{1.72}$$

If Eq. 1.71 is multiplied by $\chi_i(K)$ on both sides, and the summation is taken over all the symmetry operations, then

$$\begin{aligned}\sum_K \chi(K)\chi_i(K) &= \sum_K \sum_m a_m \chi_m(K)\chi_i(K) \\ &= \sum_m \sum_K a_m \chi_m(K)\chi_i(K)\end{aligned}$$

For a fixed m, we have

$$\sum_K a_m \chi_m(K)\chi_i(K) = a_m \sum_K \chi_m(K)\chi_i(K) = a_m h\delta_{im}$$

If we consider the sum of such a term over m, only the sum in which $m = i$ remains. Thus, we obtain

$$\sum_K \chi(K)\chi_m(K) = ha_m$$

or

$$a_m = \frac{1}{h}\sum_K \chi(K)\chi_m(K) \tag{1.73}$$

This formula is written more conveniently as

$$\boxed{a_m = \frac{1}{h}\sum n\chi(K)\chi_m(K)} \tag{1.74}$$

where n is the number of symmetry elements in any one class, and the summation is made over the different classes. As Sec. 1.8 will show, this formula is very useful in determining the number of normal vibrations belonging to each species.*

1.8. THE NUMBER OF NORMAL VIBRATIONS FOR EACH SPECIES

As shown in Sec. 1.6, the $3N-6$ (or $3N-5$) normal vibrations of an N-atom molecule can be classified into various species according to their symmetry properties. The number of normal vibrations in each species can be calculated by using the general equations given in Appendix III. These equations were derived from consideration of the vibrational degrees of freedom contributed by each set of identical nuclei for each symmetry species [1]. As an example, let us consider the NH_3 molecule belonging to the C_{3v} point group. The general equations are as follows:

$$\begin{aligned}
&A_1 \text{ species:} \quad 3m + 2m_v + m_0 - 1\\
&A_2 \text{ species:} \quad 3m + m_v - 1\\
&E \text{ species:} \quad 6m + 3m_v + m_0 - 2\\
&N(\text{total number of atoms}) = 6m + 3m_v + m_0
\end{aligned}$$

From the definitions given in the footnotes of Appendix III, it is obvious that $m = 0$, $m_0 = 1$, and $m_v = 1$ in this case. To check these numbers, we calculate the total number of atoms from the equation for N given above. Since the result is 4, these assigned numbers are correct. Then, the number of normal vibrations in each species can be calculated by inserting these numbers in the general equations given above: 2, 0, and 2, respectively, for the A_1, A_2, and E species. Since the E species is doubly degenerate, the total number of vibrations is counted as 6, which is expected from the $3N-6$ rule.

A more general method of finding the number of normal vibrations in each species can be developed by using group theory. The principle of the method is that all the

*Since this equation is not applicable to the infinite point groups ($C_{\infty v}$ and $D_{\infty h}$), several alternative approaches have been proposed (see Refs. 75 and 76).

representations are irreducible if normal coordinates are used as the basis for the representations. For example, the representations for the symmetry operations based on three normal coordinates, Q_1, Q_2, and Q_3, which correspond to the ν_1, ν_2, and ν_3 vibrations in the H_2O molecule of Fig. 1.12, are as follows:

$$I\begin{bmatrix}Q_1\\Q_2\\Q_3\end{bmatrix}=\begin{bmatrix}1&0&0\\0&1&0\\0&0&1\end{bmatrix}\begin{bmatrix}Q_1\\Q_2\\Q_3\end{bmatrix},\quad C_2(z)\begin{bmatrix}Q_1\\Q_2\\Q_3\end{bmatrix}=\begin{bmatrix}1&0&0\\0&1&0\\0&0&-1\end{bmatrix}\begin{bmatrix}Q_1\\Q_2\\Q_3\end{bmatrix}$$

$$\sigma_v(xz)\begin{bmatrix}Q_1\\Q_2\\Q_3\end{bmatrix}=\begin{bmatrix}1&0&0\\0&1&0\\0&0&-1\end{bmatrix}\begin{bmatrix}Q_1\\Q_2\\Q_3\end{bmatrix},\quad \sigma_v(yz)\begin{bmatrix}Q_1\\Q_2\\Q_3\end{bmatrix}=\begin{bmatrix}1&0&0\\0&1&0\\0&0&1\end{bmatrix}\begin{bmatrix}Q_1\\Q_2\\Q_3\end{bmatrix}$$

Let a representation be written with the $3N$ rectangular coordinates of an N-atom molecule as its basis. If it is decomposed into its irreducible components, the basis for these irreducible representations must be the normal coordinates, and the number of appearances of the same irreducible representation must be equal to the number of normal vibrations belonging to the species represented by this irreducible representation. As stated previously, however, the $3N$ rectangular coordinates involve six (or five) coordinates, which correspond to the translational and rotational motions of the molecule as a whole. Therefore, the representations that have such coordinates as their basis must be subtracted from the result obtained above. Use of the character of the representation, rather than the representation itself, yields the same result.

For example, consider a pyramidal XY_3 molecule that has six normal vibrations. At first, the representations for the various symmetry operations must be written with the 12 rectangular coordinates in Fig. 1.19 as their basis. Consider pure rotation C_p^+. If the

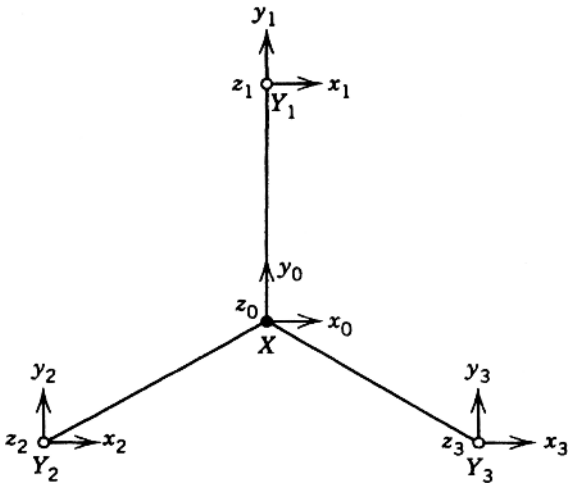

Fig. 1.19. *Rectangular coordinates in a pyramidal XY_3 molecule (Z axis is perpendicular to the paper plane).*

clockwise rotation of the point (x,y,z) around the z axis by the angle θ brings it to the point denoted by the coordinates (x',y',z'), the relations between these two sets of coordinates are given by.

$$\begin{aligned} x' &= x\cos\theta + y\sin\theta \\ y' &= -x\sin\theta + y\cos\theta \\ z' &= z \end{aligned} \tag{1.75}$$

By using matrix notation,* this can be written as

$$\begin{bmatrix} x' \\ y' \\ z' \end{bmatrix} = C_0^+ \begin{bmatrix} x \\ y \\ z \end{bmatrix} = \begin{bmatrix} \cos\theta & \sin\theta & 0 \\ -\sin\theta & \cos\theta & 0 \\ 0 & 0 & 1 \end{bmatrix} \begin{bmatrix} x \\ y \\ z \end{bmatrix} \tag{1.76}$$

Then the character of the matrix is given by

$$\chi(C_\theta^+) = 1 + 2\cos\theta \tag{1.77}$$

The same result is obtained for $\chi(C_\theta^-)$. If this symmetry operation is applied to all the coordinates of the XY_3 molecule, the result is

$$C_\theta \begin{bmatrix} x_0 \\ y_0 \\ z_0 \\ x_1 \\ y_1 \\ z_1 \\ x_2 \\ y_2 \\ z_2 \\ x_3 \\ y_3 \\ z_3 \end{bmatrix} = \left[\begin{array}{c|c|c|c} \mathbf{A} & 0 & 0 & 0 \\ \hline 0 & 0 & 0 & \mathbf{A} \\ \hline 0 & \mathbf{A} & 0 & 0 \\ \hline 0 & 0 & \mathbf{A} & 0 \end{array}\right] \begin{bmatrix} x_0 \\ y_0 \\ z_0 \\ x_1 \\ y_1 \\ z_1 \\ x_2 \\ y_2 \\ z_2 \\ x_3 \\ y_3 \\ z_3 \end{bmatrix} \tag{1.78}$$

where **A** denotes the small square matrix given by Eq. 1.76. Thus, the character of this representation is simply given by Eq. 1.77. It should be noted in Eq. 1.78 that only the small matrix **A**, related to the nuclei unchanged by the symmetry operation, appears as a diagonal element. Thus, a more general form of the character of the representation for rotation around the axis by θ is

*For matrix algebra, see Appendix II.

$$\boxed{\chi(R) = N_R(1 + 2\cos\theta)} \tag{1.79}$$

where N_R is the number of nuclei unchanged by the rotation. In the present case, $N_R = 1$ and $\theta = 120°$. Therefore, we obtain

$$\chi(C_3) = 0 \tag{1.80}$$

Identity (I) can be regarded as a special case of Eq. 1.79 in which $N_R = 4$ and $\theta = 0°$. The character of the representation is

$$\chi(I) = 12 \tag{1.81}$$

Pure rotation and identity are called *proper rotation*.

It is evident from Fig. 1.19 that a symmetry plane such as σ_1 changes the coordinates from (x_i, y_i, z_i) to ($-x_i$, y_i, z_i). The corresponding representation is therefore written as

$$\sigma_1 \begin{bmatrix} x \\ y \\ z \end{bmatrix} = \begin{bmatrix} -1 & 0 & 0 \\ 0 & 1 & 0 \\ 0 & 0 & 1 \end{bmatrix} \begin{bmatrix} x \\ y \\ z \end{bmatrix} \tag{1.82}$$

The result of such an operation on all the coordinates is

$$\sigma_1 \begin{bmatrix} x_0 \\ y_0 \\ z_0 \\ x_1 \\ y_1 \\ z_1 \\ x_2 \\ y_2 \\ z_2 \\ x_3 \\ y_3 \\ z_3 \end{bmatrix} = \left[\begin{array}{c|c|c|c} \mathbf{B} & 0 & 0 & 0 \\ \hline 0 & \mathbf{B} & 0 & 0 \\ \hline 0 & 0 & 0 & \mathbf{B} \\ \hline 0 & 0 & \mathbf{B} & 0 \end{array}\right] \begin{bmatrix} x_0 \\ y_0 \\ z_0 \\ x_1 \\ y_1 \\ z_1 \\ x_2 \\ y_2 \\ z_2 \\ x_3 \\ y_3 \\ z_3 \end{bmatrix} \tag{1.83}$$

where **B** denotes the small square matrix of Eq. 1.82. Thus, the character of this representation is calculated as $2 \times 1 = 2$. It is noted again that the matrix on the diagonal is nonzero only for the nuclei unchanged by the operation.

More generally, a reflection at a plane (σ) is regarded as $\sigma = i \times C_2$. Thus, the general form of Eq. 1.82 may be written as

$$\begin{bmatrix} -1 & 0 & 0 \\ 0 & -1 & 0 \\ 0 & 0 & -1 \end{bmatrix} \begin{bmatrix} \cos\theta & \sin\theta & 0 \\ -\sin\theta & \cos\theta & 0 \\ 0 & 0 & 1 \end{bmatrix} = \begin{bmatrix} -\cos\theta & -\sin\theta & 0 \\ \sin\theta & -\cos\theta & 0 \\ 0 & 0 & -1 \end{bmatrix}$$

Then

$$\chi(\sigma) = -(1 + 2\cos\theta)$$

As a result, the character of the large matrix shown in Eq. 1.83 is given by

$$\boxed{\chi(R) = -N_R(1 + 2\cos\theta)} \tag{1.84}$$

In the present case, $N_R = 2$ and $\theta = 180°$. This gives

$$\chi(\sigma_v) = 2 \tag{1.85}$$

Symmetry operations such as i and S_p are regarded as

$$\begin{aligned} i &= i \times I, & \theta &= 0° \\ S_3 &= i \times C_6, & \theta &= 60° \\ S_4 &= i \times C_4, & \theta &= 90° \\ S_6 &= i \times C_3, & \theta &= 120° \end{aligned}$$

Therefore, the characters of these symmetry operations can be calculated by Eq. 1.84 with the values of θ defined above. Operations such as σ, i, and S_p are called *improper rotations*. Thus, the character of the representation based on 12 rectangular coordinates is as follows:

I	$2C_3$	$3\sigma_v$
12	0	2

(1.86)

To determine the number of normal vibrations belonging to each species, the $\chi(R)$ thus obtained must be resolved into the $\chi_i(R)$ of the irreducible representations of each species in Table 1.6. First, however, the characters corresponding to the translational and rotational motions of the molecule must be subtracted from the result shown in Eq. 1.86.

The characters for the translational motion of the molecule in the x, y, and z directions (denoted by T_x, T_y, and T_z) are the same as those obtained in Eqs. 1.79 and 1.84. They are as follows:

$$\boxed{\chi_t(R) = \pm(1 + 2\cos\theta)} \tag{1.87}$$

where the $+$ and $-$ signs are for proper and improper rotations, respectively. The characters for the rotations around the x, y, and z axes (denoted by R_x, R_y, and R_z) are

given by

$$\boxed{\chi_r(R) = +(1+2\cos\theta)} \tag{1.88}$$

for both proper and improper rotations. This is due to the fact that a rotation of the vectors in the plane perpendicular to the x, y, and z axes can be regarded as a rotation of the components of angular momentum, M_x,M_y, and M_z, about the given axes. If p_x, p_y, and p_z are the components of linear momentum in the x, y, and z directions, the following relations hold:

$$M_x = yp_z - zp_y$$
$$M_y = zp_x - xp_z$$
$$M_z = xp_y - yp_x$$

Since (x,y,z) and (p_x,p_y,p_z) transform as shown in Eq. 1.76, it follows that

$$C_\theta \begin{bmatrix} M_x \\ M_y \\ M_z \end{bmatrix} = \begin{bmatrix} \cos\theta & \sin\theta & 0 \\ -\sin\theta & \cos\theta & 0 \\ 0 & 0 & 1 \end{bmatrix} \begin{bmatrix} M_x \\ M_y \\ M_z \end{bmatrix}$$

Then, a similar relation holds for R_x, R_y, and R_z:

$$C_\theta \begin{bmatrix} R_x \\ R_y \\ R_z \end{bmatrix} = \begin{bmatrix} \cos\theta & \sin\theta & 0 \\ -\sin\theta & \cos\theta & 0 \\ 0 & 0 & 1 \end{bmatrix} \begin{bmatrix} R_x \\ R_y \\ R_z \end{bmatrix}$$

Thus, the characters for the proper rotations are as given by Eq. 1.88. The same result is obtained for the improper rotation if the latter is regarded as $i \times$ (proper rotation). Therefore, the character for the vibration is obtained from

$$\boxed{\chi_v(R) = \chi(R) - \chi_t(R) - \chi_r(R)} \tag{1.89}$$

It is convenient to tabulate the foregoing calculations as in Table 1.7. By using the formula in Eq. 1.74 and the character of the irreducible representations in Table 1.6, a_m can be calculated as follows:

$$a_m(A_1) = \tfrac{1}{6}[(1)(6)(1) + (2)(0)(1) + (3)(2)(1)] = 2$$
$$a_m(A_2) = \tfrac{1}{6}[(1)(6)(1) + (2)(0)(1) + (3)(2)(-1)] = 0$$
$$a_m(E) = \tfrac{1}{6}[(1)(6)(2) + (2)(0)(-1) + (3)(2)(0)] = 2$$

TABLE 1.7.

Symmetry Operation:	I	$2C_3$	$3\sigma_v$
	Proper		Improper
Kind of Rotation: θ:	0°	120°	180°
cos θ	1	$-\frac{1}{2}$	–1
$1+2\cos\theta$	3	0	–1
N_R	4	1	2
$\chi, \pm N_R(1+2\cos\theta)$	12	0	2
$\chi_t, \pm(1+2\cos\theta)$	3	0	1
$\chi_r, +(1+2\cos\theta)$	3	0	–1
χ_v, $\chi-\chi_t-\chi_r$	6	0	2

and

$$\chi_v = 2\chi_{A1} + 2\chi_E \tag{1.90}$$

In other words, the six normal vibrations of a pyramidal XY_3 molecule are classified into two A_1 and two E species.

This procedure is applicable to any molecule. As another example, a similar calculation is shown in Table 1.8 for an octahedral XY_6 molecule. By use of Eq. 1.74 and the character table in Appendix I, the a_m are obtained as

$$\begin{aligned} a_m(A_{1g}) = \tfrac{1}{48}[&(1)(15)(1)+(8)(0)(1)+(6)(1)(1)+(6)(1)(1)\\ &+(3)(-1)(1)+(1)(-3)(1)+(6)(-1)(1)+(8)(0)(1)\\ &+(3)(5)(1)+(6)(3)(1)]\\ &=1 \end{aligned}$$

TABLE 1.8.

Symmetry Operation	I	$8C_3$	$6C_2$	$6C_4$	$3C_4^2 \equiv C_2''$	$S_2 \equiv i$	$6S_4$	$8S_6$	$3\sigma_h$[a]	$6\sigma_d$[a]
	Proper					Improper				
Kind of Rotation: θ:	0°	120°	180°	90°	180°	0°	90°	120°	180°	180°
cos θ	1	$-\frac{1}{2}$	–1	0	–1	1	0	$-\frac{1}{2}$	–1	–1
$1+2\cos\theta$	3	0	–1	1	–1	3	1	0	–1	–1
N_R	7	1	1	3	3	1	1	1	5	3
$\chi, \pm N_R(1+2\cos\theta)$	21	0	–1	3	–3	–3	–1	0	5	3
$\chi_t, \pm(1+2\cos\theta)$	3	0	–1	1	–1	–3	–1	0	1	1
$\chi_r, +(1+2\cos\theta)$	3	0	–1	1	–1	3	1	0	–1	–1
χ_v, $\chi-\chi_t-\chi_r$	15	0	1	1	–1	–3	–1	0	5	3

[a] σ_h = horizontal plane of symmetry; σ_d = diagonal plane of symmetry.

$$
\begin{aligned}
a_m(A_{1u}) = \tfrac{1}{48}[&(1)(15)(1) + (8)(0)(1) + (6)(1)(1) + (6)(1)(1) \\
&+ (3)(-1)(1) + (1)(-3)(-1) + (6)(-1)(-1) \\
&+ (8)(0)(-1) + (3)(5)(-1) + (6)(3)(-1)] \\
&= 0 \\
&\vdots
\end{aligned}
$$

and therefore

$$\chi_v = \chi_{A_{1g}} + \chi_{E_g} + 2\chi F_{1u} + \chi F_{2g} + \chi F_{2u}$$

1.9. INTERNAL COORDINATES

In Sec. 1.4, the potential and the kinetic energies were expressed in terms of rectangular coordinates. If, instead, these energies are expressed in terms of *internal coordinates* such as increments of the bond length and bond angle, the corresponding force constants have clearer physical meanings than do those expressed in terms of rectangular coordinates, since these force constants are characteristic of the bond stretching and the angle deformation involved. The number of internal coordinates must be equal to, or greater than, $3N-6$ (or $3N-5$), the degrees of vibrational freedom of an N-atom molecule. If more than $3N-6$ (or $3N-5$) coordinates are selected as the internal coordinates, this means that these coordinates are not independent of each other. Figure 1.20 illustrates the internal coordinates for various types of molecules.

In linear XYZ (a), bent XY_2 (b), and pyramidal XY_3 (c) molecules, the number of internal coordinates is the same as the number of normal vibrations. In a nonplanar X_2Y_2 molecule (d) such as H_2O_2, the number of internal coordinates is the same as the number of vibrations if the twisting angle around the central bond ($\Delta\tau$) is considered. In a tetrahedral XY_4 molecule (e), however, the number of internal coordinates exceeds the number of normal vibrations by one. This is due to the fact that the six angle coordinates around the central atom are not independent of each other, that is, they must satisfy the relation

$$\Delta\alpha_{12} + \Delta\alpha_{23} + \Delta\alpha_{31} + \Delta\alpha_{14} + \Delta\alpha_{24} + \Delta\alpha_{34} = 0 \tag{1.91}$$

This is called a *redundant condition*. In a planar XY_3 molecule (f), the number of internal coordinates is seven when the coordinate $\Delta\theta$, which represents the deviation from planarity, is considered. Since the number of vibrations is six, one redundant

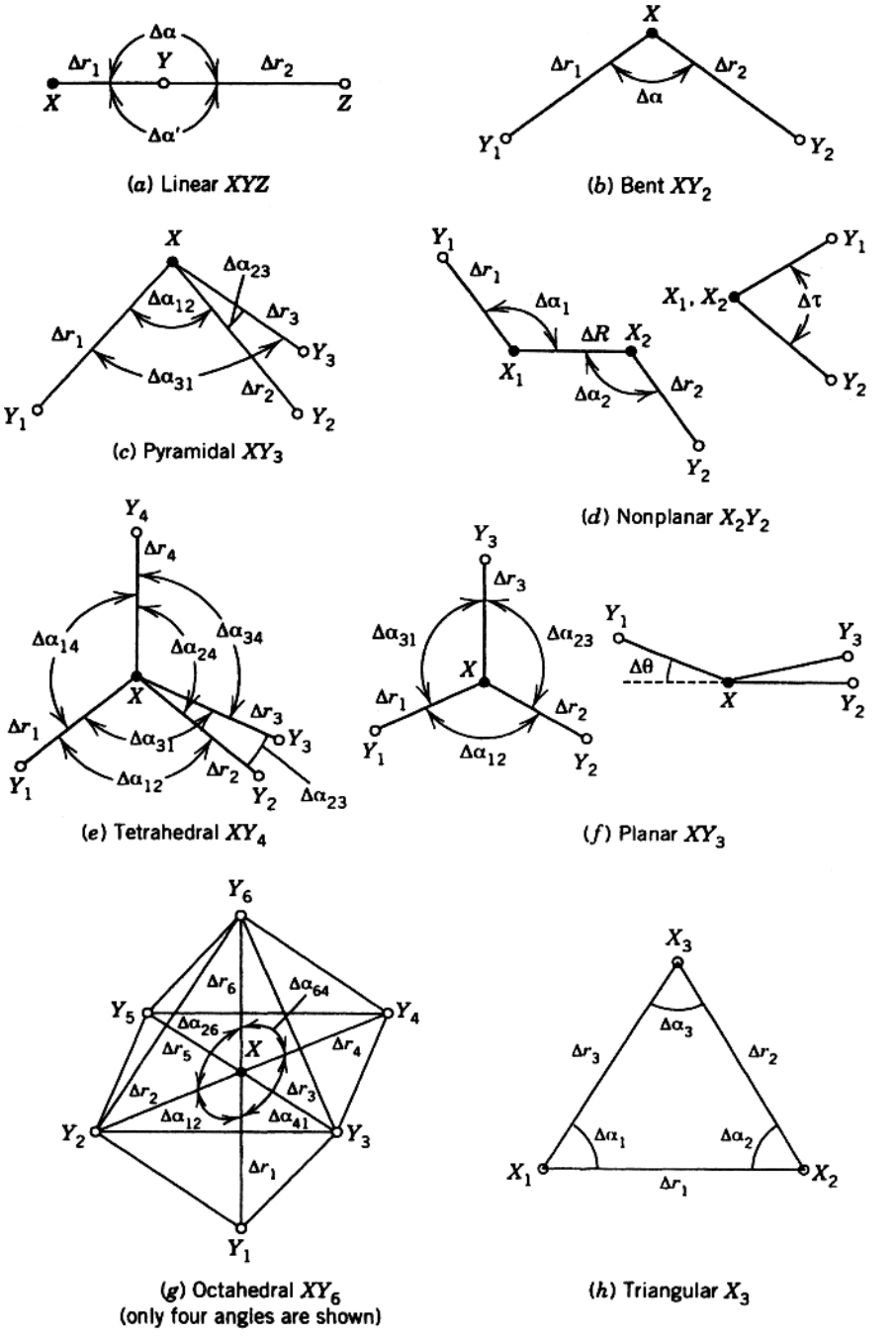

Fig. 1.20. *Internal coordinates for various molecules.*

condition such as

$$\Delta\alpha_{12} + \Delta\alpha_{23} + \Delta\alpha_{31} = 0 \tag{1.92}$$

must be involved. Such redundant conditions always exist for the angle coordinates around the central atom. In an octahedral XY_6 molecule (g), the number of internal coordinates exceeds the number of normal vibrations by three. This means that, of the 12 angle coordinates around the central atom, three redundant conditions are involved:

$$\begin{aligned} \Delta\alpha_{12} + \Delta\alpha_{26} + \Delta\alpha_{64} + \Delta\alpha_{41} &= 0 \\ \Delta\alpha_{15} + \Delta\alpha_{56} + \Delta\alpha_{63} + \Delta\alpha_{31} &= 0 \\ \Delta\alpha_{23} + \Delta\alpha_{34} + \Delta\alpha_{45} + \Delta\alpha_{52} &= 0 \end{aligned} \tag{1.93}$$

The redundant conditions are more complex in ring compounds. For example, the number of internal coordinates in a triangular X_3 molecule (h) exceeds the number of vibrations by three. One of these redundant conditions (A_1' species) is

$$\Delta\alpha_1 + \Delta\alpha_2 + \Delta\alpha_3 = 0 \tag{1.94}$$

The other two redundant conditions (E' species) involve bond stretching and angle deformation coordinates such as

$$\begin{aligned} (2\Delta r_1 - \Delta r_2 - \Delta r_3) + \frac{r}{\sqrt{3}}(\Delta\alpha_1 + \Delta\alpha_2 - 2\Delta\alpha_3) &= 0 \\ (\Delta r_2 - \Delta r_3) - \frac{r}{\sqrt{3}}(\Delta\alpha_1 - \Delta\alpha_2) &= 0 \end{aligned} \tag{1.95}$$

where r is the equilibrium length of the X–X bond. The redundant conditions mentioned above can be derived by using the method described in Sec. 1.12.

The procedure for finding the number of normal vibrations in each species was described in Sec. 1.8. This procedure is, however, considerably simplified if internal coordinates are used. Again, consider a pyramidal XY_3 molecule. Using the internal coordinates shown in Fig. 1.20c, we can write the representation for the C_3^+ operation as

$$C_3^+ \begin{bmatrix} \Delta r_1 \\ \Delta r_2 \\ \Delta r_3 \\ \Delta\alpha_{12} \\ \Delta\alpha_{23} \\ \Delta\alpha_{31} \end{bmatrix} = \begin{bmatrix} 0 & 0 & 1 & 0 & 0 & 0 \\ 1 & 0 & 0 & 0 & 0 & 0 \\ 0 & 1 & 0 & 0 & 0 & 0 \\ 0 & 0 & 0 & 0 & 0 & 1 \\ 0 & 0 & 0 & 1 & 0 & 0 \\ 0 & 0 & 0 & 0 & 1 & 0 \end{bmatrix} \begin{bmatrix} \Delta r_1 \\ \Delta r_2 \\ \Delta r_3 \\ \Delta\alpha_{12} \\ \Delta\alpha_{23} \\ \Delta\alpha_{31} \end{bmatrix} \tag{1.96}$$

Thus $\chi(C_3^+) = 0$, as does $\chi(C_3^-)$. Similarly, $\chi(\mathrm{I}) = 6$ and $\chi(\sigma_v) = 2$. This result is exactly the same as that obtained in Table 1.7 using rectangular coordinates. *When*

TABLE 1.9.

	I	$8C_3$	$6C_2$	$6C_4$	$3C_4^2 \equiv C''_2$	$S_2 \equiv i$	$6S_4$	$8S_6$	$3\sigma_h$	$6\sigma_d$
$\chi^r(R)$	6	0	0	2	2	0	0	0	4	2
$\chi^\alpha(R)$	12	0	2	0	0	0	0	0	4	2

using internal coordinates, however, the character of the representation is simply given by the number of internal coordinates unchanged by each symmetry operation.

If this procedure is made separately for stretching (Δr) and bending ($\Delta\alpha$) coordinates, it is readily seen that

$$\begin{aligned} \chi^r(R) &= \chi_{A_1} + \chi_E \\ \chi^\alpha(R) &= \chi_{A_1} + \chi_E \end{aligned} \tag{1.97}$$

Thus, it is found that both A_1 and E species have one stretching and one bending vibration, respectively. No consideration of the translational and rotational motions is necessary if the internal coordinates are taken as the basis for the representation.

Another example, for an octahedral XY_6 molecule, is given in Table 1.9. Using Eq. 1.74 and the character table in Appendix I, we find that these characters are resolved into.

$$\chi^r(R) = \chi_{A_{1g}} + \chi_{E_g} + \chi_{F_{1u}} \tag{1.98}$$

$$\chi^\alpha(R) = \chi_{A_{1g}} + \chi_{E_g} + \chi_{F_{1u}} + \chi_{F_{2g}} + \chi_{F_{2u}} \tag{1.99}$$

Comparison of this result with that obtained in Sec. 1.8 immediately suggests that three redundant conditions are included in these bending vibrations (one in A_{1g} and one in E_g). Therefore, $\chi^\alpha(R)$ for genuine vibrations becomes

$$\chi^\alpha(R) = \chi_{F_{1u}} + \chi_{F_{2g}} + \chi_{F_{2u}} \tag{1.100}$$

Thus, it is concluded that six stretching and nine bending vibrations are distributed as indicated in Eqs. 1.98 and 1.100, respectively. Although the method given above is simpler than that of Sec. 1.8, caution must be exercised with respect to the bending vibrations whenever redundancy is involved. In such a case, comparison of the results obtained from both methods is useful in finding the species of redundancy.

1.10. SELECTION RULES FOR INFRARED AND RAMAN SPECTRA

According to quantum mechanics [3], the selection rule for the infrared spectrum is determined by the following integral:

$$[\mu]_{v'v''} = \int \psi^*_{v'}(Q_a)\mu\psi_{v''}(Q_a)dQ_a \tag{1.101}$$

Here, μ is the dipole moment in the electronic ground state, ψ is the vibrational eigenfunction given by Eq. 1.21, and v' and v'' are the vibrational quantum numbers before and after the transition, respectively. The activity of the normal vibration whose normal coordinate is Q_a is being determined. By resolving the dipole moment into the three components in the x, y, and z directions, we obtain the result

$$\begin{aligned}
[\mu_x]_{v'v''} &= \int \psi^*_{v'}(Q_a)\mu_x\psi_{v''}(Q_a)dQ_a \\
[\mu_y]_{v'v''} &= \int \psi^*_{v'}(Q_a)\mu_y\psi_{v''}(Q_a)dQ_a \\
[\mu z]_{v'v''} &= \int \psi^*_{v'}(Q_a)\mu_z\psi_{v''}(Q_a)dQ_a
\end{aligned} \tag{1.102}$$

If one of these integrals is not zero, the normal vibration associated with Q_a is infrared-active. If all the integrals are zero, the vibration is infrared-inactive.

Similar to the case of infrared spectrum, the selection rule for the Raman spectrum is determined by the integral

$$[\alpha]_{v'v''} = \int \psi^*_{v'}(Q_a)\alpha\psi_{v''}(Q_a)dQ_a \tag{1.103}$$

As shown in Sec. 1.6, α consists of six components, α_{xx},α_{yy}, α_{zz}, α_{xy}, α_{yz}, and α_{xz}. Thus Eq. 1.103 may be resolved into six components:

$$\begin{aligned}
[\alpha_{xx}]_{v'v''} &= \int \psi^*_{v'}(Q_a)\alpha_{xx}\psi_{v''}(Q_a)\,dQ_a \\
[\alpha_{yy}]_{v'v''} &= \int \psi^*_{v'}(Q_a)\alpha_{yy}\psi_{v''}(Q_a)\,dQ_a \\
&\cdots\cdots\cdots\cdots\cdots\cdots\cdots\cdots
\end{aligned} \tag{1.104}$$

If one of these integrals is not zero, the normal vibration associated with Q_a is Raman-active. If all the integrals are zero, the vibration is Raman-inactive. As shown below, it is possible to determine whether the integrals of Eqs. 1.102 and 1.104 are zero or nonzero from a consideration of symmetry:

1.10.1. Selection Rules for Fundamentals

Let us consider the fundamentals in which transitions occur from $v' = 0$ to $v'' = 1$. It is evident from the form of the vibrational eigenfunction (Eq. 1.22) that $\psi_0(Q_a)$ is invariant under any symmetry operation, whereas the symmetry of $\psi_1(Q_a)$ is the same as that of Q_a. Thus, the integral does not vanish when the symmetry of μ_x, for example, is the same as that of Q_a. If the symmetry properties of μ_x and Q_a differ in even one

symmetry element of the group, the integral becomes zero. In other words, for the integral to be nonzero, Q_a must belong to the same species as μ_x. *More generally, the normal vibration associated with Q_a becomes infrared-active when at least one of the components of the dipole moment belongs to the same species as Q_a.* Similar conclusions are obtained for the Raman spectrum. Namely, *the normal vibration associated with Q_a becomes Raman-active when at least one of the components of the polarizability belongs to the same species as Q_a.*

Since the species of the normal vibration can be determined by the methods described in Sections 1.8 and 1.9, it is necessary only to determine the species of the components of the dipole moment and polarizability of the molecule. This can be done as follows. The components of the dipole moment, μ_x, μ_y, and μ_z, transform as do those of translational motion, T_x, T_y, and T_z, respectively. These were discussed in Sec. 1.8. Thus, the character of the dipole moment is given by Eq. 1.87, which is

$$\boxed{\chi_u(R) = \pm(1 + 2\cos\theta)} \tag{1.105}$$

where + and − have the same meaning as before. In a pyramidal XY_3 molecule, Eq. 1.105 gives

	I	$2C_3$	$3\sigma_v$
$\chi_\mu(R)$	3	0	1

Using Eq. 1.74, we resolve this into $A_1 + E$. It is obvious that μ_z belongs to A_1. Then, μ_x and μ_y must belong to E. In fact, the pair, μ_x and μ_y, transforms as follows:

$$I\begin{bmatrix}\mu_x\\ \mu_y\end{bmatrix} = \begin{bmatrix}1 & 0\\ 0 & 1\end{bmatrix}\begin{bmatrix}\mu_x\\ \mu_y\end{bmatrix}, \qquad C_3^+\begin{bmatrix}\mu_x\\ \mu_y\end{bmatrix} = \begin{bmatrix}-\frac{1}{2} & \frac{\sqrt{3}}{2}\\ -\frac{\sqrt{3}}{2} & -\frac{1}{2}\end{bmatrix}\begin{bmatrix}\mu_x\\ \mu_y\end{bmatrix}$$

$$\chi(I) = 2, \qquad \chi(C_3^+) = -1$$

$$\sigma_1\begin{bmatrix}\mu_x\\ \mu_y\end{bmatrix} = \begin{bmatrix}-1 & 0\\ 0 & 1\end{bmatrix}\begin{bmatrix}\mu_x\\ \mu_y\end{bmatrix}$$

$$\chi(\sigma_1) = 0$$

Thus, it is found that μ_z belongs to A_1 and (μ_x, μ_y) belongs to E.

The character of the representation of the polarizability is given by

$$\boxed{\chi_\alpha(R) = 2\cos\theta(1 + 2\cos\theta)} \tag{1.106}$$

for both proper and improper rotations. This can be derived as follows. The polarizability in the x, y, and z directions is related to that in X, Y, and Z coordinates by

$$\begin{bmatrix} \alpha_{XX} & \alpha_{XY} & \alpha_{XZ} \\ \alpha_{YX} & \alpha_{YY} & \alpha_{YZ} \\ \alpha_{ZX} & \alpha_{ZY} & \alpha_{ZZ} \end{bmatrix} = \begin{bmatrix} C_{Xx} & C_{Xy} & C_{Xz} \\ C_{Yx} & C_{Yy} & C_{Yz} \\ C_{Zx} & C_{Zy} & C_{Zz} \end{bmatrix} \begin{bmatrix} \alpha_{xx} & \alpha_{xy} & \alpha_{xz} \\ \alpha_{yx} & \alpha_{yy} & \alpha_{yz} \\ \alpha_{zx} & \alpha_{zy} & \alpha_{zz} \end{bmatrix} \begin{bmatrix} C_{Xx} & C_{Yx} & C_{Zx} \\ C_{Xy} & C_{Yy} & C_{Zy} \\ C_{Xz} & C_{Yz} & C_{Zz} \end{bmatrix}$$

where CX_x, CX_y, and so forth denote the direction cosines between the two axes subscripted. If a rotation through θ around the Z axis superimposes the X, Y, and Z axes on the x, y, and z axes, the preceding relation becomes

$$C_\theta \begin{bmatrix} \alpha_{xx} & \alpha_{xy} & \alpha_{xz} \\ \alpha_{yx} & \alpha_{yy} & \alpha_{yz} \\ \alpha_{zx} & \alpha_{zy} & \alpha_{zz} \end{bmatrix} = \begin{bmatrix} \cos\theta & \sin\theta & 0 \\ -\sin\theta & \cos\theta & 0 \\ 0 & 0 & 1 \end{bmatrix} \begin{bmatrix} \alpha_{xx} & \alpha_{xy} & \alpha_{xz} \\ \alpha_{yx} & \alpha_{yy} & \alpha_{yz} \\ \alpha_{zx} & \alpha_{zy} & \alpha_{zz} \end{bmatrix} \begin{bmatrix} \cos\theta & -\sin\theta & 0 \\ \sin\theta & \cos\theta & 0 \\ 0 & 0 & 1 \end{bmatrix}$$

This can be written as

$$C_\theta \begin{bmatrix} \alpha_{xx} \\ \alpha_{yy} \\ \alpha_{zz} \\ \alpha_{xy} \\ \alpha_{xz} \\ \alpha_{yz} \end{bmatrix} = \begin{bmatrix} \cos^2\theta & \sin^2\theta & 0 & 2\sin\theta\cos\theta & 0 & 0 \\ \sin^2\theta & \cos^2\theta & 0 & -2\sin\theta\cos\theta & 0 & 0 \\ 0 & 0 & 1 & 0 & 0 & 0 \\ -\sin\theta\cos\theta & \sin\theta\cos\theta & 0 & 2\cos^2\theta - 1 & 0 & 0 \\ 0 & 0 & 0 & 0 & \cos\theta & \sin\theta \\ 0 & 0 & 0 & 0 & -\sin\theta & \cos\theta \end{bmatrix} \cdot \begin{bmatrix} \alpha_{xx} \\ \alpha_{yy} \\ \alpha_{zz} \\ \alpha_{xy} \\ \alpha_{xz} \\ \alpha_{yz} \end{bmatrix}$$

Thus, the character of this representation is given by Eq. 1.106. The same results are obtained for improper rotations if they are regarded as the product $i \times$ (proper rotation). For a pyramidal XY_3 molecule, Eq. 1.106 gives

	I	$2C_3$	$3\sigma_v$
$\chi_\alpha(R)$	6	0	2

Using Eq. 1.74, this is resolved into $2A_1 + 2E$. Again, it is immediately seen that* the component α_{zz} belongs to A_1, and the pair a_{zx} and a_{zy} belongs to E since

$$\begin{bmatrix} zx \\ zy \end{bmatrix} = z \begin{bmatrix} x \\ y \end{bmatrix} = A_1 \times E = E$$

It is more convenient to consider the components $\alpha_{xx} + \alpha_{yy}$ and $\alpha_{xx} - \alpha_{yy}$ than α_{xx} and α_{yy}. If a vector of unit length is considered, the relation

$$x^2 + y^2 + z^2 = 1$$

holds. Since α_{zz} belongs to A_1, $\alpha_{xx} + \alpha_{yy}$ must belong to A_1. Then, the pair $\alpha_{xx} - \alpha_{yy}$ and α_{xy} must belong to E. As a result, the character table of the point group $\mathbf{C}_{3v}$, is completed as in Table 1.10. Thus, it is concluded that, in the point group $\mathbf{C}_{3v}$ both the A_1 and the E vibrations are infrared- as well as Raman-active, while the A_2 vibrations are inactive.

Complete character tables like Table 1.10 have already been worked out for all the point groups. Therefore, no elaborate treatment such as that described in this section is necessary in practice. Appendix I gives complete character tables for the point groups that appear frequently in this book. From these tables, the selection rules for the infrared and Raman spectra are obtained immediately: *The vibration is infrared- or Raman-active if it belongs to the same species as one of the components of the dipole moment or polarizability, respectively.* For example, the character table of the point group $\mathbf{O}_h$ signifies immediately that only the F_{1u} vibrations are infrared-active and only the A_{1g}, E_g, and F_{2g} vibrations are Raman-active, for the components of the dipole moment or the polarizability belong to these species in this point group. It is to be noted in these character tables that (1) a totally symmetric vibration is Raman-active in any

*The quantum mechanical expression of the polarizability [77] is

$$\alpha_{xx} = \frac{2}{3h} \sum_j \frac{(\mu_x)_{j0}^2 \nu_{j0}^2}{\nu_{j0}^2 - \nu^2}$$

$$\alpha_{xy} = \frac{2}{3h} \sum_j \frac{(\mu_x)_{j0}(\mu_y)_{j0} \nu_{j0}^2}{\nu_{j0}^2 - \nu^2} \quad \text{etc.}$$

Here, $(\mu_x)j_0$, for example, is the induced dipole moment along the x axis caused by the 0 (ground state) $\rightarrow j$ (excited state) electronic transition, ν_{j0} is the frequency of the $0 \rightarrow j$ transition, and ν is the exciting frequency. Thus, it is readily seen that the character of the polarizability components such as α_{xx} and α_{xy} is determined by considering the product of the characters of dipole moments such as μ_x and μ_y.

TABLE 1.10. Character Table of the Point Group C_{3v}

C_{3v}	I	$2C_3$	$3\sigma_v$		
A_1	+1	+1	+1	μ_z	$\alpha_{xx}+\alpha_{yy}$, α_{zz}
A_2	+1	+1	−1		
E	+2	−1	0	(μ_x, μ_y)[a]	$(\alpha_{xz}, \alpha_{yz})$,[a] $(\alpha_{xx}-\alpha_{yy}, \alpha_{xy})$[a]

[a] A doubly degenerate pair is represented by two terms in parentheses.

point group, and (2) the infrared- and Raman-active vibrations always belong to u and g types, respectively, in point groups having a center of symmetry.

1.10.2. Selection Rules for Combination and Overtone Bands

As stated in Sec. 1.3, some combination and overtone bands appear weakly because actual vibrations are not harmonic and some of these nonfundamentals are allowed by symmetry selection rules.

Selection rules for combination bands ($v_i \pm v_j$) can be derived from the characters of the *direct products* of those of individual vibrations. Thus, we obtain

$$\chi_{ij}(R) = \chi_i(R) \times \chi_j(R) \tag{1.107}$$

As an example, consider a molecule of $\mathbf{C}_{3v}$ symmetry. It is readily seen that

		$\boldsymbol{I}$	$2\boldsymbol{C}_3$	$3\sigma_v$
	$\chi_{A_1}(\boldsymbol{R})$	1	1	1
×	$\chi_E(\boldsymbol{R})$	2	−1	0
	$\chi_{A_1\times E}(\boldsymbol{R})$	2	−1	0

$$\chi_{A_1\times E}(\boldsymbol{R}) = \chi_E(\boldsymbol{R})$$

Thus, a combination band between the A_1 and E vibrations is IR- as well as Raman-active. The activity of a combination band between two E vibrations can be determined by considering the direct product of their characters:

		$\boldsymbol{I}$	$2\boldsymbol{C}_3$	$3\sigma_v$
	$\chi_E(\boldsymbol{R})$	2	−1	0
×	$\chi_E(\boldsymbol{R})$	2	−1	0
	$\chi_{E\times E}(\boldsymbol{R})$	4	1	0

Using Eq. 1.74, this set of the characters can be resolved into

$$\chi_{E\times E}(\boldsymbol{R}) = \chi_{A_1}(\boldsymbol{R}) + \chi_{A_2}(\boldsymbol{R}) + \chi_E(\boldsymbol{R})$$

Since both A_1 and E species are IR- and Raman-active, a combination band between two E vibrations is also IR- and Raman-active. It is convenient to apply the general rules of Appendix IV in determining the symmetry species of direct products.

Selection rules for overtones of nondegenerate vibrations can be obtained using the following relation:

$$\chi^n(\boldsymbol{R}) = [\chi(\boldsymbol{R})]^n \tag{1.108}$$

Here, $\chi^n(\boldsymbol{R})$ is the character of the $(n-1)$th overtone ($n=2$ for the first overtone). As an example, consider a molecule of $\mathbf{C}_{3v}$ symmetry. The character of the first overtone of the A_2 fundamental is calculated as follows:

		$\boldsymbol{I}$	$2\boldsymbol{C}_3$	$3\sigma_v$
	$\chi_{A_2}(\boldsymbol{R})$	1	1	−1
×	$\chi_{A_2}(\boldsymbol{R})$	1	1	−1
	$\chi^2_{A_2}(\boldsymbol{R})$	1	1	1

Namely, it is IR- as well as Raman-active because $\chi^2_{A_2}(\boldsymbol{R}) = \chi_{A_1}(\boldsymbol{R})$. However, the second overtone of the A_2 fundamental is IR- as well as Raman-inactive because $\chi^3_{A_2}(\boldsymbol{R}) = \chi^2_{A_2}(\boldsymbol{R}) \times \chi A_2(\boldsymbol{R}) = \chi_{A_2}(\boldsymbol{R})$ (inactive). In general, odd overtones (A_1) are IR- and Raman-active, whereas even overtones (A_2) are inactive. It is obvious that all the overtones of the A_1 fundamental are IR- and Raman-active.

Selection rules for overtones of doubly degenerate vibrations (E species) are determined by

$$\chi^n_E(\boldsymbol{R}) = \tfrac{1}{2}\left[\chi^{n-1}_E(\boldsymbol{R}) \cdot \chi_E(\boldsymbol{R}) + \chi_E(\boldsymbol{R}^n)\right] \tag{1.109}$$

For the first overtone, this is written as

$$\chi^2_E(\boldsymbol{R}) = \tfrac{1}{2}\left[\{\chi_E(R)\}^2 + \chi_E(R^2)\right]$$

Here, $\chi_E(R^2)$ is the character that corresponds to the operation R performed twice successively. Thus, one obtains

$$\chi_E(I^2) = \chi_E(I) = 2$$
$$\chi_E[(C_3^+)^2] = \chi_E(C_3^-) = -1$$
$$\chi_E[(\sigma_v)^2] = \chi_E(I) = 2$$

Therefore, $\chi^2_E(R)$ can be calculated as follows:

		$\boldsymbol{I}$	$2\boldsymbol{C}_3$	$3\sigma_v$
	$\chi_E(\boldsymbol{R})$	2	−1	0
×	$\chi_E(\boldsymbol{R})$	2	−1	0
	$\{\chi_E(\boldsymbol{R})\}^2$	4	1	0
+	$\chi_E(\boldsymbol{R}^2)$	2	−1	2
	$\{\chi_E(\boldsymbol{R})\}^2+\chi_E(\boldsymbol{R}^2)$	6	0	2
÷2	$\chi^2_E(\boldsymbol{R})$	3	0	1

$$\chi^2_E(\boldsymbol{R}) = \chi_{A_1}(\boldsymbol{R}) + \chi_{\boldsymbol{E}}(\boldsymbol{R})$$

Thus, the first overtone of the doubly degenerate vibration is IR- and Raman-active. The characters of overtones for triply degenerate vibrations are given by

$$\chi_F^n(\boldsymbol{R}) = \tfrac{1}{3}\{2\chi_F(\boldsymbol{R})\chi_F^{n-1}(\boldsymbol{R}) - \tfrac{1}{2}\chi_F^{n-2}(\boldsymbol{R})[\chi_F(\boldsymbol{R})]^2 + \tfrac{1}{2}\chi_F(\boldsymbol{R}^2)\chi_F^{n-2}(\boldsymbol{R}) + \chi_F(\boldsymbol{R}^n)\} \tag{1.110}$$

For more details, see Refs. [3,5], and [9].

1.11. STRUCTURE DETERMINATION

Suppose that a molecule has several probable structures, each of which belongs to a different point group. Then the number of infrared- and Raman-active fundamentals should be different for each structure. Therefore, the most probable model can be selected by comparing the observed number of infrared- and Raman-active fundamentals with that predicted theoretically for each model.

Consider the XeF_4 molecule as an example. It may be tetrahedral or square-planar. By use of the methods described in the preceding sections, the number of infrared- or Raman-active fundamentals can be found easily for each structure. Tables 1.11a and 1.11b summarize the results. It is seen that the distinction of these two structures can be made by comparing the number of IR- and Raman-active FXeF bending modes; the tetrahedral structure predicts one IR and two Raman bands, whereas the square–planar structure predicts two IR and one Raman bands. In general, the XeF stretching vibrations appear above 500 cm^{-1}, whereas the FXeF bending vibrations are observed below 300 cm^{-1}. The IR and Raman spectra of XeF_4 are shown in Fig. 2.17. The IR spectrum exhibits two bending bands at 291 and 123 cm^{-1}, whereas the Raman

TABLE 1.11a. Number of Fundamentals for Tetrahedral XeF_4

T_d	Activity[a]	Number of Fundamentals	XeF Stretching	FXeF Bending
A_1	R (*p*)	1	1	0
A_2	ia	0	0	0
E	R (*dp*)	1	0	1
F_1	ia	0	0	0
F_2	IR, R (*dp*)	2	1	1
Total	IR	2	1	1
	R	4	2	2

[a] *p*, polarized; *dp*, depolarized (see Sec. 1.20).

TABLE 1.11b. Number of Fundamentals for Square-Planar XeF_4

D_{4h}	Activity	Number of Fundamentals	XeF Stretching	FXeF Bending
A_{1g}	R (*p*)	1	1	0
A_{1u}	ia	0	0	0
A_{2g}	ia	0	0	0
A_{2u}	IR	1	0	1
B_{1g}	R (*dp*)	1	1	0
B_{1u}	ia	0	0	0
B_{2g}	R (*dp*)	1	0	1
B_{2u}	ia	1	0	1
E_g	R (*dp*)	0	0	0
E_u	IR	2	1	1
Total	IR	3	1	2
	R	3	2	1

spectrum shows one bending vibration at 218 cm^{-1}. Thus, the square–planar structure is preferable to the tetrahedral structure.*

Another example is given by the XeF_5^- ion, which has the three possible structures shown in Fig. 1.21. The results of vibrational analysis for each are summarized in Table 1.12. It is seen that the numbers of IR-active vibrations are 5, 6, and 3 and those of Raman-active vibrations are 6, 9, and 3, respectively, for the $\mathbf{D}_{3h}$, $\mathbf{C}_{4v}$, and $\mathbf{D}_{5h}$ structures, As discussed in Sec. 2.7.3, the XeF_5^- ion exhibits three IR bands (550–400, 290, and 274 cm^{-1}) and three Raman bands (502, 423, and 377 cm^{-1}). Thus, a pentagonal planar structure is preferable to the other two structures. The somewhat unusual structures thus obtained for XeF_4 and XeF_5^- can be rationalized by the use of the valence shell electron-pair repulsion (VSEPR) theory (Sec. 2.6.3).

This rather simple method has been used widely for the elucidation of molecular structure of inorganic and coordination compounds. In Chapter 2, the number of IR- and Raman-active vibrations is compared for possible structures of XY_n and other

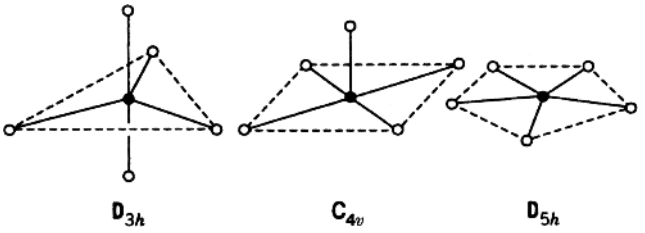

Fig. 1.21. *Three possible structures for the* XeF_5^- *ion.*

*This conclusion may be drawn directly from observation of the mutual exclusion rule, which holds for $\mathbf{D}_{4h}$ but not for $\mathbf{T}_d$.

TABLE 1.12. Number of IR- and Raman-Active Fundamentals for Three Possible Structures of the XeF_5^- Anion

Type	D_{3h}	C_{4v}	D_{5h}
IR	$2A''_2 + 3E'$	$3A_1 + 3E$	$A''_2 + 2E'_1$
Raman	$2A'_1 + 3E' + E''$	$3A_1 + 2B_1 + B_2 + 3E$	$A'_1 + 2E'_2$

molecules. Appendix V lists the number of IR- and Raman-active vibrations of MX_nY_m-type molecules. It should be noted, however, that this method does not give a clear-cut answer if the predicted numbers of infrared- and Raman-active fundamentals are similar for various probable structures. Furthermore, a practical difficulty arises in determining the number of fundamentals from the observed spectrum, since the intensities of overtone and combination bands are sometimes comparable to those of fundamentals when they appear as satellite bands of the fundamental. This is particularly true when overtone and combination bands are enhanced anomalously by *Fermi resonance* (accidental degeneracy). For example, the frequency of the first overtone of the v_2 vibration of CO_2 (667 cm^{-1}) is very close to that of the v_1 vibration (1337 cm^{-1}). Since these two vibrations belong to the same symmetry species ($\sum_g^+$), they interact with each other and give rise to two strong Raman lines at 1388 and 1286 cm^{-1}. Fermi resonances similar to the resonance observed for CO_2 may occur for a number of other molecules. It is to be noted also that the number of observed bands depends on the resolving power of the instrument used. Finally, the molecular symmetry in the isolated state is not necessarily the same as that in the crystalline state (Sec. 1.27). Therefore, this method must be applied with caution to spectra obtained for compounds in the crystalline state.

1.12. PRINCIPLE OF THE GF MATRIX METHOD*

As described in Sec. 1.4, the frequency of the normal vibration is determined by the kinetic and potential energies of the system. The kinetic energy is determined by the masses of the individual atoms and their geometrical arrangement in the molecule. On the other hand, the potential energy arises from interaction between the individual atoms and is described in terms of the force constants. Since the potential energy provides valuable information about the nature of interatomic forces, it is highly desirable to obtain the force constants from the observed frequencies. This is usually done by calculating the frequencies, assuming a suitable set of force constants. If the agreement between the calculated and observed frequencies is satisfactory, this particular set of the force constants is adopted as a representation of the potential energy of the system.

* For details, see Ref. 3. The term "normal coordinate analysis" is almost synonymous with the **GF** matrix method, since most of the normal coordinate calculations are carried out by using this method.

To calculate the vibrational frequencies, it is necessary first to express both the potential and the kinetic energies in terms of some common coordinates (Sec. 1.4). Internal coordinates (Sec. 1.9) are more suitable for this purpose than rectangular coordinates, since (1) force constants expressed in terms of internal coordinates have clearer physical meanings than those expressed in terms of rectangular coordinates, and (2) a set of internal coordinates does not involve translational and rotational motion of the molecule as a whole.

Using the internal coordinates R_i we write the potential energy as

$$2V = \tilde{\mathbf{R}}\mathbf{F}\mathbf{R} \tag{1.111}$$

For a bent Y_1XY_2 molecule such as that in Fig. 1.20b, $\mathbf{R}$ is a column matrix of the form

$$\mathbf{R} = \begin{bmatrix} \Delta r_1 \\ \Delta r_2 \\ \Delta\alpha \end{bmatrix}$$

$\tilde{\mathbf{R}}$ is its transpose:

$$\tilde{\mathbf{R}} = [\Delta r_1 \quad \Delta r_2 \quad \Delta\alpha]$$

and $\mathbf{F}$ is a matrix whose components are the force constants

$$\mathbf{F} = \begin{bmatrix} f_{11} & f_{12} & r_1 f_{13} \\ f_{21} & f_{22} & r_2 f_{23} \\ r_1 f_{31} & r_2 f_{32} & r_1 r_2 f_{33} \end{bmatrix} \equiv \begin{bmatrix} F_{11} & F_{12} & F_{13} \\ F_{21} & F_{22} & F_{23} \\ F_{31} & F_{32} & F_{33} \end{bmatrix} \tag{1.112}*$$

Here r_1 and r_2 are the equilibrium lengths of the $X-Y_1$ and $X-Y_2$ bonds, respectively.

The kinetic energy is not easily expressed in terms of the same internal coordinates. Wilson [78] has shown, however, that the kinetic energy can be written as

$$2T = \dot{\tilde{\mathbf{R}}}\mathbf{G}^{-1}\dot{\mathbf{R}} \tag{1.113}^{\dagger}$$

where $\mathbf{G}^{-1}$ is the reciprocal of the $\mathbf{G}$ matrix, which will be defined later. If Eqs. 1.111 and 1.113 are combined with Lagrange's equation

$$\frac{d}{dt}\left(\frac{\partial T}{\partial \dot{R}_k}\right) + \frac{\partial V}{\partial R_k} = 0 \tag{1.36}$$

---

*Here f_{11} and f_{22} are the stretching force constants of the $X-Y_1$ and $X-Y_2$ bonds, respectively, and f_{33} is the bending force constant of the Y_1XY_2 angle. The other symbols represent interaction force constants between stretching and stretching or between stretching and bending vibrations. To make the dimensions of all the force constants the same, f_{13} (or f_{31}), f_{23} (or f_{32}), and f_{33} are multiplied by r_1, r_2, and $r_1 r_2$, respectively.

†Appendix VI gives the derivation of Eq. 1.113.

the following secular equation, which is similar to Eq. 1.49, is obtained:

$$\begin{vmatrix} F_{11} - (G^{-1})_{11}\lambda & F_{12} - (G^{-1})_{12}\lambda & \cdots \\ F_{21} - (G^{-1})_{21}\lambda & F_{22} - (G^{-1})_{22}\lambda & \cdots \\ \vdots & \vdots & \end{vmatrix} \equiv |\mathbf{F} - \mathbf{G}^{-1}\lambda| = 0 \tag{1.114}$$

By multiplying by the determinant of **G**

$$\begin{vmatrix} G_{11} & G_{12} & \cdots \\ G_{21} & G_{22} & \cdots \\ \vdots & \vdots & \end{vmatrix} \equiv |\mathbf{G}| \tag{1.115}$$

from the left-hand side of Eq. 1.114, the following equation is obtained:

$$\begin{vmatrix} \sum G_{1t}F_{t1} - \lambda & \sum G_{1t}F_{t2} & \cdots \\ \sum G_{2t}F_{t1} & \sum G_{2t}F_{t2} - \lambda & \cdots \\ \vdots & \vdots & \end{vmatrix} \equiv |\mathbf{GF} - \mathbf{E}\lambda| = 0 \tag{1.116}$$

Here, **E** is the unit matrix, and λ is related to the wavenumber $\tilde{\nu}$ by the relation $\lambda = 4\pi^2 c^2 \tilde{\nu}^2$.* The order of the equation is equal to the number of internal coordinates used.

The **F** matrix can be written by assuming a suitable set of force constants. If the **G** matrix is constructed by the following method, the vibrational frequencies are obtained by solving Eq. 1.116. The **G** matrix is defined as

$$\mathbf{G} = \mathbf{B}\mathbf{M}^{-1}\tilde{\mathbf{B}} \tag{1.117}$$

Here $\mathbf{M}^{-1}$ is a diagonal matrix whose components are μ_i, where μ_i is the reciprocal of the mass of the *i*th atom. For a bent XY_2 molecule, we obtain

$$\mathbf{M}^{-1} = \begin{bmatrix} \mu_1 & & & & \\ & \mu_1 & & & 0 \\ & & \mu_1 & & \\ & & & \ddots & \\ 0 & & & & \mu_3 \end{bmatrix}$$

where μ_3 and μ_1 are the reciprocals of the masses of the X and Y atoms, respectively. The **B** matrix is defined as

$$\mathbf{R} = \mathbf{B}\mathbf{X} \tag{1.118}$$

where **R** and **X** are column matrices whose components are the internal and rectangular coordinates, respectively.

*Here λ should not be confused with λ_w (wavelength).

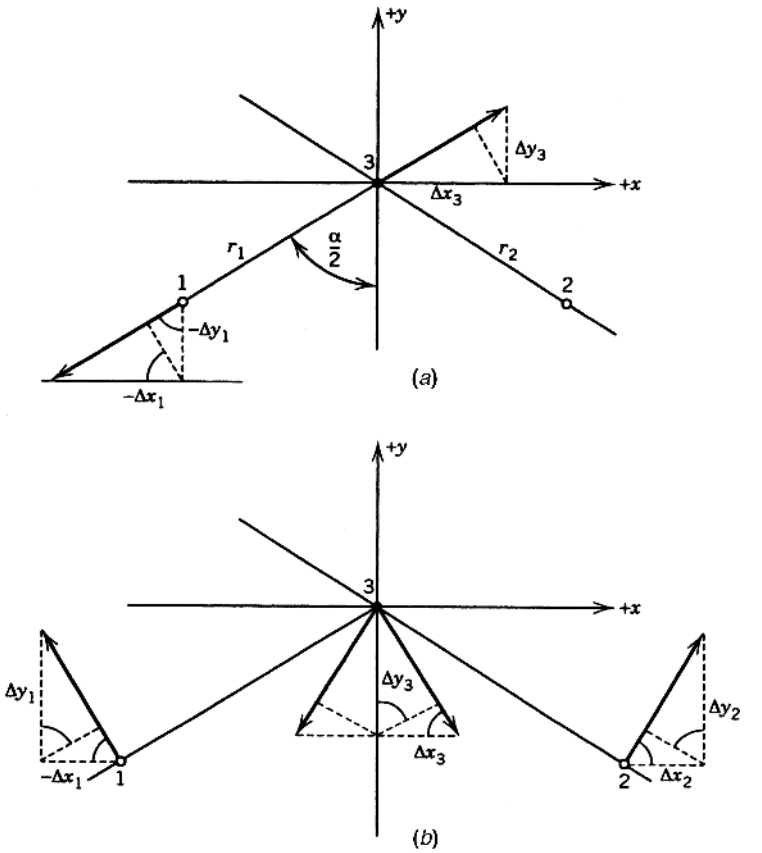

Fig. 1.22. *Relationship between internal and rectangular coordinates in (a) stretching and (b) bending vibrations of a bent XY_2 molecule.*

To write Eq. 1.118 for a bent XY_2 molecule, we express the bond stretching (Δr_1) in terms of the x and y coordinates shown in Fig. 1.22a. It is readily seen that

$$\Delta r_1 = -(\Delta x_1)(s) - (\Delta y_1)(c) + (\Delta x_3)(s) + (\Delta y_3)(c)$$

Here, $s = \sin(\alpha/2)$, $c = \cos(\alpha/2)$, and r is the equilibrium distance between the X and Y atoms. A similar expression is obtained for Δr_2. Thus

$$\Delta r_2 = (\Delta x_2)(s) - (\Delta y_2)(c) - (\Delta x_3)(s) + (\Delta y_3)(c)$$

For the bond bending ($\Delta\alpha$), consider the relationships illustrated in Fig. 1.22b. It is readily seen that

$$r(\Delta\alpha) = -(\Delta x_1)(c) + (\Delta y_1)(s) + (\Delta x_2)(c) + (\Delta y_2)(s) - 2(\Delta y_3)(s)$$

If these equations are summarized in a matrix form, we obtain

$$\begin{bmatrix} \Delta r_1 \\ \Delta r_2 \\ \Delta\alpha \end{bmatrix} = \left[\begin{array}{ccc|ccc|ccc} -s & -c & 0 & 0 & 0 & 0 & s & c & 0 \\ 0 & 0 & 0 & s & -c & 0 & -s & c & 0 \\ -c/r & s/r & 0 & c/r & s/r & 0 & 0 & -2s/r & 0 \end{array}\right] \left[\begin{array}{c} \Delta x_1 \\ \Delta y_1 \\ \Delta z_1 \\ \hline \Delta x_2 \\ \Delta y_2 \\ \Delta z_2 \\ \hline \Delta x_3 \\ \Delta y_3 \\ \Delta z_3 \end{array}\right] \tag{1.119}$$

If unit vectors such as those in Fig. 1.23 are considered, Eq. 1.119 can be written in a more compact form using vector notationr:

$$\begin{bmatrix} \Delta r_1 \\ \Delta r_2 \\ \Delta\alpha \end{bmatrix} = \begin{bmatrix} \mathbf{e}_{31} & 0 & -\mathbf{e}_{31} \\ 0 & \mathbf{e}_{32} & -\mathbf{e}_{32} \\ \mathbf{p}_{31}/r & \mathbf{p}_{32}/r & -(\mathbf{p}_{31}+\mathbf{p}_{32})/r \end{bmatrix} \begin{bmatrix} \boldsymbol{\rho}_1 \\ \boldsymbol{\rho}_2 \\ \boldsymbol{\rho}_3 \end{bmatrix} \tag{1.120}$$

Here $\boldsymbol{\rho}_1$, $\boldsymbol{\rho}_2$, and $\boldsymbol{\rho}_3$ are the displacement vectors of atoms 1, 2, and 3, respectively. Thus Eq. 1.120 can be written simply as

$$\mathbf{R} = \mathbf{S} \cdot \boldsymbol{\rho} \tag{1.121}$$

where the dot represents the scalar product of the two vectors. Here **S** is called the **S** matrix, and its components (**S** vector) can be written according to the following formulas: (1) bond stretching

$$\Delta r_1 = \Delta_{31} = \mathbf{e}_{31} \cdot \boldsymbol{\rho}_1 - \mathbf{e}_{31} \cdot \boldsymbol{\rho}_3 \tag{1.122}$$

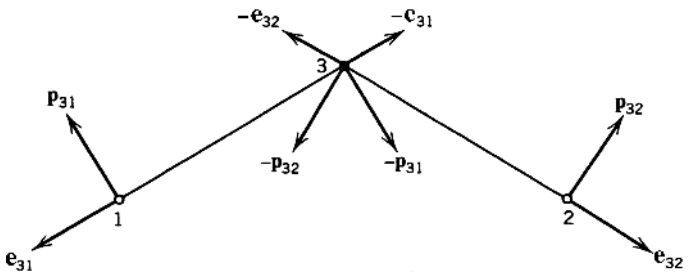

Fig. 1.23. *Unit vectors in a bent XY_2 molecule.*

and (2) angle bending:

$$\Delta\alpha = \Delta\alpha_{132} = \frac{\mathbf{p}_{31}\cdot\boldsymbol{\rho}_1 + \mathbf{p}_{32}\cdot\boldsymbol{\rho}_2 - (\mathbf{p}_{31}+\mathbf{p}_{32})\cdot\boldsymbol{\rho}_3}{r} \tag{1.123}$$

It is seen that the **S** vector is oriented in the direction in which a given displacement of the *i*th atom will produce the greatest increase in Δr or $\Delta\alpha$. Formulas for obtaining the **S** vectors of other internal coordinates such as those of out-of-plane ($\Delta\theta$) and torsional ($\Delta\tau$) vibrations are also available [3].

By using the **S** matrix, Eq. 1.117 is written as

$$\mathbf{G} = \mathbf{S}\mathbf{m}^{-1}\tilde{\mathbf{S}} \tag{1.124}$$

For a bent XY_2 molecule, this becomes

$$\mathbf{G} = \begin{bmatrix} \mathbf{e}_{31} & 0 & -\mathbf{e}_{31} \\ 0 & \mathbf{e}_{32} & -\mathbf{e}_{32} \\ \mathbf{p}_{31}/r & \mathbf{p}_{32}/r & -(\mathbf{p}_{31}+\mathbf{p}_{32})/r \end{bmatrix} \begin{bmatrix} \mu_1 & 0 & 0 \\ 0 & \mu_1 & 0 \\ 0 & 0 & \mu_3 \end{bmatrix}$$

$$\times \begin{bmatrix} \mathbf{e}_{31} & 0 & \mathbf{p}_{31}/r \\ 0 & \mathbf{e}_{32} & \mathbf{p}_{32}/r \\ -\mathbf{e}_{31} & -\mathbf{e}_{32} & -(\mathbf{p}_{31}+\mathbf{p}_{32})/r \end{bmatrix}$$

$$= \begin{bmatrix} (\mu_3+\mu_1)\mathbf{e}_{31}^2 & \mu_3\mathbf{e}_{31}\cdot\mathbf{e}_{32} & \frac{\mu_1}{r}\mathbf{e}_{31}\cdot\mathbf{p}_{31} + \frac{\mu_3}{r}\mathbf{e}_{31}\cdot(\mathbf{p}_{31}+\mathbf{p}_{32}) \\ & (\mu_3\mu_1)\mathbf{e}_{32}^2 & \frac{\mu_1}{r}\mathbf{e}_{32}\cdot\mathbf{p}_{32} + \frac{\mu_3}{r}\mathbf{e}_{32}\cdot(\mathbf{p}_{31}+\mathbf{p}_{32}) \\ & & \frac{\mu_1}{r^2}\mathbf{p}_{31}^2 + \frac{\mu_1}{r^2}\mathbf{p}_{32}^2 + \frac{\mu_3}{r^2}(\mathbf{p}_{31}+\mathbf{p}_{32})^2 \end{bmatrix}$$

Considering

$$\mathbf{e}_{31}\cdot\mathbf{e}_{31} = \mathbf{e}_{32}\cdot\mathbf{e}_{32} = \mathbf{p}_{31}\cdot\mathbf{p}_{31} = \mathbf{p}_{32}\cdot\mathbf{p}_{32} = 1, \qquad \mathbf{e}_{31}\cdot\mathbf{p}_{31} = \mathrm{e}_{32}\cdot\mathbf{p}_{32} = 0$$

$$\mathbf{e}_{31}\cdot\mathbf{e}_{32} = \cos\alpha, \qquad \mathbf{e}_{31}\cdot\mathbf{p}_{32} = \mathbf{e}_{32}\cdot\mathbf{p}_{31} = -\sin\alpha$$

$$(\mathbf{p}_{31}+\mathbf{p}_{32})^2 = 2(1-\cos\alpha)$$

we find that the **G** matrix is calculated as follows:

$$\mathbf{G} = \begin{bmatrix} \mu_3+\mu_1 & \mu_3\cos\alpha & -\frac{\mu_3}{r}\sin\alpha \\ & \mu_3+\mu_1 & -\frac{\mu_3}{r}\sin\alpha \\ & & \frac{2\mu_1}{r^2} + \frac{2\mu_3}{r^2}(1-\cos\alpha) \end{bmatrix} \tag{1.125}$$

If the **G**-matrix elements obtained are written for each combination of internal coordinates, there results

$$
\begin{aligned}
G(\Delta r_1, \Delta r_1) &= \mu_3 + \mu_1 \\
G(\Delta r_2, \Delta r_2) &= \mu_3 + \mu_1 \\
G(\Delta r_1, \Delta r_2) &= \mu_3 \cos\alpha \\
G(\Delta\alpha, \Delta\alpha) &= \frac{2\mu_1}{r^2} + \frac{2\mu_3}{r^2}(1 - \cos\alpha) \\
G(\Delta r_1, \Delta\alpha) &= -\frac{\mu_3}{r}\sin\alpha \\
G(\Delta r_2, \Delta\alpha) &= -\frac{\mu_3}{r}\sin\alpha
\end{aligned}
\tag{1.126}
$$

If such calculations are made for several types of molecules, it is immediately seen that the **G**-matrix elements themselves have many regularities. Decius [79] developed general formulas for writing **G**-matrix elements.* Some of them are as follows:

$G^2_{rr} = \mu_1 + \mu_2$

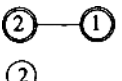

$G^1_{rr} = \mu_1 \cos\phi$

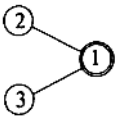

$G^2_{r\phi} = -\rho_{23}\mu_2 \sin\phi$

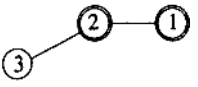

$$G^1_{r\phi}\begin{pmatrix}1\\1\end{pmatrix} = -(\rho_{13}\sin\phi_{213}\cos\psi_{234} + \rho_{14}\sin\phi_{214}\cos\psi_{243})\mu_1$$

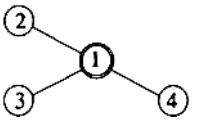

$$G^3_{\phi\phi} = \rho^2_{12}\mu_1 + \rho^2_{23}\mu_3 + (\rho^2_{12} + \rho^2_{23} - 2\rho_{12}\rho_{23}\cos\phi)\mu_2$$

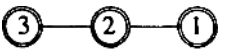

$$
\begin{aligned}
G^2_{\phi\phi}\begin{pmatrix}1\\1\end{pmatrix} = {} & (\rho^2_{12}\cos\psi_{314})\mu_1 + [\rho_{12} - \rho_{23}\cos\phi_{123} \\
& -\rho_{24}\cos\phi_{124})\rho_{12}\cos\psi_{314} \\
& +(\sin\phi_{123}\sin\phi_{124}\sin^2\psi_{314} \\
& +\cos\phi_{324}\cos\psi_{314})\rho_{23}\rho_{24}]\mu_2
\end{aligned}
$$

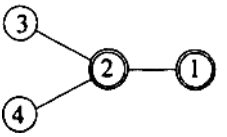

*See also Refs. 3 and 80.

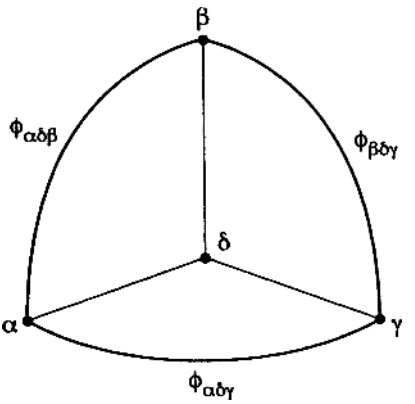

Fig. 1.24. *Spherical angles involving atomic positions,* α, β, γ, and δ.

Here, the atoms surrounded by a bold line circle are those common to both coordinates. The symbols μ and ρ denote the reciprocals of mass and bond distance, respectively. The spherical angle $\psi_{\alpha\beta\gamma}$ in Fig. 1.24 is defined as

$$\cos\psi_{\alpha\beta\gamma} = \frac{\cos\phi_{\alpha\delta\gamma} - \cos\phi_{\alpha\delta\beta}\cos\phi_{\beta\delta\gamma}}{\sin\phi_{\alpha\delta\beta}\sin\phi_{\beta\delta\gamma}} \tag{1.127}$$

The correspondence between the Decius formulas and the results obtained in Eq. 1.126 is evident.

With the Decius formulas, the **G**-matrix elements of a pyramidal XY_3 molecule have been calculated and are shown in Table 1.13.

1.13. UTILIZATION OF SYMMETRY PROPERTIES

In view of the equivalence of the two X−Y bonds of a bent XY_2 molecule, the **F** and **G** matrices obtained in Eqs. 1.112 and 1.125 are written as

$$\mathbf{F} = \begin{bmatrix} f_{11} & f_{12} & rf_{13} \\ f_{12} & f_{11} & rf_{13} \\ rf_{13} & rf_{13} & r^2 f_{33} \end{bmatrix} \tag{1.128}$$

$$\mathbf{G} = \begin{bmatrix} \mu_3 + \mu_1 & \mu_3\cos\alpha & -\dfrac{\mu_3}{r}\sin\alpha \\ \mu_3\cos\alpha & \mu_3 + \mu_1 & -\dfrac{\mu_3}{r}\sin\alpha \\ -\dfrac{\mu_3}{r}\sin\alpha & -\dfrac{\mu_3}{r}\sin\alpha & \dfrac{2\mu_1}{r^2} + \dfrac{2\mu_3}{r^2}(1-\cos\alpha) \end{bmatrix} \tag{1.129}$$

TABLE 1.13.

	Δr_1	Δr_2	Δr_3	$\Delta\alpha_{23}$	$\Delta\alpha_{31}$	$\Delta\alpha_{12}$
Δr_1	A	B	B	C	D	D
Δr_2	—	A	B	D	C	D
Δr_3	—	—	A	D	D	C
$\Delta\alpha_{23}$	—	—	—	E	F	F
$\Delta\alpha_{31}$	—	—	—	—	E	F
$\Delta\alpha_{12}$	—	—	—	—	—	E

$A = G^2_{rr} = \mu_x + \mu_y$

$B = G^1_{rr} = \mu_x \cos\alpha$

$C = G^1_{r\phi}\begin{pmatrix}1\\1\end{pmatrix} = -\frac{2}{r}\,\frac{\cos\alpha(1-\cos\alpha)\mu_x}{\sin\alpha}$

$D = G^2_{2\phi} = -\frac{\mu_x}{r}\sin\alpha$

$E = G^3_{\phi\phi} = \frac{2}{r^2}\left[\mu_y + \mu_x(1-\cos\alpha)\right]$

$F = G^2_{\phi\phi}\begin{pmatrix}1\\1\end{pmatrix} = \frac{\mu_y}{r^2}\,\frac{\cos\alpha}{1+\cos\alpha} + \frac{\mu_x}{r^2}\,\frac{(1+3\cos\alpha)(1-\cos\alpha)}{1+\cos\alpha}$

Both of these matrices are of the form

$$\begin{bmatrix} A & C & D \\ C & A & D \\ D & D & B \end{bmatrix} \tag{1.130}$$

The appearance of the same elements is evidently due to the equivalence of the two internal coordinates, Δr_1 and Δr_2. Such symmetrically equivalent sets of internal coordinates are seen in many other molecules, such as those in Fig. 1.20. In these cases, it is possible to reduce the order of the **F** and **G** matrices (and hence the order of the secular equation resulting from them) by a coordinate transformation.

Let the internal coordinates R be transformed by

$$\mathbf{R}^s = \mathbf{U}\mathbf{R} \tag{1.131}$$

Then, we obtain

$$2T = \tilde{\dot{\mathbf{R}}}\mathbf{G}^{-1}\dot{\mathbf{R}} = \tilde{\dot{\mathbf{R}}}^s\,\tilde{\mathbf{U}}^{-1}\mathbf{G}^{-1}\mathbf{U}^{-1}\dot{\mathbf{R}}^s$$

$$= \tilde{\dot{\mathbf{R}}}^s\mathbf{G}_s^{-1}\dot{\mathbf{R}}^s$$

$$2V = \tilde{\mathbf{R}}\mathbf{F}\mathbf{R} = \tilde{\mathbf{R}}^s\tilde{\mathbf{U}}^{-1}\mathbf{F}\mathbf{U}^{-1}\mathbf{R}^s$$

$$= \tilde{\mathbf{R}}^s\mathbf{F}_s\mathbf{R}^s$$

where

$$\begin{aligned} \mathbf{G}_s^{-1} &= \tilde{\mathbf{U}}^{-1}\mathbf{G}^{-1}\mathbf{U}^{-1} \quad \text{or} \quad \mathbf{G}_s = \mathbf{U}\mathbf{G}\tilde{\mathbf{U}} \\ \mathbf{F}_s &= \tilde{\mathbf{U}}^{-1}\mathbf{F}\mathbf{U}^{-1} \end{aligned} \tag{1.132}$$

If $\mathbf{U}$ is an orthogonal matrix ($\mathbf{U}^{-1} = \tilde{\mathbf{U}}$), Eq. 1.132 is written as

$$\mathbf{F}_s = \mathbf{U}\mathbf{F}\tilde{\mathbf{U}} \quad \text{and} \quad \mathbf{G}_s = \mathbf{U}\mathbf{G}\tilde{\mathbf{U}} \tag{1.133}$$

Both $\mathbf{GF}$ and $\mathbf{G}_s\mathbf{F}_s$ give the same roots, since

$$\begin{aligned} |\mathbf{G}_s\mathbf{F}_s - \mathbf{E}\lambda| &= |\mathbf{U}\mathbf{G}\tilde{\mathbf{U}}\tilde{\mathbf{U}}^{-1}\mathbf{F}\mathbf{U}^{-1} - \mathbf{E}\lambda| \\ &= |\mathbf{U}\mathbf{G}\mathbf{F}\mathbf{U}^{-1} - \mathbf{E}\lambda| \\ &= |\mathbf{U}||\mathbf{G}\mathbf{F} - \mathbf{E}\lambda||\mathbf{U}^{-1}| \\ &= |\mathbf{G}\mathbf{F} - \mathbf{E}\lambda| \end{aligned} \tag{1.134}$$

If we choose a proper $\mathbf{U}$ matrix from symmetry consideration, it is possible to factor the original $\mathbf{G}$ and $\mathbf{F}$ matrices into smaller ones. This, in turn, reduces the order of the secular equation to be solved, thus facilitating their solution. These new coordinates $\mathbf{R}^s$ are called *symmetry coordinates*.

The $\mathbf{U}$ matrix is constructed by using the equation

$$\mathbf{R}^s = N\sum_K \chi_i(K)K(\Delta r_1) \tag{1.135}$$

Here, K is a symmetry operation, and the summation is made over all symmetry operations. Also, $\chi_i(K)$ is the character of the representation to which R^s belongs. Called a generator, Δr_1 is, by symmetry operation K, transformed into $K(\Delta r_1)$, which is another coordinate of the same symmetrically equivalent set. Finally, N is a normalizing factor.

As an example, consider a bent $\mathbf{XY}_2$ molecule in which Δr_1 and Δr_2 are equivalent. Using Δr_1 as a generator, we obtain

	I	$C_2(z)$	$\sigma(xz)$	$\sigma(yz)$
$K(\Delta r_1)$	Δr_1	Δr_2	Δr_2	Δr_1
$\chi_{A_1}(K)$	1	1	1	1
$\chi_{B_2}(K)$	1	–1	–1	1

Thus

$$R^s_{A_1} = N\sum \chi_{A_1}(K)K(\Delta r_1) = 2N(\Delta r_1 + \Delta r_2)$$
$$N = \frac{1}{2\sqrt{2}} \quad \text{since} (2N)^2 + (2N)^2 = 1$$

Then

$$R^S_{A_1} = \frac{1}{\sqrt{2}}(\Delta r_1 + \Delta r_2) \tag{1.136}$$

Similarly,

$$R^s_{B_2} = \frac{1}{\sqrt{2}}(\Delta r_1 - \Delta r_2) \tag{1.137}$$

The remaining internal coordinate, $\Delta\alpha$, belongs to the A_1 species. Thus, the complete **U** matrix is written as

$$\begin{bmatrix} R^s_1(A_1) \\ R^s_2(A_1) \\ R^s_3(B_2) \end{bmatrix} = \begin{bmatrix} \frac{1}{\sqrt{2}} & \frac{1}{\sqrt{2}} & 0 \\ 0 & 0 & 1 \\ \frac{1}{\sqrt{2}} & \frac{-1}{\sqrt{2}} & 0 \end{bmatrix} \begin{bmatrix} \Delta r_1 \\ \Delta r_2 \\ \Delta\alpha \end{bmatrix} \tag{1.138}$$

If the **G** and **F** matrices of type 1.130 are transformed by relations 1.133, where **U** is given by the matrix of Eq. 1.138, they become

$$\mathbf{F_S}, \mathbf{G_S} = \left[\begin{array}{cc:c} A + C & \sqrt{2}D & 0 \\ \sqrt{2}D & B & 0 \\ \hdashline 0 & 0 & A - C \end{array}\right] \tag{1.139}$$

or, more explicitly

$$\mathbf{F_S} = \left[\begin{array}{cc:c} f_{11} + f_{12} & r\sqrt{2}f_{13} & 0 \\ r\sqrt{2}f_{13} & r^2 f_{33} & 0 \\ \hdashline 0 & 0 & f_{11} - f_{12} \end{array}\right] \tag{1.140}$$

$$\mathbf{G_S} = \left[\begin{array}{cc:c} \mu_3(1+\cos\alpha)+\mu_1 & -\dfrac{\sqrt{2}}{r}\mu_3\sin\alpha & 0 \\ -\dfrac{\sqrt{2}}{r}\mu_3\sin\alpha & \dfrac{2\mu_1}{r^2}+\dfrac{2\mu_3}{r^2}(1-\cos\alpha) & 0 \\ \hdashline 0 & 0 & \mu_3(1-\cos\alpha)+\mu_1 \end{array}\right] \tag{1.141}$$

In a pyramidal XY_3 molecule (Fig. 1.20c), Δr_1, Δr_2, and Δr_3 are the equivalent set; so are $\Delta\alpha_{23}$, $\Delta\alpha_{31}$, and $\Delta\alpha_{12}$. It is already known from Eq. 1.107 that one A_1 and one E vibration are involved both in the stretching and in the bending vibrations. Using Δr_1 as a generator, we obtain from Eq. 1.135

	I	C_3^+	C_3^-	σ_1	σ_2	σ_3
$K(\Delta r_1)$	Δr_1	Δr_2	Δr_3	Δr_1	Δr_3	Δr_2
$\chi_{A_1}(K)$	1	1	1	1	1	1
$\chi_E(K)$	2	−1	−1	0	0	0

Then, we obtain

$$R^s_{A_1} = \frac{1}{\sqrt{3}}(\Delta r_1 + \Delta r_2 + \Delta r_3) \tag{1.142}$$

$$R^s_{E_1} = \frac{1}{\sqrt{6}}(2\Delta r_1 - \Delta r_2 - \Delta r_3) \tag{1.143}$$

To find a coordinate that forms a degenerate pair with Eq. 1.143, we repeat the same procedure, using Δr_2 and Δr_3 as the generators. The results are

$$R^s_{E_2} = N(2\Delta r_2 - \Delta r_3 - \Delta r_1)$$
$$R^s_{E_2} = N(2\Delta r_3 - \Delta r_1 - \Delta r_2)$$

However, these coordinates are not orthogonal to $R^s_{E_1}$ (Eq. 1.143).

If we take a linear combination, $R^s_{E_2} + R^s_{E_3}$, we obtain Eq. 1.143. If we take $R^s_{E_2} - R^s_{E_3}$, we obtain

$$R^s_{E_4} = \frac{1}{\sqrt{2}}(\Delta r_2 - \Delta r_3) \tag{1.144}$$

Since Eqs. 1.143 and 1.144 are mutually orthogonal, these two coordinates are taken as a degenerate pair. Similar results are obtained for three angle-bending coordinates. Thus, the complete **U** matrix is written as

$$\begin{bmatrix} R_1^s(A_1) \\ R_2^s(A_1) \\ R_{3a}^s(E) \\ R_{4a}^s(E) \\ R_{3b}^s(E) \\ R_{4b}^s(E) \end{bmatrix} = \begin{bmatrix} 1/\sqrt{3} & 1/\sqrt{3} & 1/\sqrt{3} & 0 & 0 & 0 \\ 0 & 0 & 0 & 1/\sqrt{3} & 1/\sqrt{3} & 1/\sqrt{3} \\ 2/\sqrt{6} & -1/\sqrt{6} & -1/\sqrt{6} & 0 & 0 & 0 \\ 0 & 0 & 0 & 2/\sqrt{6} & -1/\sqrt{6} & -1/\sqrt{6} \\ 0 & 1/\sqrt{2} & -1/\sqrt{2} & 0 & 0 & 0 \\ 0 & 0 & 0 & 0 & 1/\sqrt{2} & -1/\sqrt{2} \end{bmatrix} \cdot \begin{bmatrix} \Delta r_1 \\ \Delta r_2 \\ \Delta r_3 \\ \Delta\alpha_{23} \\ \Delta\alpha_{31} \\ \Delta\alpha_{12} \end{bmatrix} \tag{1.145}$$

The **G** matrix of a pyramidal XY_3 molecule has already been calculated (see Table 1.14). By using Eq. 1.133, the new $\mathbf{G_s}$ matrix becomes

$$\mathbf{G_S} = \left[\begin{array}{cc|c|c} A+2B & C+2D & & \\ C+2D & E+2F & 0 & 0 \\ \hline & & A-B \quad C-D & \\ 0 & & C-D \quad E-F & 0 \\ \hline & & & A-B \quad C-D \\ 0 & & 0 & C-D \quad E-F \end{array}\right] \tag{1.146}$$

Here A, B, and so forth denote the elements in Table 1.13. The **F** matrix transforms similarly. Therefore, it is necessary only to solve two quadratic equations for the A_1 and E species.

For the tetrahedral XY_4 molecule shown in Fig. 1.20e, group theory (Secs. 1.8 and 1.9) predicts one A_1 and one F_2 stretching, and one E and one F_2 bending, vibration. The **U** matrix for the four stretching coordinates is

$$\begin{bmatrix} R_1^s(A_1) \\ R_{2a}^s(F_2) \\ R_{2b}^s(F_2) \\ R_{2c}^s(F_2) \end{bmatrix} = \begin{bmatrix} 1/2 & 1/2 & 1/2 & 1/2 \\ 1/\sqrt{6} & 1/\sqrt{6} & -2/\sqrt{6} & 0 \\ 1/\sqrt{12} & 1/\sqrt{12} & 1/\sqrt{12} & -3/\sqrt{12} \\ -1/\sqrt{2} & 1/\sqrt{2} & 0 & 0 \end{bmatrix} \begin{bmatrix} \Delta r_1 \\ \Delta r_2 \\ \Delta r_3 \\ \Delta r_4 \end{bmatrix} \tag{1.147}$$

whereas the **U** matrix for the six bending coordinates becomes

$$\begin{bmatrix} R_1^s(A_1) \\ R_{2a}^s(E) \\ R_{2b}^s(E) \\ R_{3a}^s(F_2) \\ R_{3b}^s(F_2) \\ R_{3c}^s(F_2) \end{bmatrix} = \begin{bmatrix} 1/\sqrt{6} & 1/\sqrt{6} & 1/\sqrt{6} & 1/\sqrt{6} & 1/\sqrt{6} & 1/\sqrt{6} \\ 2/\sqrt{12} & -1/\sqrt{12} & -1/\sqrt{12} & -1/\sqrt{12} & -1/\sqrt{12} & 2/\sqrt{12} \\ 0 & 1/2 & -1/2 & 1/2 & -1/2 & 0 \\ 2/\sqrt{12} & -1/\sqrt{12} & -1/\sqrt{12} & 1/\sqrt{12} & 1/\sqrt{12} & -2/\sqrt{12} \\ 1/\sqrt{6} & 1/\sqrt{6} & 1/\sqrt{6} & -1/\sqrt{6} & -1/\sqrt{6} & -1/\sqrt{6} \\ 0 & 1/2 & -1/2 & -1/2 & 1/2 & 0 \end{bmatrix} \cdot \begin{bmatrix} \Delta\alpha_{12} \\ \Delta\alpha_{23} \\ \Delta\alpha_{31} \\ \Delta\alpha_{14} \\ \Delta\alpha_{24} \\ \Delta\alpha_{34} \end{bmatrix} \tag{1.148}$$

The symmetry coordinate $R_1^s(A_1)$ in Eq. 1.148 represents a *redundant coordinate* (see Eq. 1.91). In such a case, a coordinate transformation reduces the order of the matrix by one, since all the **G**-matrix elements related to this coordinate become zero. Conversely, this result provides a general method of finding redundant coordinates. Suppose that the elements of the **G** matrix are calculated in terms of internal coordinates such as those in Table 1.13. If a suitable combination of internal coordinates is made so that $\Sigma_j G_{ij} = 0$ (where j refers to all the equivalent internal coordinates), such a combination is a redundant coordinate. By using the **U** matrices in Eqs. 1.147 and 1.148, the problem of solving a tenth-order secular equation for a tetrahedral XY_4 molecule is reduced to that of solving two first-order (A_1 and E) and one quadratic (F_2) equation.

The normal modes of vibration of the tetrahedral XY_4 molecule are shown in Fig. 2.12 of Chapter 2. It can be seen that the normal modes, ν_1 and ν_3, correspond to the symmetry coordinates $R_1^s(A_1)$ and $R_{2b}^s(F_2)$ of Eq. 1.147, respectively, and that the normal modes, ν_2 and ν_4, correspond to the symmetry coordinates $R_{2a}^s(E)$ and $R_{3b}^s(F_2)$ of Eq. 1.148, respectively.

1.14. POTENTIAL FIELDS AND FORCE CONSTANTS

Using Eqs. 1.111 and 1.128, we write the potential energy of a bent XY_2 molecule as

$$\begin{aligned} 2V = {} & f_{11}(\Delta r_1)^2 + f_{11}(\Delta r_2)^2 + f_{33}r^2(\Delta\alpha)^2 + 2f_{12}(\Delta r_1)(\Delta r_2) \\ & + 2f_{13}r(\Delta r_1)(\Delta\alpha) + 2f_{13}r(\Delta r_2)(\Delta\alpha) \end{aligned} \tag{1.149}$$

This type of potential field is called a *generalized valence force* (GVF) field.* It consists of stretching and bending force constants, as well as the interaction force constants between them. When using such a potential field, four force constants are needed to describe the potential energy of a bent XY_2 molecule. Since only three vibrations are observed in practice, it is impossible to determine all four force constants simultaneously. One method used to circumvent this difficulty is to calculate the vibrational frequencies of isotopic molecules (e.g., D_2O and HDO for H_2O), assuming the same set of force constants.† This method is satisfactory, however, only for simple molecules. As molecules become more complex, the number of interaction force constants in the GVF field becomes too large to allow any reliable evaluation.

In another approach, Shimanouchi [82] introduced the *Urey–Bradley force* (UBF) field, which consists of stretching and bending force constants, as well as repulsive force constants between nonbonded atoms. The general form of the potential field is given by

$$\begin{aligned} V = &\sum_i \left(\frac{1}{2} K_i (\Delta r_i)^2 + K_i' r_i (\Delta r_i) \right) \\ &+ \sum_i \left(\frac{1}{2} H_i r_{i\alpha}^2 (\Delta \alpha_i)^2 + H_i' r_{i\alpha}^2 (\Delta \alpha_i) \right) \\ &+ \sum_i \left(\frac{1}{2} F_i (\Delta q_i)^2 + F_i' q_i (\Delta q_i) \right) \end{aligned} \tag{1.150}$$

Here Δr_i, $\Delta \alpha_i$, and Δq_i, are the changes in the bond lengths, bond angles, and distances between nonbonded atoms, respectively. The symbols K_i, K_i', H_i, H_i' and F_i, F_i' represent the stretching, bending, and repulsive force constants, respectively. Furthermore, r_i, $r_{i\alpha}$, and q_i are the values of the distances at the equilibrium positions and are inserted to make the force constants dimensionally similar. Linear force constants (K_i', H_i' and F_i') must be included since Δr_i, $\Delta \alpha_i$, and Δq_i are not completely independent of each other.

Using the relation

$$q_{ij}^2 = r_i^2 + r_j^2 - 2 r_i r_j \cos \alpha_{ij} \tag{1.151}$$

*A potential field consisting of stretching and bending force constants only is called a *simple valence force* field.

†In addition to isotope frequency shifts, mean amplitudes of vibration, Coriolis coupling constants, centrifugal distortion constants, and so forth may be used to refine the force constants of small molecules (see Ref. 81).

and considering that the first derivatives can be equated to zero in the equilibrium case, we can write the final form of the potential field as

$$\begin{aligned} V = \frac{1}{2}\sum_i \left[K_i + \sum_{j(\neq i)}(t_{ij}^2 F_{ij}^{'} + s_{ij}^2 F_{ij})\right](\Delta r_i)^2 \\ + \frac{1}{2}\sum_{i<j}(H_{ij} - s_{ij}s_{ji}F_{ij}^{'} + t_{ij}t_{ji}F_{ij})(\sqrt{r_i r_j}\Delta\alpha_{ij})^2 \\ + \sum_{i<j}(-t_{ij}t_{ji}F_{ij}^{'} + s_{ij}s_{ji}F_{ij})(\Delta r_i)(\Delta r_j) \\ + \sum_{i\neq j}(t_{ij}s_{ji}F_{ij}^{'} + t_{ji}s_{ij}F_{ij})\left(\frac{r_j}{r_i}\right)^{1/2}(\Delta r_i)(\sqrt{r_i r_j}\Delta\alpha_{ij}) \end{aligned} \quad (1.152)^*$$

Here

$$\begin{aligned} s_{ij} &= \frac{r_i - r_j\cos\alpha_{ij}}{q_{ij}} \\ s_{ji} &= \frac{r_j - r_i\cos\alpha_{ij}}{q_{ij}} \\ t_{ij} &= \frac{r_j\sin\alpha_{ij}}{q_{ij}} \\ t_{ji} &= \frac{r_i\sin\alpha_{ij}}{q_{ij}} \end{aligned} \quad (1.153)$$

In a bent XY_2 molecule, Eq. 1.152 becomes

$$\begin{aligned} V = \tfrac{1}{2}(K + t^2F^{'} + s^2F)\left[(\Delta r_1)^2 + (\Delta r_2)^2\right] + \tfrac{1}{2}(H - s^2F^{'} + t^2F)(r\Delta\alpha)^2 \\ + (-t^2F^{'} + s^2F)(\Delta r_1)(\Delta r_2) + ts(F^{'} + F)(\Delta r_1)(r\Delta\alpha) \\ + ts(F^{'} + F)(\Delta r_2)(r\Delta\alpha) \end{aligned} \quad (1.154)$$

where

*In the case of tetrahedral molecules, a term

$$\sum_{i\neq j\neq k}\left(\frac{\kappa}{\sqrt{2}}\right)r_{ij}r_{ik}(r_{ij}\Delta\alpha_{ij})(r_{ik}\Delta\alpha_{ik})$$

must be added, where κ is called the *internal tension*.

$$s = \frac{r(1-\cos\alpha)}{q}$$

$$t = \frac{r\sin\alpha}{q}$$

Comparing Eqs. 1.154 and 1.149, we obtain the following relations between the force constants of the generalized valence force field and those of the Urey–Bradley force field:

$$\begin{aligned} f_{11} &= K + t^2F' + s^2F \\ r^2f_{33} &= (H - s^2F' + t^2F)r^2 \\ f_{12} &= -t^2F' + s^2F \\ rf_{13} &= ts(F' + F)r \end{aligned} \tag{1.155}$$

Although the Urey–Bradley field has four force constants, F' is usually taken as $-\frac{1}{10}F$, on the assumption that the repulsive energy between nonbonded atoms is proportional to $1/r^9$.* Thus, only three force constants, K, H, and F, are needed to construct the **F** matrix. The *orbital valence force* (OVF) field developed by Heath and Linnett [83] is similar to the UBF field. The OVF field uses the angle ($\Delta\beta$), which represents the distortion of the bond from the axis of the bonding orbital instead of the angle between two bonds ($\Delta\alpha$).

The number of force constants in the Urey–Bradley field is, in general, much smaller than that in the generalized valence force field. In addition, the UBF field has the advantage that (1) the force constants have clearer physical meanings than those of the GVF field, and (2) they are often transferable from molecule to molecule. For example, the force constants obtained for $SiCl_4$ and $SiBr_4$ can be used for $SiCl_3Br$, $SiCl_2Br_2$, and $SiClBr_3$. Mizushima, Shimanouchi, and their coworkers [81] and Overend and Scherer [84] have given many examples that demonstrate the transferability of the force constants in the UBF field. This property of the Urey–Bradley force constants is highly useful in calculations for complex molecules. It should be mentioned, however, that ignorance of the interactions between nonneighboring stretching vibrations and between bending vibrations in the Urey–Bradley field sometimes causes difficulties in adjusting the force constants to fit the observed frequencies. In such a case, it is possible to improve the results by introducing more force constants [84,85].

*This assumption does not cause serious error in final results, since F' is small in most cases.

Evidently, the values of force constants depend on the force field initially assumed. Thus, a comparison of force constants between molecules should not be made unless they are obtained by using the same force field. The normal coordinate analysis developed in Secs. 1.12–1.14 has already been applied to a number of molecules of various structures. Appendix VII lists the **G** and **F** matrix elements for typical molecules.

1.15. SOLUTION OF THE SECULAR EQUATION

Once the **G** and **F** matrices are obtained, the next step is to solve the matrix secular equation:

$$|\mathbf{GF} - \mathbf{E}\lambda| = 0 \tag{1.116}$$

In diatomic molecules, $\mathbf{G} = G_{11} = 1/\mu$ and $\mathbf{F} = F_{11} = K$. Then $\lambda = G_{11}F_{11}$ and $\tilde{\nu} = \sqrt{\lambda}/2\pi c = \sqrt{K/\mu}/2\pi c$ (Eq. 1.20). If the units of mass and force constant are atomic weight and mdyn/Å (or 10^5 dyn/cm), respectively,* λ is related to $\tilde{\nu}(\mathrm{cm}^{-1})$ by

$$\tilde{\nu} = 1302.83\sqrt{\lambda}$$

or

$$\lambda = 0.58915\left(\frac{\tilde{\nu}}{1000}\right)^2 \tag{1.156}$$

As an example, for the HF molecule $\mu = 0.9573$ and $K = 9.65$ in these units. Then, from Eqs. 1.20 and 1.156, $\tilde{\nu}$ is $4139\,\mathrm{cm}^{-1}$.

The **F** and **G** matrix elements of a bent XY_2 molecule are given in Eqs. 1.140 and 1.141, respectively. The secular equation for the A_1 species is quadratic:

$$|\mathbf{GF} - \mathbf{E}\lambda| = \begin{vmatrix} G_{11}F_{11} + G_{12}F_{21} - \lambda & G_{11}F_{12} + G_{12}F_{22} \\ G_{21}F_{11} + G_{22}F_{21} & G_{21}F_{12} + G_{22}F_{22} - \lambda \end{vmatrix} = 0 \tag{1.157}$$

If this is expanded into an algebraic equation, the following result is obtained:

$$\lambda^2 - (G_{11}F_{11} + G_{22}F_{22} + 2G_{12}F_{12})\lambda + (G_{11}G_{22} - G_{12}^2)(F_{11}F_{22} - F_{12}^2) = 0 \tag{1.158}$$

*Although the bond distance is involved in both the **G** and **F** matrices, it is canceled during multiplication of the **G** and **F** matrix elements. Therefore, any unit can be used for the bond distance.

For the H_2O molecule, we obtain

$$\mu_1 = \mu_H = \frac{1}{1.008} = 0.99206$$

$$\mu_3 = \mu_O = \frac{1}{15.995} = 0.06252$$

$$r = 0.96(\text{Å}), \qquad \alpha = 105^\circ$$
$$\sin\alpha = \sin 105^\circ = 0.96593$$
$$\cos\alpha = \cos 105^\circ = -0.25882$$

Then, the **G** matrix elements of Eq. 1.141 are

$$G_{11} = \mu_1 + \mu_3(1 + \cos\alpha) = 1.03840$$
$$G_{12} = -\frac{\sqrt{2}}{r}\mu_3 \sin\alpha = -0.08896$$
$$G_{22} = \frac{1}{r^2}[2\mu_1 + 2\mu_3(1 - \cos\alpha)] = 2.32370$$

If the force constants in terms of the generalized valence force field are selected as

$$f_{11} = 8.4280, \qquad f_{12} = -0.1050$$
$$f_{13} = 0.2625, \qquad f_{33} = 0.7680$$

the **F** matrix elements of Eq. 1.140 are

$$F_{11} = f_{11} + f_{12} = 8.32300$$
$$F_{12} = \sqrt{2} r f_{13} = 0.35638$$
$$F_{22} = r^2 f_{33} = 0.70779$$

Using these values, we find that Eq. 1.158 becomes

$$\lambda^2 - 10.22389\lambda + 13.86234 = 0$$

The solution of this equation gives

$$\lambda_1 = 8.61475, \qquad \lambda_2 = 1.60914$$

If these values are converted to $\tilde{\nu}$ through Eq. 1.156, we obtain

$$\tilde{\nu}_1 = 3824\,\text{cm}^{-1}, \qquad \tilde{\nu}_2 = 1653\,\text{cm}^{-1}$$

With the same set of force constants, the frequency of the B_2 vibration is calculated as

$$\begin{aligned}\lambda_3 = G_{33}F_{33} &= [\mu_1 + \mu_3(1 - \cos\alpha)]\,(f_{11} - f_{12}) \\ &= 9.13681 \\ \tilde{\nu}_3 &= 3938\ \text{cm}^{-1}\end{aligned}$$

The observed frequencies corrected for anharmonicity are as follows: $\omega_1 = 3825\,\text{cm}^{-1}$, $\omega_2 = 1654\,\text{cm}^{-1}$, and $\omega_3 = 3936\,\text{cm}^{-1}$.

If the secular equation is third order, it gives rise to a cubic equation:

$$\begin{aligned}&\lambda^3 - (G_{11}F_{11} + G_{22}F_{22} + G_{33}F_{33} + 2G_{12}F_{12} + 2G_{13}F_{13} + 2G_{23}F_{23})\lambda^2 \\ &\quad + \left\{ \begin{vmatrix} G_{11} & G_{12} \\ G_{21} & G_{22} \end{vmatrix} \begin{vmatrix} F_{11} & F_{12} \\ F_{21} & F_{22} \end{vmatrix} + \begin{vmatrix} G_{12} & G_{13} \\ G_{22} & G_{23} \end{vmatrix} \begin{vmatrix} F_{12} & F_{13} \\ F_{22} & F_{23} \end{vmatrix} + \begin{vmatrix} G_{11} & G_{13} \\ G_{21} & G_{23} \end{vmatrix} \begin{vmatrix} F_{11} & F_{13} \\ F_{21} & F_{23} \end{vmatrix} \right. \\ &\quad + \begin{vmatrix} G_{11} & G_{12} \\ G_{31} & G_{32} \end{vmatrix} \begin{vmatrix} F_{11} & F_{12} \\ F_{31} & F_{32} \end{vmatrix} + \begin{vmatrix} G_{12} & G_{13} \\ G_{32} & G_{33} \end{vmatrix} \begin{vmatrix} F_{12} & F_{13} \\ F_{32} & F_{33} \end{vmatrix} \\ &\quad + \begin{vmatrix} G_{11} & G_{13} \\ G_{31} & G_{33} \end{vmatrix} \begin{vmatrix} F_{11} & F_{13} \\ F_{31} & F_{33} \end{vmatrix} + \begin{vmatrix} G_{21} & G_{22} \\ G_{31} & G_{32} \end{vmatrix} \begin{vmatrix} F_{21} & F_{22} \\ F_{31} & F_{32} \end{vmatrix} + \begin{vmatrix} G_{22} & G_{23} \\ G_{32} & G_{33} \end{vmatrix} \begin{vmatrix} F_{22} & F_{23} \\ F_{32} & F_{33} \end{vmatrix} \\ &\quad \left. + \begin{vmatrix} G_{21} & G_{23} \\ G_{31} & G_{33} \end{vmatrix} \begin{vmatrix} F_{21} & F_{23} \\ F_{31} & F_{33} \end{vmatrix} \right\} \lambda - \begin{vmatrix} G_{11} & G_{12} & G_{13} \\ G_{21} & G_{22} & G_{33} \\ G_{31} & G_{32} & G_{33} \end{vmatrix} \begin{vmatrix} F_{11} & F_{12} & F_{13} \\ F_{21} & F_{23} & F_{33} \\ F_{31} & F_{32} & F_{33} \end{vmatrix} = 0 \quad (1.159)\end{aligned}$$

Thus, it is possible to solve the secular equation by expanding it into an algebraic equation. If the order of the secular equation is higher than three, however, direct expansion such as that just shown becomes too cumbersome. There are several methods of calculating the coefficients of an algebraic equation using indirect expansion [3]. The use of an electronic computer greatly reduces the burden of calculation. Excellent programs written by Schachtschneider [86] and other workers are available for the vibrational analysis of polyatomic molecules.

1.16. VIBRATIONAL FREQUENCIES OF ISOTOPIC MOLECULES

As stated in Sec. 1.14, the vibrational frequencies of isotopic molecules are very useful in refining a set of force constants in vibrational analysis. For large molecules, isotopic substitution is indispensable in making band assignments, since only vibrations involving the motion of the isotopic atom will be shifted by isotopic substitution.

Two important rules hold for the vibrational frequencies of isotopic molecules. The first, called the *product rule*, can be derived as follows.

Let $\lambda_1, \lambda_2, \ldots, \lambda_n$ be the roots of the secular equation $|\mathbf{GF} - \mathbf{E}\lambda| = 0$. Then

$$\lambda_1\lambda_2 \cdots \lambda_n = |\mathbf{G}||\mathbf{F}| \quad (1.160)$$

holds for a given molecule. Since the isotopic molecule has exactly the same $|\mathbf{F}|$ as that in Eq. 1.160, a similar relation

$$\lambda'_1\lambda'_2\cdots\lambda'_n = |\mathbf{G}'||\mathbf{F}|$$

holds for this molecule. It follows that

$$\frac{\lambda_1\lambda_2\cdots\lambda_n}{\lambda'_1\lambda'_2\cdots\lambda'_n} = \frac{|\mathbf{G}|}{|\mathbf{G}'|} \tag{1.161}$$

Since

$$\tilde{\nu} = \frac{1}{2\pi c}\sqrt{\lambda}$$

Equation 1.161 can be written as

$$\frac{\tilde{\nu}_1\tilde{\nu}_2\cdots\tilde{\nu}_n}{\tilde{\nu}'_1\tilde{\nu}'_2\cdots\tilde{\nu}'_n} = \sqrt{\frac{|\mathbf{G}|}{|\mathbf{G}'|}} \tag{1.162}$$

This rule has been confirmed by using pairs of molecules such as H_2O and D_2O and CH_4 and CD_4. The rule is also applicable to the product of vibrational frequencies belonging to a single symmetry species.

A more general form of Eq. 1.162 is given by the *Redlich-Teller product rule* [1]:

$$\frac{\tilde{\nu}_1\tilde{\nu}_2\cdots\tilde{\nu}_n}{\tilde{\nu}'_1\tilde{\nu}'_2\cdots\tilde{\nu}'_n} = \sqrt{\left(\frac{m'_1}{m_1}\right)^{\alpha}\left(\frac{m'_2}{m_2}\right)^{\beta}\cdots\left(\frac{M}{M'}\right)^{t}\left(\frac{I_x}{I'_x}\right)^{\delta_x}\left(\frac{I_y}{I'_y}\right)^{\delta_y}\left(\frac{I_z}{I'_z}\right)^{\delta_z}} \tag{1.163}$$

Here m_1, m_2,... are the masses of the representative atoms of the various sets of equivalent nuclei (atoms represented by m,m_0,m_{xy},... in the tables given in Appendix III); α, β,... are the coefficients of m,m_0,m_{xy},...; M is the total mass of the molecule; t is the number of T_x,T_y,T_z in the symmetry type considered; I_x,I_y,I_z are the moments of inertia about the x, y, z axes, respectively, which go through the center of the mass; and δ_x,δ_y,δ_z are 1 to 0, depending on whether R_x,R_y,R_z belong to the symmetry type considered. A degenerate vibration is counted only once on both sides of the equation.

Another useful rule in regard to the vibrational frequencies of isotopic molecules, called the *sum rule*, can be derived as follows. It is obvious from Eqs. 1.158 and 1.159 that

$$\lambda_1 + \lambda_2 + \cdots + \lambda_n = \sum_n \lambda = \sum_{i,j} G_{ij}F_{ij} \tag{1.164}$$

Let σ_k denote $\Sigma_{ij} G_{ij} F_{ij}$ for k different isotopic molecules, all of which have the same **F** matrix. If a suitable combination of molecules is taken, so that

$$\begin{aligned}\sigma_1 + \sigma_2 + \cdots + \sigma_k &= \left(\sum G_{ij}F_{ij}\right)_1 + \left(\sum G_{ij}F_{ij}\right)_2 + \cdots + \left(\sum G_{ij}F_{ij}\right)_k \\ &= \left[\left(\sum G_{ij}\right)_1 + \left(\sum G_{ij}\right)_2 + \cdots + \left(\sum G_{ij}\right)_k\right]\left(\sum F_{ij}\right) \\ &= 0\end{aligned}$$

then it follows that

$$\left(\sum \lambda\right)_1 + \left(\sum \lambda\right)_2 + \cdots + \left(\sum \lambda\right)_k = 0 \qquad (1.165)$$

This rule has been verified for such combinations as H_2O, D_2O, and HDO, where

$$2\sigma(\mathrm{HDO}) - \sigma(\mathrm{H_2O}) - \sigma(\mathrm{D_2O}) = 0$$

Such relations between the frequencies of isotopic molecules are highly useful in making band assignments.

1.17. METAL–ISOTOPE SPECTROSCOPY [87,88]

As a first approximation, vibrational spectra of coordination compounds (Chapter 3, in Part B) can be classifed into ligand vibrations that occur in the high-frequency region (4000–600 cm^{-1}) and metal–ligand vibrations that appear in the low-frequency region (below 600 cm^{-1}). The former provide information about the effect of coordination on the electronic structure of the ligand, while the latter provide direct information about the structure of the coordination sphere and the nature of the metal–ligand bond. Since the main interest of coordination chemistry is the coordinate bond, it is the metal–ligand vibrations that have held the interest of inorganic vibrational spectroscopists. It is difficult, however, to make unequivocal assignments of metal–ligand vibrations since the interpretation of the low-frequency spectrum is complicated by the appearance of ligand vibrations as well as lattice vibrations in the case of solid-state spectra.

Conventional methods that have been used to assign metal–ligand vibrations are

(1) Comparison of spectra between a free ligand and its metal complex; the metal–ligand vibration should be absent in the spectrum of the free ligand. This method often fails to give a clear-cut assignment because some ligand vibrations activated by complex formation may appear in the same region as the metal–ligand vibrations.

(2) The metal–ligand vibration should be metal sensitive and be shifted by changing the metal or its oxidation state. This method is applicable only when a series of metal complexes have exactly the same structure, where only the central metal is different. Also, it does not provide definitive assignments since some ligand vibrations (such as chelate ring deformations) are also metal-sensitive.

(3) The metal–ligand stretching vibration should appear in the same frequency region if the metal is the same and the ligands are similar. For example, the ν(Zn-N) (ν: stretching) of Zn(II) pyridine complexes are expected to be similar to those of Zn(II) α-picoline complexes. This method is applicable only when the metal–ligand vibration is known for one parent compound.

(4) The metal–ligand vibration exhibits an isotope shift if the ligand is isotopically substituted. For example, the ν(Ni-N) of $[Ni(NH_3)_6]Cl_2$ at $334\,cm^{-1}$ is shifted to $318\,cm^{-1}$ on deuteration of the ammonia ligands. The observed shift ($16\,cm^{-1}$) is in good agreement with that predicted theoretically for this mode. This method was used to assign the metal–ligand vibrations of chelate compounds such as oxamido ($^{14}N/^{15}N$) and acetylacetonato($^{16}O/^{18}O$) complexes. However, isotopic substitution of the α-atom (atom directly bonded to the metal) causes shifts of not only metal–ligand vibrations but also of ligand vibrations involving the motion of the α-atom. Thus, this method alone cannot provide an unequivocal assignment of the metal–ligand vibration.

(5) The frequency of a metal–ligand vibration may be predicted if the metal–ligand stretching and other force constants are known *a priori*. At present, this method is not practical since only a limited amount of information is available on the force constants of coordination compounds.

It is obvious that none of the above methods is perfect in assigning metal–ligand vibrations. Furthermore, these methods encounter more difficulties as the structure of the complex (and hence the spectrum) becomes more complicated. Fortunately, the "metal isotope technique" which was developed in 1969 may be used to obtain reliable metal–ligand assignments [89]. Isotope pairs such as (H/D) and ($^{16}O/^{18}O$) had been used routinely by many spectroscopists. However, isotopic pairs of heavy metals such as ($^{58}Ni/^{62}Ni$) and ($^{104}Pd/^{110}Pd$) were not employed until 1969 when the first report on the assignments of the Ni−P vibrations of *trans*-$Ni(PEt_3)_2X_2$ (X = Cl and Br) was made. The delay in their use was probably due to two reasons:

(1) It was thought that the magnitude of isotope shifts arising from metal isotope substitution might be too small to be of practical value.

(2) Pure metal isotopes were too expensive to use routinely in the laboratory. Nakamoto and coworkers [87,88] have shown, however, that the magnitudes of metal isotope shifts are generally of the order of $2–10\,cm^{-1}$ for stretching modes and $0–2\,cm^{-1}$ for bending modes, and that the experimental error in measuring the frequency could be as small as $\pm 0.2\,cm^{-1}$ if proper precautions

are taken. They have also shown that this technique is financially feasible if the compounds are prepared on a milligram scale. Normally, the vibrational spectrum of a compound can be obtained with a sample less than 10 mg. Table 1.14 lists metal isotopes that are useful for vibrational studies of coordination compounds.

TABLE 1.14. Some Stable Metal Isotopes[a]

Element	Inventory Form	Isotope	Natural Abundance (%)	Purity (%)
Magnesium	Oxide	Mg-24	78.99	99.9
		Mg-25	10.00	94
		Mg-26	11.01	97
Silicon	Oxide	Si-28	92.23	>99.8
		Si-30	3.10	>94
Titanium	Oxide	Ti-46	8.0	70–96
		Ti-48	73.8	>99
Chromium	Oxide	Cr-50	4.345	>95
		Cr-52	83.79	>99.7
		Cr-53	9.50	>96
Iron	Oxide	Fe-54	5.9	>96
		Fe-56	91.72	>99.9
		Fe-57	2.1	86–93
Nickel	Metal	Ni-58	68.27	>99.9
	Oxide	Ni-60	26.1	>99
	Oxide	Ni-62	3.59	>96
Copper	Oxide	Cu-63	69.17	>99.8
		Cu-65	30.83	>99.6
Zinc	Oxide	Zn-64	48.6	>99.8
		Zn-66	27.9	>98
		Zn-68	18.8	97–99
Germanium	Oxide	Ge-72	27.4	>97
		Ge-74	36.5	>98
Zirconium	Oxide	Zr-90	51.45	97–99
		Zr-94	17.38	>98
Molybdenum	Metal/oxide	Mo-92	14.84	>97
		Mo-95	15.92	>96
		Mo-97	9.55	>92
		Mo-100	9.63	>97
Ruthenium	Metal	Ru-99	12.7	>98
		Ru-102	31.6	>99
Palladium	Metal	Pd-104	11.4	>95
		Pd-108	26.46	>98
Tin	Oxide	Sn-116	14.53	>95
		Sn-120	32.59	>98
		Sn-124	5.79	>94
Barium	Carbonate	Ba-135	6.593	>93
		Ba-138	71.70	>99

[a]Available at Oak Ridge National Laboratory.

It should be noted that the central atom of a highly symmetrical molecule ($\mathbf{T}_d$, $\mathbf{O}_h$, etc.) does not move during the totally symmetric vibration. Thus, no metal–isotope shifts are expected in these cases [90]. When the central atom is coordinated by several different donor atoms, multiple isotope labeling is necessary to distinguish different coordinate bond-stretching vibrations. For example, complete assignments of bis (glycino)nickel(II) require $^{14}N/^{15}N$ and/or $^{16}O/^{18}O$ isotope shift data as well as $^{58}Ni/^{62}Ni$ isotope shift data [91]. This book contains many other applications of metal–isotope techniques. These results show that metal–isotope data are indispensable not only in assigning the metal–ligand vibrations but also in refining metal–ligand stretching force constants in normal coordinate analysis [88]. The presence of vibrational coupling between metal–ligand and other vibrations can also be detected by combining metal–isotope data with normal coordinate calculations (Sec. 1.18) since both experimental and theoretical isotope shift values would be smaller when such couplings occur.

The metal–isotope techniques become more important as the molecules become larger and complex. In biological molecules such as heme proteins, structural and bonding information about the active site (iron porphyrin) can be obtained through definitive assignments of coordinate bond-stretching vibrations around the iron atom. Using resonance Raman techniques (Sec. 1.22), it is possible to observe iron porphyrin and iron-axial ligand vibrations without interference from peptide chain vibrations. Thus, these vibrations can be assigned by comparing resonance Raman spectra of a natural heme protein with that of a ^{54}Fe-reconstituted heme protein. Chapter 5 (in Part B) includes several examples of applications of metal-isotope techniques to bioinorganic compounds [hemoglobin (^{54}Fe, ^{57}Fe), oxy-hemocyanin (^{63}Cu, ^{65}Cu), etc.]. An example of a multiple labeling is seen in the case of cytochrome $P450_{cam}$ having the axial Fe–S linkage in addition to four Fe–N (porphyrin) bonds; Champion et al. [92] were able to assign its Fe–S stretching vibration (351 cm^{-1}) by combining ^{32}S–^{34}S and ^{54}Fe–^{56}Fe isotope shift data.

1.18. GROUP FREQUENCIES AND BAND ASSIGNMENTS

From observation of the infrared spectra of a number of compounds having a common group of atoms, it is found that, regardless of the rest of the molecule, this common group absorbs over a narrow range of frequencies, called the *group frequency*. For example, the methyl group exhibits the antisymmetric stretching [$\nu_a(CH_3)$], symmetric stretching [$\nu_s(CH_3)$], degenerate bending [$\delta_d(CH_3)$], symmetric bending [$\delta_s(CH_3)$], and rocking [$\rho_s(CH_3)$] vibrations in the ranges 3050–2950, 2970–2860, 1480–1410, 1385–1250, and 1200–800 cm^{-1}, respectively. Figure 1.25 illustrates their vibrational modes together with the observed frequencies for CH_3C1, The methylene group vibrations are also well known; the antisymmetric stretching [$\nu_a(CH_2)$], symmetric stretching [$\nu_s(CH_2)$], scissoring [$\delta(CH_2)$], wagging [$\rho_w(CH_2)$], twisting [$\rho_t,(CH_2)$], and rocking [$\rho_r(CH_2)$] vibrations appear

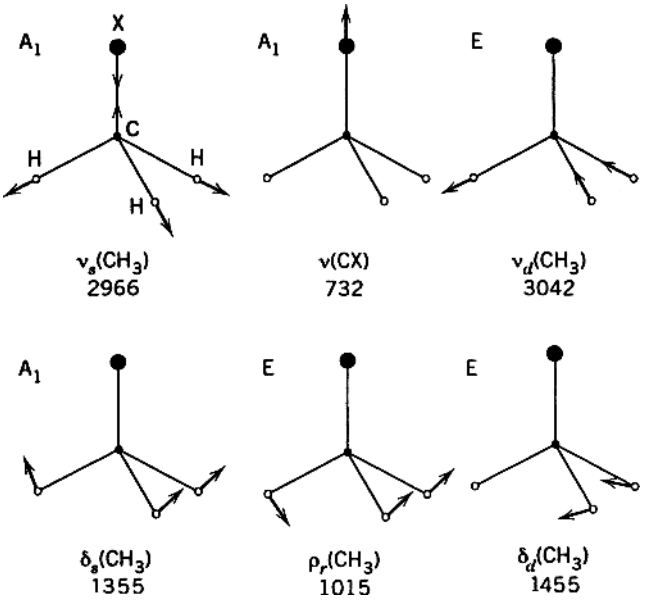

Fig. 1.25. *Approximate normal modes of a CH_3X-type molecule (frequencies are given for X=Cl). The subscripts s, d, and r denote symmetric, degenerate, and rocking vibrations, respectively. Only the displacements of the H or X atoms are shown.*

in the regions 3100–3000, 3060–2980, 1500–1350, 1400–1100, 1260–1030, and 1180–750 cm^{-1}, respectively. Figure 1.26 illustrates the normal modes of these vibrations together with the observed frequencies for CH_2C1_2. The normal modes illustrated for CH_3C1 and CH_2C1_2 are applicable to vibrational assignments of coordination and organometallic compounds, which will be discussed in Chapters 3 and 4, respectively. Group frequencies have been found for a number of organic and inorganic groups, and they have been summarized as *group frequency charts* [39,40] which are highly useful in identifying the atomic groups from observed spectra. Group frequency charts for inorganic compounds are given in Appendix VIII as well as in Figs. 2.55 and 2.61.

The concept of group frequency rests on the assumption that the vibrations of a particular group are relatively independent of those of the rest of the molecule. As stated in Sec. 1.4, however, all the nuclei of the molecule perform their harmonic oscillations in a normal vibration. Thus, an *isolated vibration*, which the group frequency would have to be, cannot be expected in polyatomic molecules. If, however, a group includes relatively light atoms such as hydrogen (OH, NH, NH_2, CH, CH_2, CH_3, etc.) or relatively heavy atoms such as the halogens (CC1, CBr, CI, etc.), as compared to other atoms in the molecule, the idea of an isolated vibration may be justified, since the amplitudes (or velocities) of the harmonic oscillation of these atoms are relatively larger or smaller than those of the other atoms in the same molecule. Vibrations of groups having multiple bonds (C≡C, C≡N, C=C, C=N, C=O, etc.) may

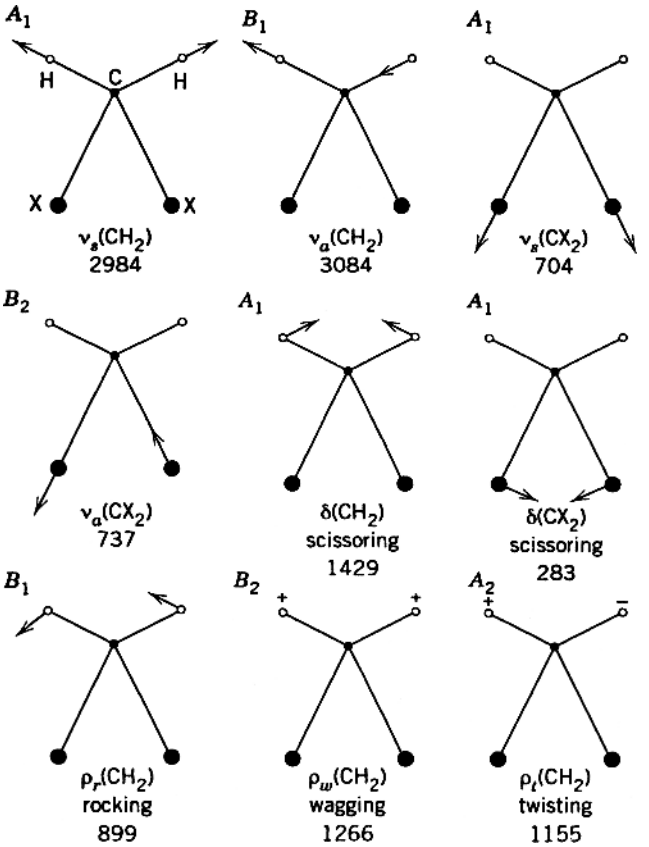

Fig. 1.26. *Approximate normal modes of a CH_2X_2-type molecule (frequencies are given for X=Cl). Only the displacements of the H or X atoms are shown.*

also be relatively independent of the rest of the molecule if the groups do not belong to a conjugated system.

If atoms of similar mass are connected by bonds of similar strength (force constant), the amplitude of oscillation is similar for each atom of the whole system. Therefore, it is not possible to isolate the group frequencies in a system like the following:

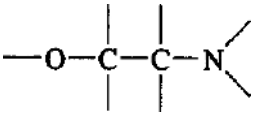

A similar situation may occur in a system in which resonance effects average out the single and multiple bonds by conjugation. Examples of this effect are seen for

the metal chelate compounds discussed in Chapter 3. When the group frequency approximation is permissible, the mode of vibration corresponding to this frequency can be inferred empirically from the band assignments obtained theoretically for simple molecules. If *coupling* between various group vibrations is serious, it is necessary to make a theoretical analysis for each individual compound, using a method like the following one.

As stated in Sec. 1.4, the generalized coordinates are related to the normal coordinates by

$$q_k = \sum_i B_{ki} Q_i \tag{1.40}$$

In matrix form, this is written as

$$\mathbf{q} = \mathbf{B}_q \mathbf{Q} \tag{1.166}$$

It can be shown [3] that the internal coordinates are also related to the normal coordinates by

$$\mathbf{R} = \mathbf{L}\mathbf{Q} \tag{1.167}$$

This is written more explicitly as

$$\begin{aligned} R_1 &= l_{11}Q_1 + l_{12}Q_2 + \cdots + l_{1N}Q_N \\ R_2 &= l_{21}Q_1 + l_{22}Q_2 + \cdots + l_{2N}Q_N \\ &\vdots \qquad\qquad \vdots \\ R_i &= l_{i1}Q_1 + l_{i2}Q_2 + \cdots + l_{iN}Q_N \end{aligned} \tag{1.168}$$

In a normal vibration in which the normal coordinate Q_N changes with frequency ν_N, all the internal coordinates, $R_1, R_2, \ldots, R_i$, change with the same frequency. The amplitude of oscillation is, however, different for each internal coordinate. The relative ratio of the amplitudes of the internal coordinates in a normal vibration associated with Q_N is given by

$$l_{1N} : I_{2N} : \cdots : I_{iN} \tag{1.169}$$

If one of these elements is relatively large compared to the others, the normal vibration is said to be predominantly due to the vibration caused by the change of this coordinate.

The ratio of l's given by Eq. 1.169 can be obtained as a column matrix (or eigenvector) $\boldsymbol{l}_N$, which satisfies the relation [3]

$$\mathbf{GF}\boldsymbol{l}_N = \boldsymbol{l}_N\boldsymbol{\lambda}_N \tag{1.170}$$

It consists of i elements, $l_{1N}, l_{2N}, \ldots, l_{iN}$, where i is the number of internal coordinates, and can be calculated if the **G** and **F** matrices are known. An assembly by columns of the l elements obtained for each λ gives the relation

$$\mathbf{GFL} = \mathbf{L}\Lambda \tag{1.171}$$

where Λ is a diagonal matrix whose elements consist of λ values.

As an example, calculate the **L** matrix of the H_2O molecule, using the results obtained in Sec. 1.15. The **G** and **F** matrices for the A_1 species are as follows:

$$\mathbf{G} = \begin{bmatrix} 1.03840 & -0.08896 \\ -0.08896 & 2.32370 \end{bmatrix}, \qquad \mathbf{F} = \begin{bmatrix} 8.32300 & 0.35638 \\ 0.35638 & 0.70779 \end{bmatrix}$$

with $\lambda_1 = 8.61475$ and $\lambda_2 = 1.60914$. The **GF** product becomes

$$\mathbf{GF} = \begin{bmatrix} 8.61090 & 0.30710 \\ 0.08771 & 1.61299 \end{bmatrix}$$

The **L** matrix can be calculated from Eq. 1.171:

$$\begin{bmatrix} 8.61090 & 0.30710 \\ 0.08771 & 1.61299 \end{bmatrix} \begin{bmatrix} l_{11} & l_{12} \\ l_{21} & l_{22} \end{bmatrix} = \begin{bmatrix} l_{11} & l_{12} \\ l_{21} & l_{22} \end{bmatrix} \begin{bmatrix} 8.61475 & 0 \\ 0 & 1.60914 \end{bmatrix}$$

However, this equation gives only the ratios l_{11}: l_{21} and l_{12}: l_{22} To determine their values, it is necessary to use the following normalization condition:

$$\mathbf{L}\tilde{\mathbf{L}} = \mathbf{G} \tag{1.172}^*$$

Then the final result is

$$\begin{bmatrix} l_{11} & l_{12} \\ l_{21} & l_{22} \end{bmatrix} = \begin{bmatrix} 1.01683 & -0.06686 \\ 0.01274 & 1.52432 \end{bmatrix}$$

---

*This equation can be derived as follows. According to Eq. 1.113, $2T = \tilde{\dot{\mathbf{R}}}\mathbf{G}^{-1}\dot{\mathbf{R}}$. On the other hand, Eq. 1.167 gives $\dot{\mathbf{R}} = \mathbf{L}\dot{\mathbf{Q}}$ and $\tilde{\dot{\mathbf{R}}} = \dot{\mathbf{Q}}\tilde{\mathbf{L}}$. Thus $2T = \dot{\mathbf{Q}}\tilde{\mathbf{L}}\mathbf{G}^{-1}\mathbf{L}\dot{\mathbf{Q}}$. Comparing this with $2T = \dot{\mathbf{Q}}\mathbf{E}\dot{\mathbf{Q}}$ (matrix form of Eq. 1.41), we obtain $\tilde{\mathbf{L}}\mathbf{G}^{-1}\mathbf{L} = \mathbf{E}$ or $\mathbf{L}\tilde{\mathbf{L}} = \mathbf{G}$.

This result indicates that, in the normal vibration Q_1, the relative ratio of amplitudes of two internal coordinates, R_1 (symmetric OH stretching) and R_2 (HOH bending), is 1.0168: 0.0127. Therefore, this vibration (3824 cm^{-1}) is assigned to an almost pure OH stretching mode. The relative ratio of amplitudes for the Q_2 vibration is −0.0669: 1.5243. Thus, this vibration is assigned to an almost pure HOH bending mode. In other cases, the l values do not provide the band assignments that are expected empirically. This occurs because the dimension of l for a stretching coordinate is different from that for a bending coordinate.

The potential energy due to a normal vibration, Q_N is written as

$$V(Q_N) = \frac{1}{2} Q_N^2 \sum_{ij} F_{ij} l_{iN} l_{jN} \qquad (1.173)^*$$

Individual $F_{ij}l_{iN}l_{jN}$ terms in the summation represent the potential energy distribution (PED) in Q_N, which gives a better measure for making band assignments [93]. In general, the value of $F_{ij}l_{iN}l_{jN}$ is large when $i = j$. Therefore, the $F_{ii}l_{iN}^2$ terms are most important in determining the distribution of the potential energy. Thus, the ratios of the $F_{ii}l_{iN}^2$ terms provide a measure of the relative contribution of each internal coordinate R_i to the normal coordinate Q_N. If any $F_{ii}l_{iN}^2$ term is exceedingly large compared with the others, the vibration is assigned to the mode associated with R_i. If $F_{ii}l_{iN}^2$ and $F_{jj}l_{jN}^2$ are relatively large compared with the others, the vibration is assigned to a mode associated with both R_i and R_j (coupled vibration).

As an example, let us calculate the potential energy distribution for the H_2O molecule. Using the **F** and **L** matrices obtained previously, we find that the $\tilde{\mathbf{L}}\mathbf{F}\mathbf{L}$ matrix is calculated to be

$$\begin{bmatrix} \begin{pmatrix} l_{11}^2F_{11} & + & l_{21}^2F_{22} & + & 2l_{21}l_{11}F_{12} \\ 8.60551 & & 0.00011 & & 0.00923 \end{pmatrix} & 0 \\ 0 & \begin{pmatrix} l_{12}^2F_{11} & + & l_{22}^2F_{22} & + & 2l_{12}l_{22}F_{12} \\ 0.03721 & & 1.644459 & & 0.07264 \end{pmatrix} \end{bmatrix}$$

Then, the potential energy distribution in each normal vibration ($F_{ii}l_{iN}^2$) is given by

$$\begin{array}{c} \\ R_1 \\ R_2 \end{array} \begin{array}{c} \begin{array}{cc} \lambda_1 & \lambda_2 \end{array} \\ \begin{bmatrix} 8.60551 & 0.03721 \\ 0.00011 & 1.64459 \end{bmatrix} \end{array}$$

---

*According to Eq. 1.111, the potential energy is written as $2V = \tilde{\mathbf{R}}\mathbf{F}\mathbf{R}$. Using Eq. 1.167, we can write this as $2V = \tilde{\mathbf{Q}}\tilde{\mathbf{L}}\mathbf{F}\mathbf{L}\mathbf{Q}$. On the other hand, Eq. 1.42 can be written as $2V = \mathbf{Q}\Lambda\mathbf{Q}$. A comparison of these two expressions gives $\Lambda = \tilde{\mathbf{L}}\mathbf{F}\mathbf{L}$. If this is written for one normal vibration whose frequency is λ_N, we have

$$\lambda_N = \sum_{ij} \tilde{l}_{Ni} F_{ij} l_{jN} = \sum_{ij} F_{ij} l_{iN} l_{jN}$$

Then the potential energy due to this vibration is expressed by Eq. 1.173.

More conveniently, PED is expressed by calculating $(F_{ii}l_{iN}^2/\Sigma F_{ii}l_{iN}^2) \times 100$ for each coordinate:

$$\begin{array}{c} \\ R_1 \\ R_2 \end{array} \begin{array}{c} \begin{array}{cc} \lambda_1 & \lambda_2 \end{array} \\ \begin{bmatrix} 99.99 & 2.21 \\ 0.01 & 97.79 \end{bmatrix} \end{array}$$

In this case, the final results are the same whether the band assignments are based on the **L** matrix or on the potential energy distribution: Q_1 is the symmetric OH stretching and Q_2 is the HOH bending. In other cases, different results may be obtained, depending on which criterion is used for band assignments.

In the example above, no serious coupling occurs between the OH stretching and HOH bending modes of H_2O in the A_1 species. This is because the vibrational frequencies of these two modes are far apart. In other cases, however, vibrational frequencies of two or more modes in the same symmetry species are relatively close to each other. Then, the l_{iN} values for these modes become comparable.

A more rigorous method of determining the vibrational mode involves drawing the displacements of individual atoms in terms of rectangular coordinates. As in Eq. 1.167, the relationship between the rectangular and normal coordinates is given by

$$\mathbf{X} = \mathbf{L}_x\mathbf{Q} \tag{1.174}$$

The $\mathbf{L}_x$ matrix can be obtained from the relationship [94]

$$\mathbf{L}_x = \mathbf{M}^{-1}\tilde{\mathbf{B}}\mathbf{G}^{-1}\mathbf{L} \tag{1.75)*}$$

The matrices on the right-hand sides have already been defined.

Three-dimensional drawings of normal modes, such as those shown in Chapter 2, can be made from the Cartesian displacement calculations obtained above. However, hand plotting of these data is laborious and complicated. Use of computer plotting programs greatly facilitates this process [95].

1.19. INTENSITY OF INFRARED ABSORPTION [16]

The absorption of strictly monochromatic light (v) is expressed by the Lambert–Beer law:

$$I_v = I_{0,v}e^{-\alpha_v pl} \tag{1.176}$$

*By combining Eqs. 1.118 and 1.174, we have $\mathbf{R} = \mathbf{BX} = \mathbf{BL}_x\mathbf{Q}$. Since $\mathbf{R} = \mathbf{LQ}$ (Eq. 1.167), it follows that $\mathbf{LQ} = \mathbf{BL}_x\mathbf{Q}$ or $\mathbf{L} = \mathbf{BL}_x$. The kinetic energy is written as $2T = \dot{\tilde{\mathbf{X}}}\mathbf{M}\dot{\mathbf{X}}$. In terms of internal coordinates, it is written as $2T = \dot{\tilde{\mathbf{R}}}\mathbf{G}^{-1}\dot{\mathbf{R}} = \dot{\tilde{\mathbf{X}}}\tilde{\mathbf{B}}\mathbf{G}^{-1}\mathbf{B}\dot{\mathbf{X}}$. By comparing these two expressions, we have $\mathbf{M} = \tilde{\mathbf{B}}\mathbf{G}^{-1}\mathbf{B}$. Then we can write $\mathbf{L}_x = \mathbf{M}^{-1}\mathbf{M}\mathbf{L}_x = \mathbf{M}^{-1}\tilde{\mathbf{B}}\,\mathbf{G}^{-1}\mathbf{B}\mathbf{L}_x = \mathbf{M}^{-1}\tilde{\mathbf{B}}\mathbf{G}^{-1}\mathbf{L}$.

where I_v is the intensity of the light transmitted by a cell of length l containing a gas at pressure p, $I_{0,v}$ is the intensity of the incident light, and α_v is the absorption coefficient for unit pressure. The true integrated absorption coefficient A is defined by

$$A = \int_{\text{band}} \alpha_v dv = \frac{1}{pl} \int_{\text{band}} \ln\left(\frac{I_{0,v}}{I_v}\right) dv \tag{1.177}$$

where the integration is carried over the entire frequency region of a band.

In practice, I_v and $I_{0,v}$ cannot be measured accurately, since no spectrophotometers have infinite resolving power. Therefore we measure instead the apparent intensity T_v:

$$T_v = \int_{\text{slit}} I(v) g(v, v') dv \tag{1.178}$$

where $g(v, v')$ is a function indicating the amount of light of frequency v when the spectrophotometer reading is set at v'. Then the apparent integrated absorption coefficient B is defined by

$$B = \frac{1}{pl} \int_{\text{band}} \ln \frac{\int_{\text{slit}} I_0(v) g(v, v') dv}{\int_{\text{slit}} I(v) g(v, v') dv} dv' \tag{1.179}$$

It can be shown that

$$\lim_{pl \to 0} (A - B) = 0 \tag{1.180}$$

if I_0 and α_v are constant within the slit width used. (This condition is approximated by using a narrow slit.) In practice, we plot B/pl against pl, and extrapolate the curve to $pl \to 0$. To apply this method to gaseous molecules, it is necessary to broaden the vibrational–rotational bands by adding a high-pressure inert gas (pressure broadening).

For liquids and solutions, p and α in the preceding equations are replaced by M (molar concentration) and ε (molar absorption coefficient), respectively. However, the extrapolation method just described is not applicable, since experimental errors in determining B values become too large at low concentration or at small cell length. The true integrated absorption coefficient of a liquid can be calculated if we assume that the shape of an absorption band is represented by the Lorentz equation and that the slit function is triangular [96].

Theoretically, the true integrated absorption coefficient A_N of the Nth normal vibration is given by [3]

$$A_N = \frac{n\pi}{3c} \left[\left(\frac{\partial \mu_x}{\partial Q_N}\right)_0^2 + \left(\frac{\partial \mu_y}{\partial Q_N}\right)_0^2 + \left(\frac{\partial \mu_z}{\partial Q_N}\right)_0^2 \right] \tag{1.181}$$

where n is the number of molecules per cubic centimeter, and c is the velocity of light. As shown by Eq. 1.167, an internal coordinate R_i is related to a set of normal

coordinates by

$$R_i = \sum_N L_{iN} Q_N \tag{1.182}$$

If the additivity of the bond dipole moment is assumed, it is possible to write

$$\begin{aligned} \frac{\partial \mu}{\partial Q_N} &= \sum_i \left(\frac{\partial \mu}{\partial R_i}\right)\left(\frac{\partial R_i}{\partial Q_N}\right) \\ &= \sum_i \left(\frac{\partial \mu}{\partial R_i}\right) L_{iN} \end{aligned} \tag{1.183}$$

Then Eq. 1.181 is written as

$$\begin{aligned} A_N &= \frac{n\pi}{3c}\left[\left(\sum_i \frac{\partial \mu_x}{\partial R_i} L_{iN}\right)_0^2 + \left(\sum_i \frac{\partial \mu_y}{\partial R_i} L_{iN}\right)_0^2 + \left(\sum \frac{\partial \mu_z}{\partial R_i} L_{iN}\right)_0^2\right] \\ &= \frac{n\pi}{3c}\sum_i \left[\left(\frac{\partial \mu_x}{\partial R_i}\right)_0^2 + \left(\frac{\partial \mu_y}{\partial R_i}\right)_0^2 + \left(\frac{\partial \mu_z}{\partial R_i}\right)_0^2\right](L_{iN})^2 \end{aligned} \tag{1.184}$$

This equation shows that the intensity of an infrared band depends on the values of the $\partial\mu/\partial R$ terms as well as the L matrix elements.

Equation 1.184 has been applied to relatively small molecules to calculate the $\partial\mu/\partial R$ terms from the observed intensity and known L_{iN} values [7]. However, the additivity of the bond dipole moment does not strictly hold, and the results obtained are often inconsistent and conflicting. Thus far, very few studies have been made on infrared intensities of large molecules because of these difficulties.

As seen in Eq. 1.184, the IR band becomes stronger as the $\partial\mu/\partial R$ term becomes larger if the L_{iN} term does not vary significantly. In general, the more polar the bond, the larger the $\partial\mu/\partial R$ term. Thus, the IR intensities of the stretching vibrations follow the general trends:

$$\nu(\mathrm{OH}) > \nu(\mathrm{NH}) > \nu(\mathrm{CH})$$
$$\nu(\mathrm{C{=}O}) > \nu(\mathrm{C{=}N}) > \nu(\mathrm{C{=}C})$$

It is also noted that the antisymmetric stretching vibration is always stronger than the symmetric stretching vibration because the $\partial\mu/\partial R$ term is larger for the former than for the latter. This can be seen for functional groups such as $\rangle\mathrm{CH_2}$ and $\rangle\mathrm{CCl_2}$. These trends are entirely opposite to those found in Raman spectra (Sec. 1.21), and make both IR and Raman spectroscopy complementary.

1.20. DEPOLARIZATION OF RAMAN LINES

As stated in Secs. 1.8 and 1.9, it is possible, by using group theory, to classify the normal vibration into various symmetry species. Experimentally, measurements of the

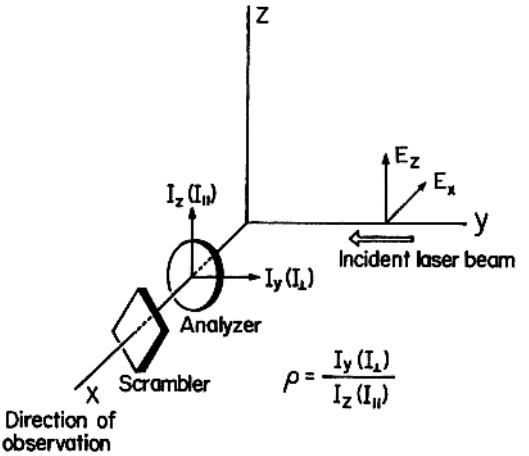

Fig. 1.27. *Experimental configuration for measuring depolarization ratios. The scrambler is placed after the analyzer because the monochromator gratings show different efficiencies for ⊥ and ∥ directions.*

infrared dichroism and polarization properties of Raman lines of an orientated crystal provide valuable information about the symmetry of normal vibrations (Sec. 1.31). Here, we consider the polarization properties of Raman lines in liquids and solutions in which molecules or ions take completely random orientations.*

Suppose that we irradiate a molecule fixed at the origin of a space-fixed coordinate system with natural light from the positive-y direction, and observe the Raman scattering in the x direction as shown in Fig. 1.27. The incident light vector E may be resolved into two components, E_x and E_z, of equal magnitude ($E_y = 0$). Both components give induced dipole moments, P_x, P_y, and P_z. However, only P_y and P_z contribute to the scattering along the x axis, since an oscillating dipole cannot radiate in its own direction. Then, from Eq. 1.66, we have.

$$P_y = \alpha_{yx}E_x + \alpha_{yz}E_z \tag{1.185}$$
$$P_z = \alpha_{zx}E_x + \alpha_{zz}E_z \tag{1.186}$$

The intensity of the scattered light is proportional to the sum of squares of the individual $\alpha_{ij}E_j$ terms. Thus, the ratio of the intensities in the y and z directions is

$$\rho_n = \frac{I_y}{I_z} = \frac{\alpha_{yx}^2E_x^2 + \alpha_{yz}^2E_z^2}{\alpha_{zx}^2E_x^2 + \alpha_{zz}^2E_z^2} \tag{1.187}$$

where ρ_n is called the *depolarization ratio for natural light* (n).

In a homogeneous liquid or gas, the molecules are randomly oriented, and we must consider the polarizability components averaged over all molecular

*It is possible to obtain approximate depolarization ratios of fine powders where the molecules or ions take pseudorandom orientations (see Ref. 97).

orientations. The results are expressed in terms of two quantities: $\bar{\alpha}$ (*mean value*) and γ (*anisotropy*):

$$\bar{\alpha} = \frac{1}{3}(\alpha_{xx} + \alpha_{yy} + \alpha_{zz}) \tag{1.188}$$

$$\gamma^2 = \frac{1}{2}\left[(\alpha_{xx} - \alpha_{yy})^2 + (\alpha_{yy} - \alpha_{zz})^2 + (\alpha_{zz} - \alpha_{xx})^2 + 6(\alpha_{xy}^2 + \alpha_{yz}^2 + \alpha_{zx}^2)\right] \tag{1.189}$$

These two quantities are invariant to any coordinate transformation. It can be shown [3] that the average values of the squares of α_{ij} are

$$\overline{(\alpha_{xx})^2} = \overline{(\alpha_{yy})^2} = \overline{(\alpha_{zz})^2} = \frac{1}{45}[45(\bar{\alpha})^2 + 4\gamma^2] \tag{1.190}$$

$$\overline{(\alpha_{xy})^2} = \overline{(\alpha_{yz})^2} = \overline{(\alpha_{zx})^2} = \frac{1}{15}\gamma^2 \tag{1.191}$$

Since $E_x = E_z = E$, Eq. 1.187 can be written as

$$\rho_n = \frac{I_y}{I_z} = \frac{6\gamma^2}{45(\bar{\alpha})^2 + 7\gamma^2} \tag{1.192}$$

The total intensity I_n is given by

$$I_n = I_y + I_z = \text{const}\left\{\frac{1}{45}[45(\bar{\alpha})^2 + 13\gamma^2]\right\}E^2 \tag{1.193}$$

If the incident light is plane-polarized (e.g., a laser beam), with its electric vector in the z direction ($E_x = 0$), Eq. 1.192 becomes

$$\rho_p = \frac{I_y}{I_z} = \frac{3\gamma^2}{45(\bar{\alpha})^2 + 4\gamma^2} \tag{1.194}$$

where ρ_p is the *depolarization ratio for polarized light* (p). In this case, the total intensity is given by

$$I_p = I_y + I_z = \text{const}\left\{\frac{1}{45}[45(\bar{\alpha})^2 + 7\gamma^2]\right\}E^2 \tag{1.195}$$

The symmetry property of a normal vibration can be determined by measuring the depolarization ratio. From an inspection of character tables (Appendix I), it is obvious that $\bar{\alpha}$ is nonzero only for totally symmetric vibrations. Then, Eq. 1.192 gives $0 \leq \rho_n < \frac{6}{7}$, and the Raman lines are said to be *polarized*. For all nontotally symmetric vibrations, $\bar{\alpha}$ is zero, and $\rho_n = \frac{6}{7}$. Then, the Raman lines are said to be *depolarized*. If the exciting line is plane polarized, these criteria must be changed according to

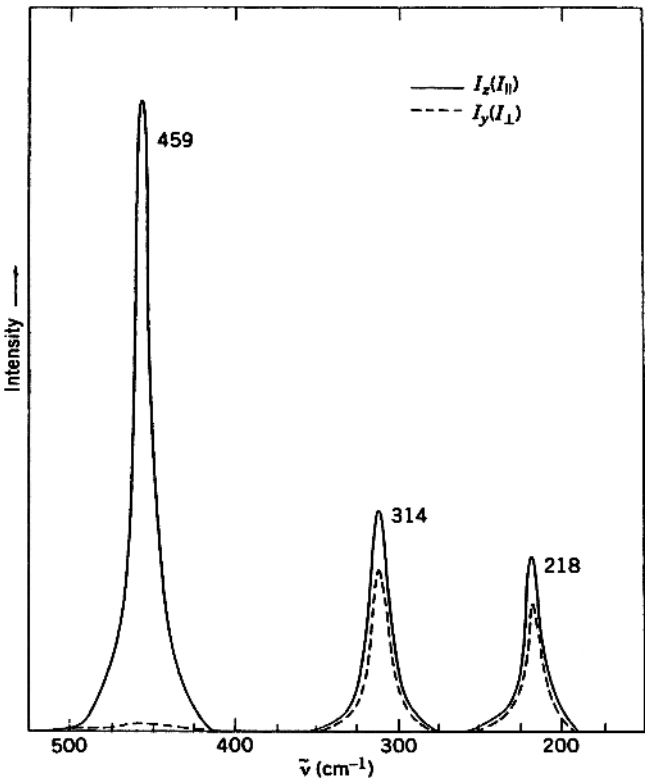

Fig. 1.28. *Raman spectra of CCl_4 in two directions of polarization (488 nm excitation).*

Eq. 1.194. Thus, $0 \leq \rho_p < \frac{3}{4}$ for totally symmetric vibrations, and $\rho_p = \frac{3}{4}$ for nontotally symmetric vibrations. Figure 1.28 shows the Raman spectra of CCl_4 (500–150 cm^{-1}) in two directions of polarization obtained with the 488 nm excitation. The three bands at 459, 314, and 218 cm^{-1} give ρ_p values of approximately 0.02, 0.75, and 0.75, respectively. Thus, it is concluded that the 459 cm^{-1} band is polarized (A_1), whereas the two bands at 314 (F_2) and 218 (E) cm^{-1} are depolarized.

As stated in Sec. 1.6, the polarizability tensors are symmetric in normal Raman scattering. If the exciting frequency approaches that of an electronic absorption, some scattering tensors become antisymmetric,* and resonance Raman scattering can occur (Sec. 1.22). In this case, Eq. 1.194 must be written in a more general form [98]

$$\rho_p = \frac{3g^s + 5g^a}{10g^o + 4g^s} \tag{1.196}$$

*A tensor is called antisymmetric if $\alpha_{xx} = \alpha_{yy} = \alpha_{zz} = 0$ and $\alpha_{xy} = -\alpha_{yx}, \alpha_{yz} = -\alpha_{zy}$, and $\alpha_{zx} = -\alpha_{xz}$.

where

$$
\begin{aligned}
g^o &= 3(\bar{\alpha})^2 \\
g^s &= \frac{1}{3}\left[(\alpha_{xx}-\alpha_{yy})^2+(\alpha_{yy}-\alpha_{zz})^2+(\alpha_{zz}-\alpha_{xx})^2\right] \\
&\quad + \frac{1}{2}\left[(\alpha_{xy}+\alpha_{yx})^2+(\alpha_{xz}+\alpha_{zx})^2+(\alpha_{yz}+\alpha_{zy})^2\right] \\
g^a &= \frac{1}{2}\left[(\alpha_{xy}-\alpha_{yx})^2+(\alpha_{xz}-\alpha_{zx})^2+(\alpha_{yz}-\alpha_{zy})^2\right]
\end{aligned}
\tag{1.197}
$$

If we define

$$
\gamma_s^2 = \frac{3}{2}g^s \quad \text{and} \quad \gamma_{as}^2 = \frac{3}{2}g^a \tag{1.198}
$$

Eq. 1.196 can be written as

$$
\rho_p = \frac{3\gamma_s^2 + 5\gamma_{as}^2}{45(\bar{\alpha})^2 + 4\gamma_s^2} \tag{1.199}
$$

In normal Raman scattering, $\gamma_s^2 = \gamma^2$ and $\gamma_{as}^2 = 0$. Then Eq. 1.199 is reduced to Eq. 1.194.

The symmetry properties of resonance Raman lines can be predicted on the basis of Eq. 1.199. For totally symmetric vibrations, $\bar{\alpha} \neq 0$ and $\gamma_{as} = 0$. Then, Eq. 20.15 gives $0 \leq \rho_p < \frac{3}{4}$. Nontotally symmetric vibrations ($\bar{\alpha} = 0$) are classified into two types: those that have symmetric scattering tensors, and those that have antisymmetric scattering tensors. If the tensor is symmetric, $\gamma_{as} = 0$ and $\gamma_s \neq 0$. Then Eq. 1.199 gives $\rho_p = \frac{3}{4}$ (depolarized). If the tensor is antisymmetric, $\gamma_{as} \neq 0$ and $\gamma_s = 0$. Then, Eq. 1.199 gives $\rho_p = \infty$ (*inverse polarization*). In the case of the $\mathbf{D}_{4h}$ point group, the B_{1g} and B_{2g} representations belong to the former type, whereas the A_{2g} representations belongs to the latter [99]. As will be shown in Sec. 1.22, Spiro and Strekas [98] observed for the first time A_{2g} vibrations which exhibit ρ_p values $\frac{3}{4} < \rho_p < \infty$. For these vibrations, the term "anomalous polarization (*ap*)" is used instead of "inverse polarization (*ip*)" [100].

1.21. INTENSITY OF RAMAN SCATTERING

According to the quantum mechanical theory of light scattering, the intensity per unit solid angle of scattered light arising from a transition between states m and n is given by

$$
I_{n \leftarrow m} = \text{const}(\nu_0 \pm \nu_{mn})^4 \sum_{\rho\sigma} |(P_{\rho\sigma})_{mn}|^2 \tag{1.200}
$$

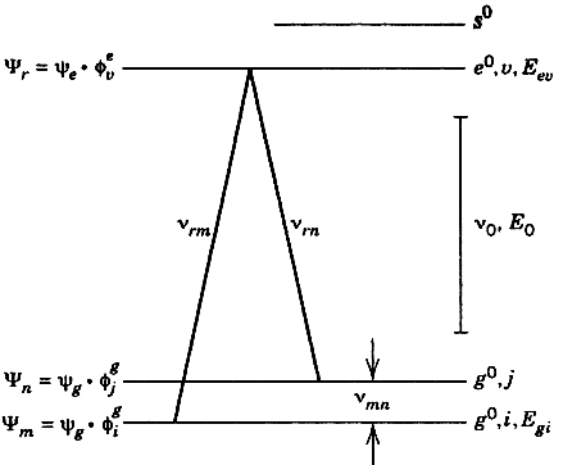

Fig. 1.29. *Energy-level diagram for Raman scattering.*

where

$$(P_{\rho\sigma})_{mn} = (\alpha_{\rho\sigma})_{mn}E = \frac{1}{h}\sum_r \left[\frac{(M_\rho)_{rn}(M_\sigma)_{mr}}{\nu_{rm} - \nu_0} + \frac{(M_\rho)_{mr}(M_\sigma)_{rn}}{\nu_{rn} + \nu_0}\right]E \qquad (1.201)$$

Here ν_0 is the frequency of the incident light: ν_{rm}, ν_{rn}, and ν_{mn} are the frequencies corresponding to the energy differences between subscripted states; terms of the type $(M_\sigma)_{mr}$ are the Cartesian components of transition moments such as $\int \Psi_r^* \mu_\sigma \Psi_m d\tau$; and E is the electric vector of the incident light. It should be noted here that the states denoted by m, n, and r represent vibronic states $\psi_g(\xi, Q)\phi_i^g(Q)$, $\psi_g(\xi, Q)\phi_j^g(Q)$ and $\psi_e(\xi, Q)\phi_v^e(Q)$, respectively, where ψ_g and ψ_e are electronic ground- and excited-state wavefunctions, respectively, and ϕ_i^g, ϕ_j^g, and ϕ_v^e vibrational functions. The symbols ξ and Q represent the electronic and nuclear coordinates, respectively. These notations are illustrated in Fig. 1.29. Finally, σ and ρ denote x, y, and z components.

Since the electric dipole operator acts only on the electronic wavefunctions, the $(\alpha_{\rho\sigma})_{mn}$ term in Eq. 1.201 can be written in the form

$$(\alpha_{\rho\sigma})_{mn} = \frac{1}{h}\int \phi_j^g (\alpha_{\rho\sigma})_{gg} \phi_j^g dQ \qquad (1.202)$$

where

$$(\alpha_{\rho\sigma})_{gg} = \sum_e \left(\frac{\int \psi_g^* \mu_\sigma \psi_e d\tau \cdot \int \psi_e^* \mu_\rho \psi_g d\tau}{\bar{\nu}_{eg} - \nu_0} + \frac{\int \psi_g^* \mu_\rho \psi_e d\tau \cdot \int \psi_e^* \mu_\sigma \psi_g d\tau}{\bar{\nu}_{eg} + \nu_0}\right)$$

Here $\bar{\nu}_{eg}$ corresponds to the energy of a pure electronic transition between the ground and excited states.

To discuss the Raman scattering, we expand the $(\alpha_{\rho\sigma})_{gg}$ term as a Taylor series with respect to the normal coordinate Q:

$$(\alpha_{\rho\sigma})_{gg} = (\alpha_{\rho\sigma})^0_{gg} + \left[\frac{\partial(\alpha_{\rho\sigma})_{gg}}{\partial Q}\right]_0 Q + \cdots \tag{1.203}$$

Then, we write Eq. 1.202 as

$$(\alpha_{\rho\sigma})_{mn} = \frac{1}{h}(\alpha_{\rho\sigma})^0_{gg}\int \phi^g_j \phi^g_i dQ + \frac{1}{h}\left[\frac{\partial(\alpha_{\rho\sigma})_{gg}}{\partial Q}\right]_0 \int \phi^g_j Q \phi^g_i dQ \tag{1.204}$$

The first term on the right-hand side is zero unless $i = j$. This term is responsible for Rayleigh scattering. The second term determines the activity of fundamental vibrations in Raman scattering; it vanishes for a harmonic oscillator unless $j = i \pm 1$ (Sec. 1.10).

If we consider a Stokes transition, $\upsilon \rightarrow \upsilon + 1$, Eq. 1.204 is written as [3]

$$(\alpha_{\rho\sigma})_{\upsilon,\upsilon+1} = \frac{1}{h}\left[\frac{\partial(\alpha_{\rho\sigma})_{gg}}{\partial Q}\right]_0 \sqrt{\frac{(\upsilon+1)h}{8\pi^2\mu\nu}} \tag{1.205}$$

where μ and ν are the reduced mass and the Stokes frequency. Then Eq. 1.200 is written as

$$I = \text{const}(\nu_0 - \nu)^4 \frac{E^2}{h^2}\left[\frac{\partial(\alpha_{p\sigma})_{gg}}{\partial Q}\right]^2_0 \frac{(\upsilon+1)h}{8\pi^2\mu\nu} \tag{1.206}$$

In Sec. 1.20, we derived a classical equation for Raman intensity:

$$\begin{aligned} I_n &= \text{const}\left(\frac{\partial\alpha}{\partial Q}\right)^2 E^2 \\ &= \text{const}\left\{\frac{1}{45}[45(\bar{\alpha})^2 + 13\gamma^2]\right\}E^2 \end{aligned} \tag{1.193}$$

By replacing the $\partial\alpha/\partial Q$ term of Eq. 1.206 with the term enclosed in braces in Eq. 1.193, we obtain

$$I_n = \text{const}(\nu_0 - \nu)^4 \frac{(\upsilon+1)}{8\pi^2\mu\nu}\frac{E^2}{h^2}\left\{\frac{1}{45}[45(\bar{\alpha})^2 + 13\gamma^2]\right\} \tag{1.207}$$

At room temperature, most of the scattering molecules are in the $\upsilon = 0$ state, but some are in higher vibrational states. Using the Maxwell–Bolztmann distribution

law, we find that the fraction of molecules f_v with vibrational quantum number v is given by

$$f_v = \frac{e^{-[v+(1/2)]hv/kT}}{\sum_v e^{-[v+(1/2)]hv/kT}} \tag{1.208}$$

Then the total intensity is proportional to $\sum_v f_v(v+1)$, which is equal to $(1-e^{-hv/kT})^{-1}$ (see Ref. 23). Hence we can rewrite Eq. 1.207 in the form

$$I_n = KI_0 \frac{(v_0 - v)^4}{\mu v(1-e^{-hv/kT})}[45(\bar{\alpha})^2 + 13\gamma^2] \tag{1.209}$$

Here I_0 is the incident light intensity which is proportional to E^2, and K summarizes all other constant terms.

If the incident light is polarized, the form of Eq. 1.209 is slightly modified:

$$I_\rho = KI_0 \frac{(v_0 - v)^4}{\mu v(1-e^{-hv/kT})}[45(\bar{\alpha})^2 + 7\gamma^2] \tag{1.210}$$

As shown in Sec. 1.20, the degree of depolarization ρ_p is

$$\rho_p = \frac{3\gamma^2}{45(\bar{\alpha})^2 + 4\gamma^2} \quad \text{or} \quad \gamma^2 = \frac{45(\bar{\alpha})^2\rho_p}{3-4\rho_p} \tag{1.211}$$

Since $\rho_p = \frac{3}{4}$ for nontotally symmetric vibrations, Eq. 1.211 holds only for totally symmetric vibrations. Then Eq. 1.210 is written as

$$I_p = K' I_0 \frac{(v_0 - v)^4}{\mu v(1-e^{-hv/kT})}\left(\frac{1+\rho_p}{3-4\rho_p}\right)(\bar{\alpha})^2 \tag{1.212}$$

In the case of a solution, the intensity is proportional to the molar concentration C. Then Eq. 1.212 is written as

$$I_p = K'' I_0 \frac{C(v_0 - v)^4}{\mu v(1-e^{-hv/kT})}\left(\frac{1+\rho_p}{3-4\rho_p}\right)(\bar{\alpha})^2 \tag{1.213}$$

If we compare the intensities of totally symmetric vibrations (A_1 mode) of two tetrahedral XY_4-type molecules, the intensity ratio is given by

$$\frac{I_1}{I_2} = \frac{C_1}{C_2}\left(\frac{\tilde{\nu}_0 - \tilde{\nu}_1}{\tilde{\nu}_0 - \tilde{\nu}_2}\right)^4 \frac{\tilde{\nu}_2\mu_2}{\tilde{\nu}_1\mu_1}\frac{(1-e^{-hc\tilde{\nu}_2/kT})(\bar{\alpha}_1)^2}{(1-e^{-hc\tilde{\nu}_1/kT})(\bar{\alpha}_2)^2} \tag{1.214}$$

In this case, the ρ_p term drops out, since $\gamma^2 = 0$ for isotropic molecules such as tetrahedral XY_4 and octahedral XY_6 types. By using CCl_4 as the standard, it is possible to determine the relative value of the $\partial\alpha/\partial Q$ term, which provides information about the degree of covalency and the bond order [23].

As seen above, the intensity of Raman scattering increases as the $(\partial\alpha/\partial Q)_0$ term becomes larger. The following general rules may reflect the trends in the $(\partial\alpha/\partial Q)_0$ values: (1) stretching vibrations produce stronger Raman bands than do bending vibrations; (2) symmetric vibrations produce stronger Raman bands than do antisymmetric vibrations, and totally symmetric "breathing" vibrations produce the most intense Raman bands; (3) stretching vibrations of covalent bonds produce Raman bands stronger than those of ionic bonds (among the covalent bonds, Raman intensities increase as the bond order increases; thus, the ratio of relative intensities of the C≡C, C=C, and C−C stretching vibrations is approximately 3:2:1); and (4) bonds involving heavier atoms produce stronger Raman bands than do those involving lighter atoms. For example, the ν(S−S) is stronger than the ν(C−C). Coordination compounds containing heavy metals and sulfur ligands are ideal for Raman studies.

1.22. PRINCIPLE OF RESONANCE RAMAN SPECTROSCOPY

In normal Raman spectroscopy, the exciting frequency lies in the region where the compound has no electronic absorption band. In resonance Raman spectroscopy, the exciting frequency falls within the electronic band (Sec. 1.2). In the gaseous phase, this tends to cause resonance fluorescence since the rotational–vibrational levels are discrete. In the liquid and solid states, however, these levels are no longer discrete because of molecular collisions and/or intermolecular interactions. If such a broad vibronic bands is excited, it tends to give resonance Raman rather than resonance fluorescence spectra [101,102].

Resonance Raman spectroscopy is particularly suited to the study of biological macromolecules such as heme proteins because only a dilute solution (biological condition) is needed to observe the spectrum and only vibrations localized within the chromophoric group are enhanced when the exciting frequency approaches that of the relevant chromophore. This *selectivity* is highly important in studying the theoretical relationship between the electronic transition and the vibrations to be resonance-enhanced.

The origin of resonance Raman enhancement is explained in terms of Eq. 1.201. In normal Raman spectroscopy, ν_0 is chosen in the region that is far from the electronic absorption. Then, $\nu_{rm} \gg \nu_0$, and $\alpha_{\rho\sigma}$ is independent of the exciting frequency ν_0. In resonance Raman spectroscopy, the denominator, $\nu_{rm} - \nu_0$, becomes very small as ν_0 approaches ν_{rm}. Thus, the first term in the square brackets of Eq. 1.201 dominates all other terms and results in striking enhancement of Raman lines. However, Eq. 1.201 cannot account for the selectivity of resonance Raman enhancement since it is not specific about the states of the molecule. Albrecht [103] derived a more specific equation for the initial and final states of resonance Raman scattering by

introducing the Herzberg–Teller expansion of electronic wave functions into the Kramers–Heisenberg dispersion formula. The results are as follows:

$$(\alpha_{\rho\sigma})_{gi,gj} = A + B + C \tag{1.215}$$

$$A = \sum_{e\neq g}{}' \sum_{v} \left[\frac{(g^0|R_\sigma|e^0)(e^0|R_\rho|g^0)}{E_{ev} - E_{gi} - E_0} + (\text{nonresonance term}) \right] \langle i|v\rangle\langle v|j\rangle \tag{1.216}$$

$$B = \sum_{e\neq g}{}' \sum_{v} \sum_{s\neq e}{}' \sum_{a} \left\{ \left[\frac{(g^0|R_\sigma|e^0)(e^0|h_a|s^0)(s^0|R_\rho|g^0)}{E_{ev} - E_{gi} - E_0} + (\text{nonresonance term}) \right] \times \frac{\langle i/v\rangle\langle v/Q_a|j\rangle}{E_e^0 - E_s^0} + \left[\frac{(g^0|R_\sigma|s^0)(s^0|h_a|e^0)(e^0|R_\rho|g^0)}{E_{ev} - E_{gi} - E_0} + (\text{nonresonance term}) \right] \times \frac{\langle i|Q_a|v\rangle\langle v/j\rangle}{E_e^0 - E_s^0} \right\} \tag{1.217}$$

$$C = \sum_{e\neq g}{}' \sum_{t\neq g}{}' \sum_{v} \sum_{a} \left\{ \left[\frac{(e^0|R_\rho|g^0)(g^0|h_a|t^0)(t^0|R_\sigma|e^0)}{E_{ev} - E_{gi} - E_0} + (\text{nonresonance term}) \right] \times \frac{\langle i|v\rangle\langle v|Q_a|j\rangle}{E_g^0 - E_t^0} + \left[\frac{(e^0|R_\rho|t^0)(t^0|h_a|g^0)(g^0|R_\sigma|e^0)}{E_{ev} - E_{gi} - E_0} + (\text{nonresonance term}) \right] \times \frac{\langle i|Q_a|v\rangle\langle v|j\rangle}{E_g^0 - E_t^0} \right\} \tag{1.218}$$

The notations g, i, j, e, and v were explained in Sec. 1.21. Other notations are as follows: s, another excited electronic state; h_a, the vibronic coupling operator $\partial\mathcal{H}/\partial Q_a$, $\mathcal{H}$, and Q_a, the electronic Hamiltonian and the ath normal coordinate of the electronic ground state, respectively; E_{gi} and E_{ev}, the energies of states gi and ev, respectively; $|g^0)$, $|e^0)$, and $|s^0)$, the electronic wavefunctions for the equilibrium nuclear positions of the ground and excited states; E_e^0 and E_s^0, the corresponding energies of the electronic states, e^0 and s^0, respectively; and E_0, the energy of the exciting light. The nonresonance terms are similar to the preceding terms except that the denominator is $(E_{ev} - E_{gj} + E_0)$ instead of $(E_{ev} - E_{gj} - E_0)$ and that R_σ and R_p (Cartesian components of the transition moment) in the numerator are interchanged. These terms can be neglected under the strict resonance condition since the resonance terms become very large. The C term is usually neglected because its components are denominated by $E_g^0 - E_t^0$, where t refers to an excited state that is much higher in energy than the first excited state. These notations are shown on the right-hand side of Fig. 1.29. In more rigorous expressions, the damping factor $i\Gamma$ must be added to the

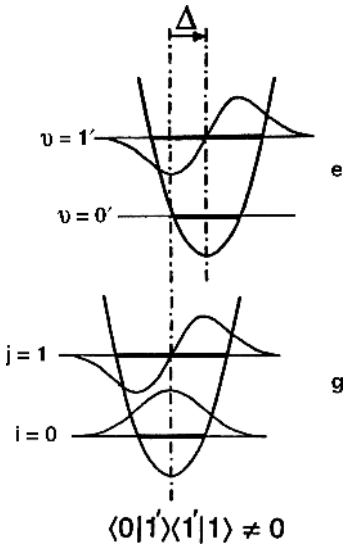

Fig. 1.30. *Shift of equilibrium position caused by totally symmetric vibration.*

denominators such as $E_{ev} - E_{gj} - E_0$ so that the resonance term does not become infinity under rigorous resonance conditions [103].

For the A term to be nonzero, the $g \leftrightarrow e$ electronic transition must be allowed, and the product of the integrals $\langle i \mid v \rangle \langle v \mid j \rangle$ (Franck–Condon factor) must be nonzero. The latter condition is satisfied if the equilibrium position is shifted by a transition ($\Delta \neq 0$ as shown in Fig. 1.30). Totally symmetric vibrations tend to be resonance-enhanced via the A term since they tend to shift the equilibrium position upon electronic excitation. If the equilibrium position is not shifted by the $g \leftrightarrow e$ transition, the A term becomes zero since either one of the integrals, $(i \mid v)$ or $(v \mid j)$, becomes zero. This situation tends to occur for nontotally symmetric vibrations.

In contrast to the A term, the B term resonance requires at least one more electronic excited state(s), which must be mixed with the e state via normal vibration, Q_a. Namely, the integral $(e^0 \mid h_a \mid s^0)$ must be nonzero. The B-term resonance is significant only when these two excited states are closely located so that the denominator, $E_e^0 - E_s^0$, is small. Other requirements are that the $g \leftrightarrow e$ and $g \leftrightarrow s$ transitions should be allowed and that the integrals $\langle i \mid v \rangle$ and $\langle v \mid Q_a \mid j \rangle$ should not be zero. The B term can cause resonance enhancement of nontotally symmetric as well as totally symmetric vibrations, although it is mainly responsible for resonance enhancement of the former.

As seen in Eqs. 1.216 and 1.217, both A and B terms involve summation over v, which is the vibrational quantum number at the electronic excited state. Since the harmonic oscillator selection rule ($\Delta v = \pm 1$) does not hold for a large v, overtones and combination bands may appear under resonance conditions. In fact, series of these nonfundamental vibrations have been observed in the case of A-term resonance (Sec. 1.23).

In Sec. 1.20, we have shown that the depolarization ratio for totally symmetric vibrations is in the range $0 \leq \rho_p < \frac{3}{4}$. For the A term to be nonzero, however, the term $(g^0 | R_\sigma | e^0)(e^0 | R_\rho | g^0)$ must be nonzero. Since g^0 is totally symmetric, this condition is realized only when both $\chi(R_\sigma)\chi(e^0)$ and $\chi(R_\rho)\chi(e^0)$ belong to the totally symmetric species. Thus, $\chi(R_\sigma) = \chi(R_\rho)$, and only one of the diagonal terms of the polarizability tensor (α_{xx}, α_{yy}, or α_{zz}) becomes nonzero. Then, it is readily seen from Eq. 1.199 that $\rho_p = \frac{1}{3}$. This rule has been confirmed by many observations. If the electronic excited state is degenerate, two of the diagonal terms must be nonzero. In this case, $\rho_p = \frac{1}{8}$. These rules hold for any point group with at least one C_3 or higher axis, with the exception of the cubic groups in which the Cartesian coordinates transform as a single irreducible degenerate representation.

1.23. RESONANCE RAMAN SPECTRA

Because of the advantages mentioned in the preceding section, resonance Raman (RR) spectroscopy has been applied to vibrational studies of a number of inorganic as well as organic compounds. It is currently possible to cover the whole range of electronic transitions continuously by using excitation lines from a variety of lasers and Raman shifters [26]. In particular, the availability of excitation lines in the UV region has made it possible to carry out UV resonance Raman (UVRR) spectroscopy [104].

In RR spectroscopy, the excitation line is chosen inside the electronic absorption band. This condition may cause thermal decomposition of the sample by local heating. To minimize thermal decomposition, several techniques have been developed. These include the rotating sample technique, the rotating (or oscillating) laser beam technique, and their combinations with low-temperature techniques [21,26]. It is always desirable to keep low laser power so that thermal decomposition is minimal. This will also minimize photodecomposition, which occurs depending on laser lines in some compounds.

An example of the A-term resonance is given by I_2, which has an absorption band near 500 nm and its fundamental at $\sim 210\ \text{cm}^{-1}$. Figure 1.31 shows the RR spectrum of I_2 in solution obtained by Kiefer and Bernstein [105] (excitation at 514.5 nm). It shows a series of overtones up to the seventeenth. The vibrational energy of an anharmonic oscillator including the cubic term is expressed as

$$E_v = hc\omega_e\left(v + \frac{1}{2}\right) - hc\chi_e\omega_e\left(v + \frac{1}{2}\right)^2 + hcy_e\omega_e\left(v + \frac{1}{2}\right)^3 \cdots$$

The anharmonicity constants, $\chi_e\omega_e$ and $y_e\omega_e$ can be determined by plotting the $\tilde{\nu}(\text{obs})/v$ against the vibrational quantum number v, as shown in Fig. 1.32. The straight line gives $\chi_e\omega_e$ and the deviation from the straight line (at higher v) gives $y_e\omega_e$ The results (CCl_4 solution) in cm^{-1} are

$$\omega_e = 212.59 \pm 0.08, \quad \chi_e\omega_e = 0.62 \pm 0.03, \quad y_e\omega_e = -0.005 \pm 0.002$$

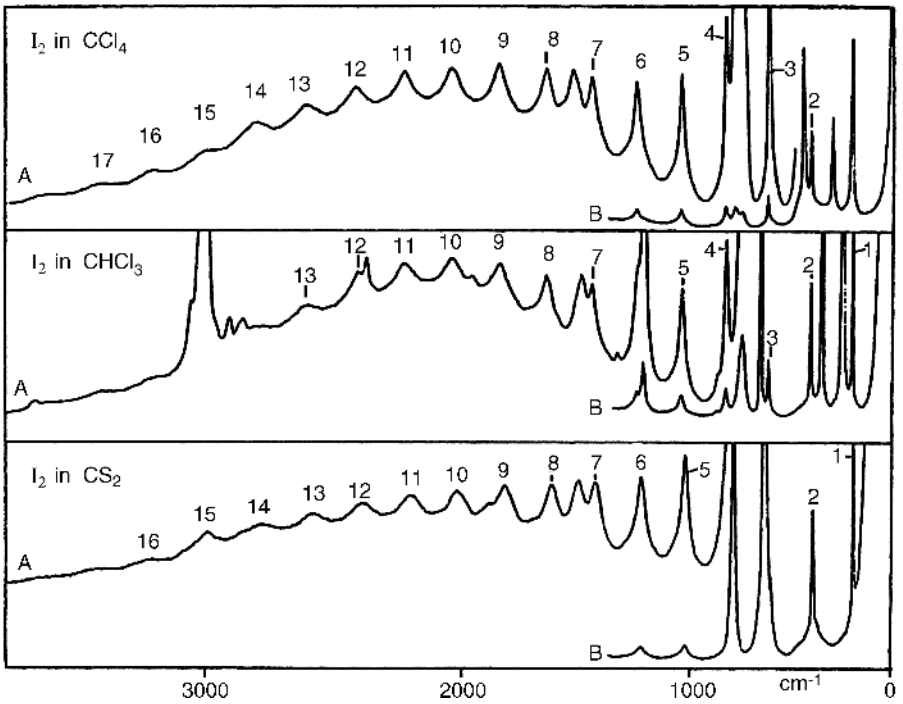

Fig. 1.31. *Resonance Raman spectra of I_2 in CCl_4, $CHCl_3$, and CS_2 (514.5 nm excitation) [105].*

As stated in the preceding section, the depolarization ratio (ρ_p) is expected to be closed to $\frac{1}{3}$ for totally symmetric vibrations. However, this value increases as the change in vibrational quantum number (Δv) increases. For example, it is 0.48 for the tenth overtone of I_2 in CCl_4 [100].

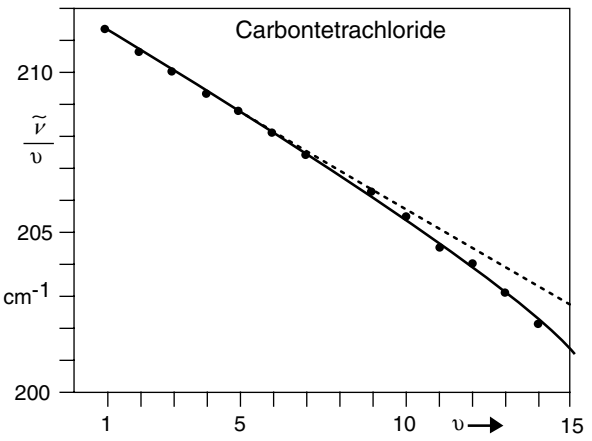

Fig. 1.32. *Plot of $\tilde{\nu}/v$ vs. v for I_2 in CCl_4 [105].*

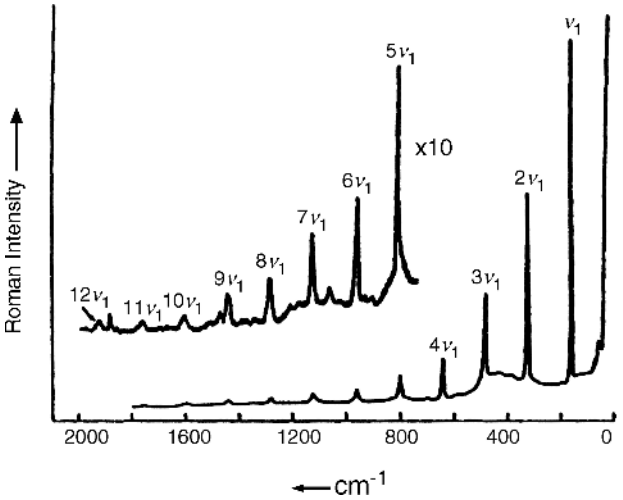

Fig. 1.33. *Resonance Raman spectrum of solid TiI_4 (514.5 nm excitation) [106].*

The second example is given by TiI_4, which has the absorption maximum near 514 nm. Figure 1.33 shows the RR spectrum of solid TiI_4 obtained by Clark and Mitchell [106] with 514.5 nm excitation. In this case, a series of overtones up to the twelfth has been observed. Using these data, they obtained the following constants (cm^{-1}):

$$\omega_e = 161.0 \pm 0.2 \quad \text{and} \quad X_{11} = 0.11 \pm 0.03$$

Here, X_{11} is the anharmonicity constant corresponding to $\chi_e\omega_e$ of a diatomic molecule (Sec. 1.3).

Theoretical treatments of Raman intensities of these overtone series under rigorous resonance conditions have been made by Nafie et al. [107]. There are many other examples of RR spectra of small molecules and ions that exhibit *A*-term resonance. Section 2.6 includes references on RR spectra of the CrO_4^{2-} and MnO_4^- ions. Kiefer [101] reviewed RR studies of small molecules and ions.

Hirakawa and Tsuboi [108] noted that among the totally symmetric modes, the mode that leads to the excited-state configuration is most strongly resonance enhanced. For example, the NH_3 molecule is pyramidal in the ground state and planar in the excited state (216.8 nm above the ground state). Then, the symmetric bending mode near 950 cm^{-1} is enhanced 10 times more than the symmetric stretching mode near 3300 cm^{-1} when the excitation wavelength is changed from 514.5 to 351.1 nm.

A typical example of the *B*-term resonance is given by metalloporphyrins and heme proteins. As shown in Fig. 1.34, Ni(OEP) (OEP:octaethylporphyrin) exhibits two electronic transitions referred to as the Q_0 (or α) and **B** (or Soret) bands along with a vibronic side band (Q_1 or β) in the 350–600 nm region. According to MO (molecular orbital) calculations on the porphyrin core of $\mathbf{D}_{4h}$, symmetry, Q_0 and **B** transitions

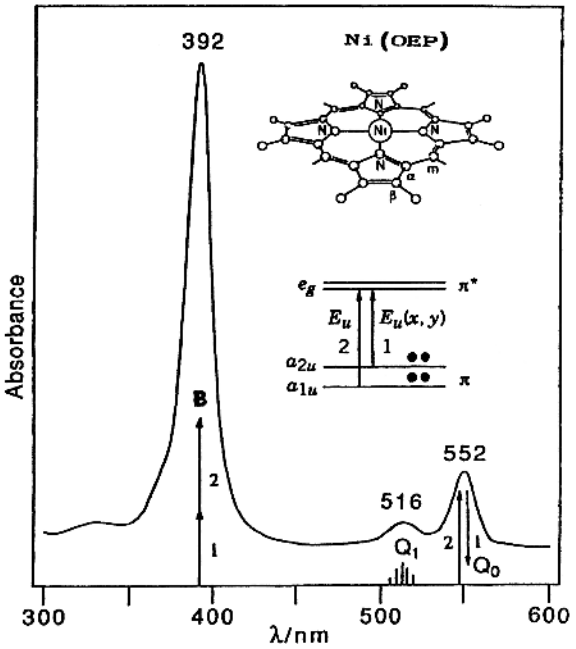

Fig. 1.34. *Structure, energy-level diagram, and electronic spectrum of Ni(OEP) [109].*

result from strong interaction between the $a_{1u}(\pi) \rightarrow e_g\ (\pi^*)$ and $a_{2u}(\pi) \rightarrow e_g\ (\pi^*)$ transitions which have similar energies and the same excited-state symmetry (E_u). The transition dipoles add up for the strong **B** transition and nearly cancel out for the weak Q_0 transition. This is an ideal situation for *B*-term resonance. According to Eq. 1.217, any normal modes which give nonzero values for the integral $(e^0 \mid h_a \mid s^0)$ are enhanced via the *B* term. These vibrations must belong to one of the symmetry species given by $E_u \times E_u$, that is, $A_{1g} + B_{1g} + B_{2g} + A_{2g}$.*

Figure 1.35 shows the RR spectra of Ni(OEP) with excitation near the **B**, Q_1 and Q_0 transitions as obtained by Spiro and coworkers [109]. As discussed in Sec. 1.20, polarization properties are expected to be A_{1g} (*p*, polarized), B_{1g} and B_{2g} (*dp*, depolarized), and A_{2g} (*ap*, anomalous polarization). These polarization properties, together with normal coordinate analysis, were used to make complete vibrational assignments of Ni(OEP) [110]. It is seen that the spectra obtained by excitation near the Q_0 band (bottom traces) are dominated by the *dp* bands (B_{1g} and B_{2g} species), while those obtained by excitation between the Q_0 and Q_1 bands (middle traces) are dominated by the *ap* bands (A_{2g} species). The spectra obtained by excitation near the **B** band (top traces) are dominated by the *p* bands (A_{1g} species). In this

*For symmetry species of the direct products, see Appendix IV. Also note that the A_{1g} vibrations are not effective in vibronic mixing.

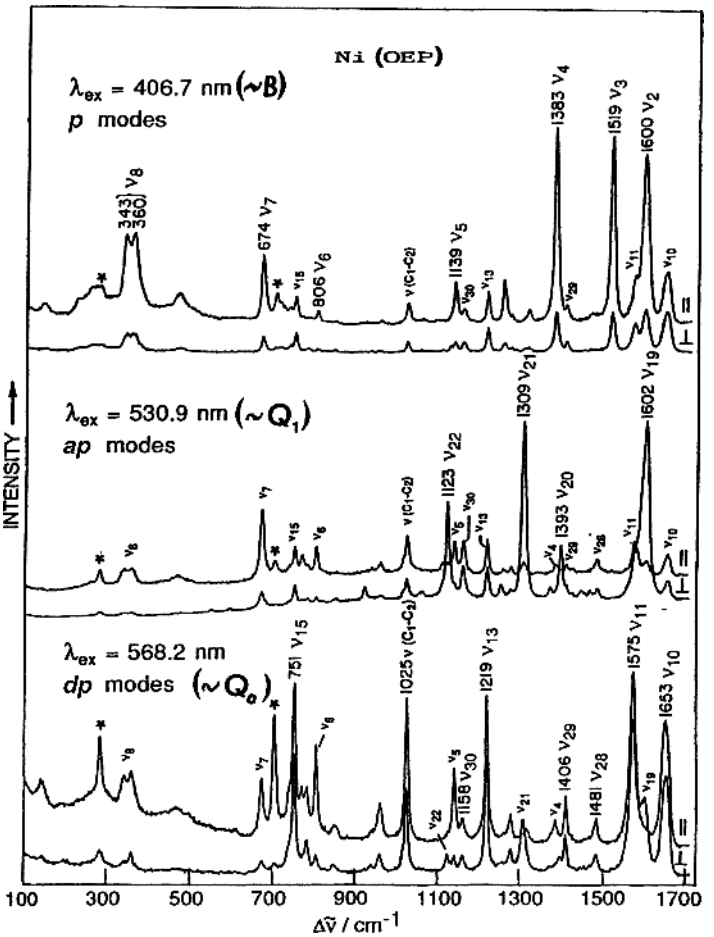

Fig. 1.35. *Resonance Raman spectra of Ni(OEP) obtained by excitation near the B, Q_1, and Q_0 bands [110].*

case, the *A*-term resonance is much more important than the *B*-term resonance because of the very strong absorption strength of the **B** band. Mizutani and coworkers [110a] analyzed the resonance Raman spectra of Ni(OEP) obtained at the *d–d* excited state.

As will be shown in Sec. 2.8, anomalously polarized bands have also been observed in the RR spectra of the $IrCl_6^{2-}$ ion, although their origin is different from the vibronic coupling mentioned above [111,112].

The majority of compounds studied thus far exhibit the *A*-term rather than the *B*-term resonance. A more complete study of resonance Raman spectra involves the observation of *excitation profiles* (Raman intensity plotted as a function of the excitation frequency for each mode), and the simulation of observed excitation profiles based on theoretical treatments of resonance Raman scattering [113].

1.24. THEORETICAL CALCULATION OF VIBRATIONAL FREQUENCIES

The procedure for calculating harmonic vibrational frequencies and force constants by **GF** matrix method has been described in Sec. 1.12. In this method, both **G** (kinetic energy) and **F** (potential energy) matrices are expressed in terms of internal coordinates (**R**) such as increments of bond distances and bond angles. Then, the kinetic (T) and potential (V) energies are written as:

$$2T = \tilde{\dot{\mathbf{R}}}\mathbf{G}^{-1}\dot{\mathbf{R}} \tag{1.113}$$

$$2V = \tilde{\mathbf{R}}\mathbf{F}\mathbf{R} \tag{1.111}$$

and the secular equation

$$|\mathbf{GF} - \mathbf{E}\lambda| = 0 \tag{1.116}$$

is solved to obtain vibrational frequencies. Here, **E** is a unit matrix, and λ is related to the wavenumber by the relation given by Eq. 1.156. The **G** matrix elements can be calculated from the known bond distances and angles, and the **F** matrix elements (force constants) are refined until the differences between the observed and calculated frequencies are minimized. Force constants thus obtained can be transferred to similar molecules to predict their vibrational frequencies.

On the other hand, quantum mechanical methods utilize an entirely different approach to this problem. The principle of the method is to express the total electronic energy (E) of a molecule as a function of nuclear displacements near the equilibrium positions and to calculate its second derivatives with respect to nuclear displacements, namely, vibrational force constants. In the past, *ab initio* calculations of force constants were limited to small molecules [114] such as H_2O and C_2H_2 because computational time required for large molecules was prohibitive. This problem has been solved largely by more recent progress in density functional theory (DFT) [115] coupled with commercially available computer software. Currently, the DFT method is used almost routinely to calculate vibrational parameters of a variety of inorganic, organic, coordination, and organometallic compounds. The advent of high-speed personal computers further facilitated this trend.

Using a commercially available computer program such as "Gaussian 03," DFT calculations of the H_2O molecule proceed in the following order: First, molecular parameters (masses of constituent atoms, approximate bond distances and angles) are used as input data. As an example, let us assume that the O−H distance is 0.96 Å and the HOH angle is 109.5°. Then, the program calculates the cartesian coordinates of the three atoms by placing the origin at the center of gravity (CG) of the molecule. It also determines the point group of the molecule as $\mathbf{C}_{2v}$ on the basis of the given geometry.

Since the total electronic enegy (E) of the H_2O molecule is a function of the nine Cartesian coordinates (x_i, i where $i = 1, 2, \ldots, 9$), the equilibrium configuration that renders all the nine first derivatives ($\partial E/\partial x_i$) zero can be determined (energy optimization). Accuracy of the results depends on the level of the approximation method

TABLE 1.15. Calculated Cartesian Coordinates of H_2O

Center Number	Atomic Number	Coordinate (Å)		
		X	Y	Z
1	8	0.0000	0.0000	0.1110
2	1	0.0000	0.8010	−0.4440
3	1	0.0000	−0.8010	−0.4440

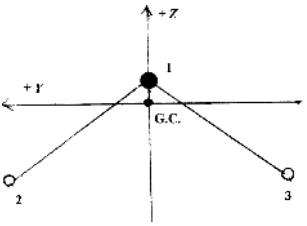

chosen in calculating E. Using 6-31G* basis set with B3LYP functional [116], for example, the optimal geometry was found to be: OH distance = 0.9745 Å and HOH angle = 110.5670° These values were used to recalculate the Cartesian coordinates listed in Table 1.15

The next step is to calculate the second derivatives near the equilibrium positions $[(\partial E^2/\partial x_i\,\partial x_j)_0, i,j = 1\sim 9]$, namely, the force constants in terms of Cartesian coordinates $(f_{i,j})$, using analytical methods [116a]. The force constants thus obtained are converted to mass-weighted Cartesian coordinates $(X_{M,i})$ by

$$x_{M,1} = \sqrt{m_1}x_1, \qquad x_{M,2} = \sqrt{m_1}x_2, \ldots \tag{1.219}$$

$$f_{M,i,j} = \frac{f_{i,j}}{\sqrt{m_i m_j}} = \left(\frac{\partial^2 V}{\partial x_{Mi}\partial x_{Mj}}\right)_0 \tag{1.220}$$

These $f_{M,i,j}$ terms are the elements of the force constant (Hessian) matrix.

Using matrix expression, the relationship between mass-weighted Cartesian ($\mathbf{X_M}$) and Cartesian ($\mathbf{X}$) coordinates is written as follows:

$$\mathbf{X}_\mathrm{M} = \mathbf{M}^{1/2}\mathbf{X} \tag{1.221}$$

Here, $\mathbf{M}^{1/2}$ is a diagonal matrix whose elements are $\sqrt{m_1}, \ldots \sqrt{m_9}$ and $\mathbf{X}$ is a column matrix, $[x_1,\ldots,x_9]$. The product, $\mathbf{M}^{1/2}\mathbf{X}$, gives a column matrix, $\mathbf{X_M}$, $[\sqrt{m_1}x_1, \ldots, \sqrt{m_9}x_9]$. Equation (1.221) is rewritten as

$$\mathbf{X} = \mathbf{M}^{-(1/2)}\mathbf{X}_\mathbf{M} \tag{1.222}$$

The relationship between the internal coordinate $\mathbf{R}$ and $\mathbf{X}$ (Eqs. 1.118 and 1.119) is now written as

$$\mathbf{R} = \mathbf{B}\mathbf{X} = \mathbf{B}\mathbf{M}^{-(1/2)}\mathbf{X}_\mathbf{M} \tag{1.223}$$

and its transpose is

$$\tilde{\mathbf{R}} = \tilde{\mathbf{X}}_\mathbf{M}\mathbf{M}^{-(1/2)}\tilde{\mathbf{B}} \tag{1.224}$$

where $\mathbf{B}$ is a rectangular (3×9) matrix shown by Eq. 1.119.

The kinetic energy (Eq. 1.113) in terms of $\mathbf{X_M}$ is written as

$$2T = \tilde{\dot{\mathbf{X}}}_{\mathbf{M}}\dot{\mathbf{X}}_{\mathbf{M}} \tag{1.225}$$

and the potential energy (Eq. 1.111) in terms of the same coordinate, $\mathbf{X_M}$, is

$$2V = \tilde{\mathbf{R}}\mathbf{F_R}\mathbf{R} = \tilde{\mathbf{X}}_{\mathbf{M}}\mathbf{M}^{-(1/2)}\tilde{\mathbf{B}}\mathbf{F_R}\mathbf{B}\mathbf{M}^{-(1/2)}\mathbf{X_M} = \tilde{\mathbf{X}}_{\mathbf{M}}\mathbf{F_{XM}}\mathbf{X_M} \tag{1.226}$$

where

$$\mathbf{F_{XM}} = \mathbf{M}^{-(1/2)}\tilde{\mathbf{B}}\mathbf{F_R}\mathbf{B}\mathbf{M}^{-(1/2)} \tag{1.227}$$

or

$$\tilde{\mathbf{B}}\mathbf{F_R}\mathbf{B} = \mathbf{M}^{1/2}\mathbf{F_{XM}}\mathbf{M}^{1/2} \tag{1.228}$$

Vibrational frequencies are calculated by solving the following equation:

$$|\mathbf{F_{XM}} - \mathbf{E}\lambda| = 0 \tag{1.229}$$

In the case of H_2O, we obtain nine frequencies, six of which are near zero. These six frequencies must be eliminated from the results because they correspond to the translational and rotational motions of the molecule as a whole ($3N$–6 rule). Thus, the remaining three frequencies correspond to the normal modes of the H_2O molecule. It should be noted that vibrational frequencies are intrinsic of individual molecules and do not depend on the coordinate system chosen ($\mathbf{R}$ or $\mathbf{X_M}$).

The next step is to convert the force constants ($\mathbf{F_{XM}}$) in terms of $\mathbf{X_M}$ coordinates to those of internal coordinates ($\mathbf{F_R}$), which have clearer physical meanings. For this purpose, Eq. 1.228 is rewritten as [117–119]

$$\mathbf{F_R} = \mathbf{U}\Gamma^{-1}\tilde{\mathbf{U}}\mathbf{B}\mathbf{M}^{1/2}\mathbf{F_{XM}}\mathbf{M}^{1/2}\tilde{\mathbf{B}}\mathbf{U}\Gamma^{-1}\tilde{\mathbf{U}} \tag{1.230}$$

Here, $\mathbf{U}$ is an orthogonal matrix ($\mathbf{U} = \tilde{\mathbf{U}}^{-1}$) that diagonalizes $\mathbf{B}\tilde{\mathbf{B}}$, and Γ is a diagonal matrix that is defined as follows:

$$\mathbf{B}\tilde{\mathbf{B}}\mathbf{U} = \mathbf{U}\Gamma \tag{1.231}$$

In the case of H_2O, $\mathbf{B}$ is a 3×9 matrix, whereas $\mathbf{U}$, Γ, and $\mathbf{F_R}$ are 3×3 matrices. To take advantage of symmetry properties, internal coordinates are further transformed to internal symmetry coordinates ($\mathbf{R}^S$) by the relation

$$\mathbf{R}^S = \mathbf{U}^S\mathbf{R} \tag{1.131}$$

where $\mathbf{U}^S$ is an orthogonal matrix chosen by symmetry consideration. Then, the force constants in terms of internal symmetry coordinates ($\mathbf{F}_{\mathbf{R}}^S$) are given by

$$\mathbf{F}_{\mathbf{R}}^S = \mathbf{U}^S\mathbf{F_R}\tilde{\mathbf{U}}^S \tag{1.232}$$

TABLE 1.16. Comparison of Observed and Calculated Frequencies (cm^{-1}) and Normal Modes of H_2O

Normal Vibration:	$\nu_1(A_1)$			$\nu_2(A_1)$			$\nu_3(B_2)$		
Observed frequencies[a]	1595			3657			3756		
Calculated frequencies	1565.5			3639.2			3804.7		
Normal modes[b]	X	Y	Z	X	Y	Z	X	Y	Z
O(1)	0.00	0.00	0.08	0.00	0.00	0.04	0.00	0.07	0.00
H(2)	0.00	−0.38	−0.60	0.00	0.62	−0.35	0.00	−0.58	0.40
H(3)	0.00	0.38	−0.60	0.00	−0.62	−0.35	0.00	−0.58	−0.40
Assignment	HOH bending			Symmetric OH stretch			Antisymmetric OH stretch		

[a]IR spectrum (Table 2.2d of Chapter 2).
[b]The normal modes shown in Fig. 1.12 are obtained by plotting these displacement coordinates.

Thus, $\mathbf{F_{XM}}$ can be coverted to $\mathbf{F_R^S}$ using Eqs. 1.230 and 1.232. Several computer programs are available for this conversion [118].

Table 1.16 summarizes the results of DFT calculation of H_2O. It is seen that the calculated frequencies are in good agreement with the observed values. In other cases, however, the former becomes higher than the latter because (1) the effect of anharmonicity is not included in the calculation and (2) systematic errors result from the use of finite basis sets and incomplete inclusion of electron correlation effects. In such cases, several empirical "scaling methods" are applied to the force constants [120] or frequencies [121] obtained by DFT calculations.

Computer programs such as "Gaussian 03" can simultaneously calculate several other parameters including normal modes (shown in Table 1.15), IR intensities, Raman scattering intensities, and depolarization ratios.

1.25. VIBRATIONAL SPECTRA IN GASEOUS PHASE [122] AND INERT GAS MATRICES [29,30]

As distinct from molecules in condensed phases, those in the gaseous phase are free from intermolecular interactions. If the molecules are relatively small, vibrational spectra of gases exhibit rotational fine structure (see Fig. 1.3) from which moments of inertia and hence internuclear distances and bond angles can be calculated [1,2]. Furthermore, detailed analysis of rotational fine structure provides information about the magnitude of rotation–vibration interaction (Coriolis coupling), centrifugal distortion, anharmonicity, and even nuclear spin statistics in some cases. In the past, infrared spectroscopy was the main tool in measuring gas-phase vibrational spectra. However, Raman spectroscopy is also playing a significant role because of the development of powerful laser sources and high-resolution spectrophotometers. For example, Clark and Rippon [123] measured gas-phase Raman spectra of Group IV tetrahalides, and calculated the Coriolis coupling constants from the observed band contours. For gas-phase Raman spectra of other inorganic compounds, see

Ref. [122]. Unfortunately, the majority of inorganic and coordination compounds exist as solids at room temperature. Although some of these compounds can be vaporized at high temperatures without decomposition, it is rather difficult to measure their spectra by the conventional method. Furthermore, high-temperature spectra are difficult to interpret because of the increased importance of rotational and vibrational hot bands.

In 1954, Pimentel and his colleagues [124] developed the *matrix isolation technique* to study the infrared spectra of unstable and stable species. In this method, solute molecules and inert gas molecules such as Ar and N_2 are mixed at a ratio of 1:500 or greater and deposited on an IR window such as a CsI crystal cooled to 10–15 K. Since the solute molecules trapped in an inert gas matrix are completely isolated from each other, the matrix isolation spectrum is similar to the gas-phase spectrum; no crystal field splittings and no lattice modes are observed. However, the former spectrum is simpler than the latter because, except for a few small hydride molecules, no rotational transitions are observed because of the rigidity of the matrix environment at low temperatures. The lack of rotational structure and intermolecular interactions results in a sharpening of the solute band so that even very closely located metal isotope peaks can be resolved in a matrix environment. This technique is also applicable to a compound which is not volatile at room temperature. For example, matrix isolation spectra of metal halides can be measured by vaporizing these compounds at high temperatures in a Knudsen cell and co-condensing their vapors with inert gas molecules on a cold window [125].

More recent developments of laser ablation techniques coupled with closed-cycle helium refrigerators greatly facilitated its application. Thus, matrix isolation technique has now been utilized to obtain structural and bonding information of a number of inorganic and coordination compounds. Some important features and applications are described in this and the following sections.

1.25.1. Vibrational Spectra of Radicals

Highly reactive radicals can be produced *in situ* in inert gas matrices by photolysis and other techniques. Since these radicals are stabilized in matrix environments, their spectra can be measured by routine spectroscopic techniques. For example, the spectrum of the HOO radical [126] was obtained by measuring the spectrum of the photolysis product of a mixture of HI and O_2 in an Ar matrix at $\sim$4 K. Chapter 2 lists the vibrational frequencies of many other radicals, such as CN, OF, and HSi, obtained by similar methods.

1.25.2. Vibrational Spectra of High-Temperature Species

Alkali halide vapors produced at high temperatures consist mainly of monomers and dimers. The vibrational spectra of these salts at high temperatures are difficult to measure and difficult to interpret because of the presence of hot bands. The matrix isolation technique utilizing a Knudsen cell has solved this problem. The

vibrational frequencies of some of these high-temperature species are listed in Chapter 2.

1.25.3. Isotope Splittings

As stated before, it is possible to observe individual peaks due to heavy-metal isotopes in inert gas matrices since the bands are extremely sharp (half-band width, 1.5–1.0 cm^{-1}) under these conditions. Figure 1.36a shows the infrared spectrum of the ν_7 band (coupled vibration between CrC stretching and CrCO bending modes) of $Cr(CO)_6$ in a N_2 matrix [127]. The bottom curve shows a computer simulation using the measured isotope shift of 2.5 cm^{-1} per atomic mass unit, a 1.2 cm^{-1} half-band width, and the percentages of natural abundance of Cr isotopes: ^{50}Cr (4.31%), ^{52}Cr (83.76%), ^{53}Cr (9.55%), and ^{54}Cr (2.38%). The isotope splittings of $SnCl_4$ and $GeCl_4$ in Ar matrices are discussed in Sec. 2.6. These isotope frequencies are highly important in refining force constants in normal coordinate analysis.

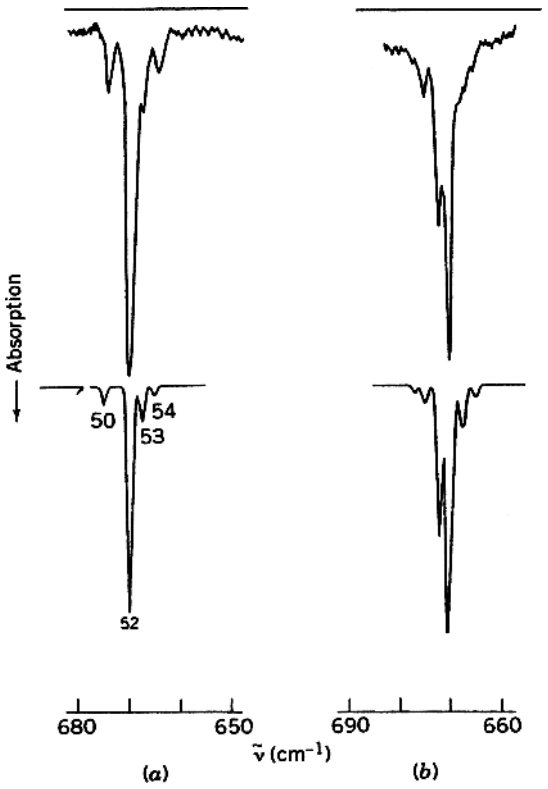

Fig. 1.36. *Matrix isolation IR spectra of $Cr(CO)_6$ in N_2 (a) and Ar (b) matrices. The bottom spectra were obtained by computer simulation [127].*

1.25.4. Matrix Effect

The vibrational frequencies of matrix-isolated molecules give slight shifts when the matrix gas is changed. This result suggests the presence of weak interaction between the solute and matrix molecules. In some cases, the spectra are complicated by the presence of more than one trapping site. For example, the infrared spectrum of $Cr(CO)_6$ in an Ar matrix (Fig. 1.36b) is markedly different from that in a N_2 matrix (Fig. 1.36a) [127]. The former spectrum can be interpreted by assuming two different sites in an Ar matrix. The computer-simulation spectrum (bottom curve) was obtained by assuming that these two sites are populated in a 2:1 ratio, the frequency separation of the corresponding peaks being $2\,cm^{-1}$. Thus, it is always desirable to obtain the matrix isolation spectra in several different environments.

1.26. MATRIX COCONDENSATION REACTIONS

A number of unstable and transient species have been synthesized via matrix cocondensation reactions, and their structure and bonding have been studied by vibrational spectroscopy. The principle of the method is to cocondense two solute vapors (atom, salt, or molecule) diluted by an inert gas on an IR window (IR spectroscopy) or a metal plate (Raman spectroscopy) that is cooled to low temperature by a cryocooler. Solid compounds can be vaporized by conventional heating (Knudsen cell), laser ablation, or other techniques, and mixed with inert gases at proper ratios [128]. In general, the spectra of the cocondensation products thus obtained exhibit many peaks as a result of the mixed species produced. In order to make band assignments, the effects of changing the temperature, concentration (dilution ratios), and isotope substitution on the spectra must be studied. In some cases, theoretical calculations (Sec. 1.24) must be carried out to determine the structure and to make band assignments. Vibrational frequencies of many molecules and ions obtained by matrix cocondensation reactions are listed in Chapter 2.

Matrix cocondensation reactions are classified into the following five types:

1. *Atom-Atom Reaction*. Liang et al. [129] studied the reaction: $U + S \rightarrow US_n (n = 1–3)$, Figure 1.37 shows the IR spectra of laser-ablated U atom vapor cocondensed with microwave-discharged S atom in Ar at 7 K. In (a) (^{32}S with higher concentration) and (b) (^{32}S with low concentration), the prominent band at $438.7\,cm^{-1}$ and a weak band at $449.8\,cm^{-1}$ show a consistent intensity ratio of 6 : 1, and are shifted to 427.8 and $437.4\,cm^{-1}$ respectively, by $^{32}S/^{34}S$ substitution (c). In the mixed $^{32}S + {}^{34}S$ experiments [traces] (d) and (e), both bands split into asymmetric triplets marked in (e). These results suggest that two equivalent S atoms are involved in this species. The bands at 438.7 and $449.8\,cm^{-1}$ were assigned to the antisymmetric (ν_3) and symmetric (ν_1) stretching modes, respectively, of the nonlinear U $^{32}S_2$ molecule. Although the analogous UO_2 molecule is linear, the US_2 molecule is bent because of more favorable U(6*d*)–S(3*p*) overlap. The weak band at $451.1\,cm^{-1}$, which is partly overlapped by the ν_1 mode of US_2 in (a), is shifted to $439.2\,cm^{-1}$ by $^{32}S/^{34}S$ substitution (c), and was assigned to the diatomic US molecule. Another weak band at $458.2\,cm^{-1}$ in (a) shows a

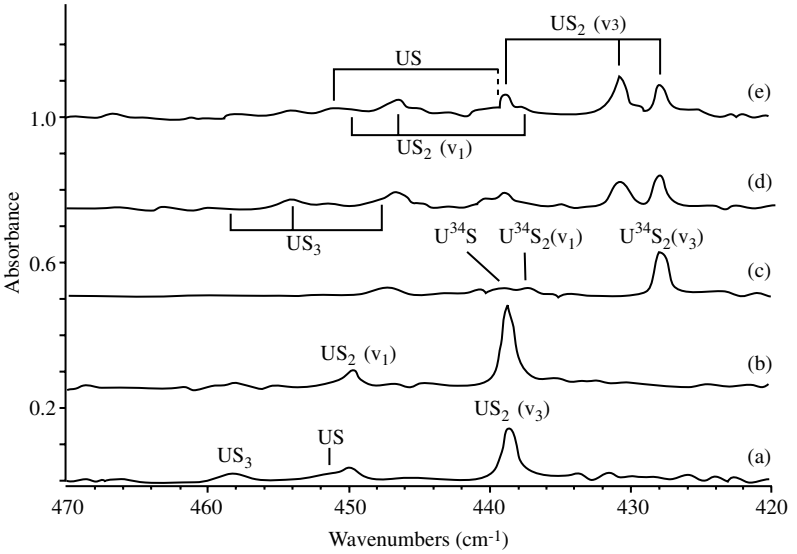

Fig. 1.37. *Infrared spectra of laser-ablated U co-deposited with discharged isotopic S atoms in Ar at 7 K: (a) ^{32}S with higher concentration, (b) ^{32}S with lower concentration, (c) ^{34}S, (d) 35/65 $^{32}S + {}^{34}S$ mixture, and (e) 50/50 $^{32}S + {}^{34}S$ mixture [129].*

triplet pattern in the mixed-isotope experiment shown in (d), and was assigned to the antisymmetric stretching vibration of the near-linear S−U−S unit of a T-shaped US_3 molecule similar to UO_3 All these structures and band assignments are supported by DFT calculations.

2. *Atom–Molecule Reaction*. Zhou and Andrews [130] studied the reaction of Sc + CO → $Sc(CO)_n (n = 1–4)$ via cocondensation of laser-ablated Sc atoms with CO in excess Ar or Ne, and made band assignments based on the results of ^{13}CO and $C^{18}O$ isotope shifts, matrix annealing, broadband photolysis, and DFT calculations. Figure 1.38a shows the IR spectrum of the cocondensation product after one hour deposition at 10 K in Ar. The strong and sharp band at 1834.2 cm^{-1} is shifted to 1792.9 and 1792.3 cm^{-1} by ^{13}CO and $C^{18}O$ substitutions, respectively, and its intensity decreases upon annealng to 25 K (b) but increases on photolysis (c,d). Two weak bands near 1920 cm^{-1} in (a) are also isotope-sensitive and become stronger on annealing to 25 K (b). These bands were assigned to the $Sc(CO)^+$ cation produced by the reaction of laser-ablated Sc^+ ion with CO. In a Ne matrix, a similar experiment exhibits a sharp band at 1732.0 cm^{-1} that was assigned to the $Sc(CO)^-$ ion produced via electron capture by Sc(CO). The pair of bands at 1851.4 and 1716.3 cm^{-1} in (b) were assigned to the antisymmetric and symmetric stretching vibrations of the bent $Sc(CO)_2$ molecule while the strong and sharp band at 1775.5 cm^{-1} in (c) was attributed to the linear $Sc(CO)_2$ molecule. DFT calculations predict $Sc(CO)_3$ to be trigonal pyramidal ($\mathbf{C}_{3v}$ symmetry) in the ground state. The bands at 1968.0 and 1822.2 cm^{-1} in (b) become weaker by photolysis (c,d) and stronger by annealing at 35 K (e), These bands were assigned to the nondegenerate symmetric and degenerate CO stretching

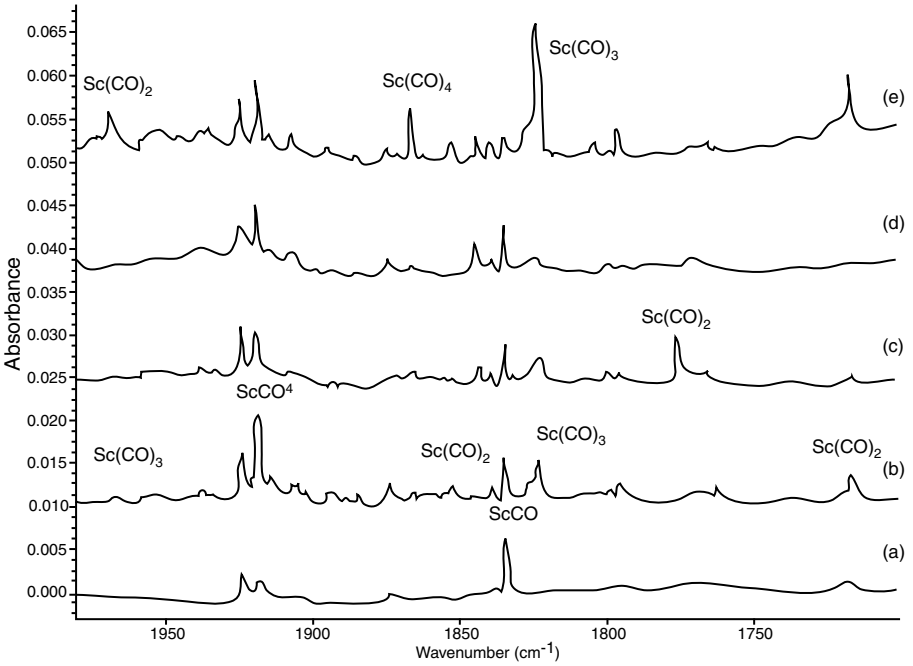

Fig. 1.38. *Infrared spectra of laser-ablated Sc atoms co-deposited with 0.5 % CO in excess Ar.: (a) after 1 hr sample deposition at 10 K, (b) after annealing to 25 K, (c) after 20 min $\lambda > 470$ nm photolysis, (d) after 20 min full-arc photolysis, and (e) after annealing to 35 K [130].*

vibrations, respectively, of the $Sc(CO)_3$ molecule. The band at 1865.4 cm^{-1} appeared last when the matrix was annealed to 35 K (e), and was tentatively assigned to a degenerate vibration of $Sc(CO)_4$. Matrix cocondensation reactions of this type have been studied most extensively as shown in Part B, Sec. 3.18.6.

3. *Salt–Molecule Reaction.* Tevault and Nakamoto [131] carried out matrix cocondensation reactions of metal salts such as PbF_2 with L(CO, NO and N_2) in Ar, and confirmed the formation of PbF_2–L adducts by observing the shifts of IR bands of both components. These spectra are shown in Fig. 3.67 (of Sec. 3.18.6).

4. *Salt–Salt Reaction.* Ault [132] obtained the IR spectrum of the PbF_3^- ion via the reaction of the type, $MF + PbF_2 \rightarrow M[PbF_3]$ (M = Na, K, Rb, and Cs). Both salts were premixed, and the mixture was heated in a single Knudsen cell at 300–325°C, which is roughly 200°C below that is needed to vaporize either PbF_2 or MF. Figure 1.39 shows the IR spectra of PbF_2 and its cocondensation products with MF in Ar matrices. It is seen that, except for M = Na, the cocondensation products exhibit two prominent bands near 456 and 405 cm^{-1} with no bands due to PbF_2 Thus, these two bands were assigned to the A_1 and E stretching vibrations, respectively, of the PbF_3^- ion of $\mathbf{C}_{3v}$ symmetry. The band at 242 cm^{-1} was observed weakly only in high-yield experiments, and tentatively assigned to a bending mode of the PbF_3^- ion.

5. *Molecule–Molecule Reaction.* The reaction $Fe(TPP) + O_2 \rightarrow$ (TPP) Fe-O_2 (TPP tetraphenylporphyrin) was carried out by Watanabe et al. [133] using $^{16}O_2$ and $^{18}O_2$

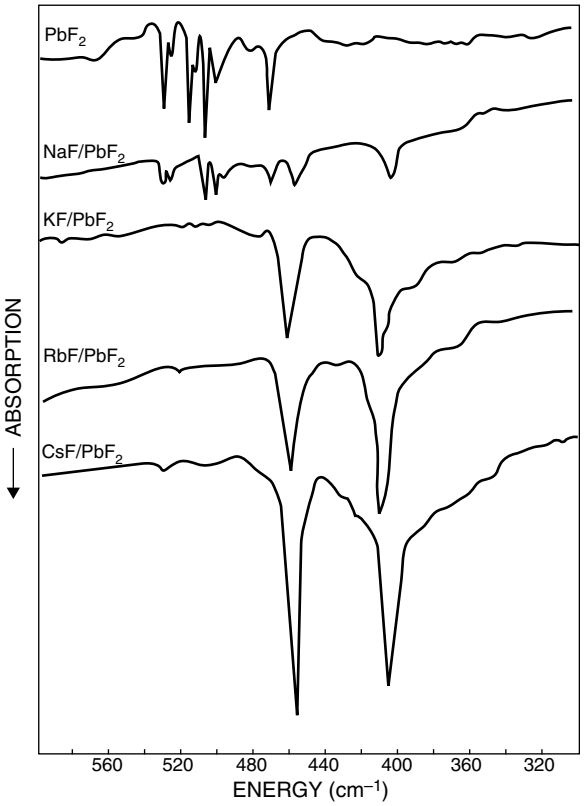

Fig. 1.39. *Infrared spectra of the $M^{+}PbF_3^{-}$ isolated in Ar matrices. The top trace shows the spectrum of the parent PbF_2 salt, while the next four spectra show the bands attributable to the vaporization products from the solid mixtures of NaF/PbF_2, KF/PbF_2, RbF/PbF_2, and CsF/PbF_2 in the 580 ~ 300 cm^{-1} region [132].*

diluted in Ar. The IR spectra shown in Fig. 3.76 (in Sec. 3.21.4) indicate that two new bands appear at 1195 and 1108 cm^{-1} which are due to the O_2 stretching vibrations of the end-on and side-on type Fe(TPP)O_2, respectively. Bajdor and Nakamoto [134] obtained a novel oxoferrylporphyrin [O=Fe(IV)(TPP)] via laser photolysis of Fe (TPP)O_2 in pure O_2 matrices at ~15 K. As seen in Fig. 1.82 (Sec. 1.22.4 of Part B), it exhibits the Fe(IV)=O stretching vibration at 852 cm^{-1}.

1.27. SYMMETRY IN CRYSTALS

The symmetry elements and point groups of molecules and ions in the free state have been discussed in Sec. 1.5. For molecules and ions in crystals, however, it is necessary to consider some additional symmetry operations that characterize translational symmetries in the lattice. Addition of these translational operations results in the formation of the space groups that can be used to classify the symmetry of molecules and ions in crystals.

TABLE 1.17. Seven Crystallographic Systems and 32 Crystallographic Point Groups

System	Axes and Angles	32 Crystallographic Point Groups
Triclinic	a b c α β γ	1 $\bar{1}$ $\mathbf{C}_1$ C_i
Monoclinic	a b c 90° β 90°	2 m or $\bar{2}$ $2/m$ $\mathbf{C}_2$ $\mathbf{C}_s$ $\mathbf{C}_{2h}$
Orthorthombic	a b c 90° 90° 90°	222 $mm2$ mmm $\mathbf{D}_2$ $\mathbf{C}_{2v}$ $\mathbf{D}_{2h}$
Tetragonal	a b c 90° 90° 90°	4 $\bar{4}$ $4/m$ 422 $4mm$ $\bar{4}2m$ $4/mmm$ $\mathbf{C}_4$ S_4 C_{4h} $\mathbf{D}_4$ $\mathbf{C}_{4v}$ $\mathbf{D}_{2d}$ $\mathbf{D}_{4h}$
Trigonal (rhombohedral)	aaa $\alpha\alpha\alpha$ or a a c 90° 90° 120°	3 $\bar{3}$ 32 $3m$ $\bar{3}m$ $\mathbf{C}_3$ $\mathbf{C}_{3i}$ $\mathbf{D}_3$ $\mathbf{C}_{3v}$ $\mathbf{D}_{3d}$
Hexagonal	a a c 90° 90° 120°	6 $\bar{6}$ $6/m$ 622 6mm $\bar{6}m2$ $6/mmm$ $\mathbf{C}_6$ $\mathbf{C}_{3h}$ C_{6h} $\mathbf{D}_6$ $\mathbf{C}_{6v}$ $\mathbf{D}_{3h}$ $\mathbf{D}_{6h}$
Cubic	a a c 90° 90° 90°	23 $m3$ 432 $\bar{4}3m$ $m3m$ $\mathbf{T}$ $\mathbf{T}_h$ $\mathbf{O}$ $\mathbf{T}_d$ $\mathbf{O}_h$

1.27.1. 32 Crystallographic Point Groups

As discussed in Sec. 1.5, molecular symmetry can be described by point groups that are derived from the combinations of symmetry operations, I (identity), C_p (p-fold axis of symmetry), a (plane of symmetry), i (center of symmetry), and S_p (p-fold rotation–reflection axis), where p may range from 1 to ∞. In the case of crystal symmetry, p is limited to 1, 2, 3, 4, and 6 because of space-filling requirement in a crystal lattice. As a result, only the 32 crystallographic point groups listed in Table 1.17 are possible. Here, Hermann–Mauguin (HM) as well as Schönflies (S) notations are shown. In the HM notation, 1, 2, 3, 4, and 6 denote the principal axis of rotation, C_p, where p is 1, 2, 3, 4, and 6, respectively, and $\bar{1}, \bar{2}, \bar{3}, \bar{4}$, and $\bar{6}$ denote a combination of respective rotation about an axis and inversion through a point on the axis. Thus, $\bar{1}$ means the center of inversion (i), $\bar{2}$ indicates σ on a mirror plane (m), and $\bar{3}, \bar{4}$, and $\bar{6}$ correspond to S_6, S_4, and S_3, respectively. For example, the point group $\mathbf{C}_{2h}$, (I, C_2, a, and i) can be written as $2m\bar{1}$, which can be simplified to $2/m$ where the slash means the C_2 axis is perpendicular to m. As shown in Table 1.17, these 32 crystallographic point groups which describe the symmetry of the unit cell can be classified into seven crystallographic systems according to the most simple choice of reference axes.

1.27.2. Symmetry of the Crystal Lattice

A crystal has a lattice structure that is a repetition of identical units. Bravais has shown that only the 14 different types of lattices shown in Fig. 1.40 are possible. These

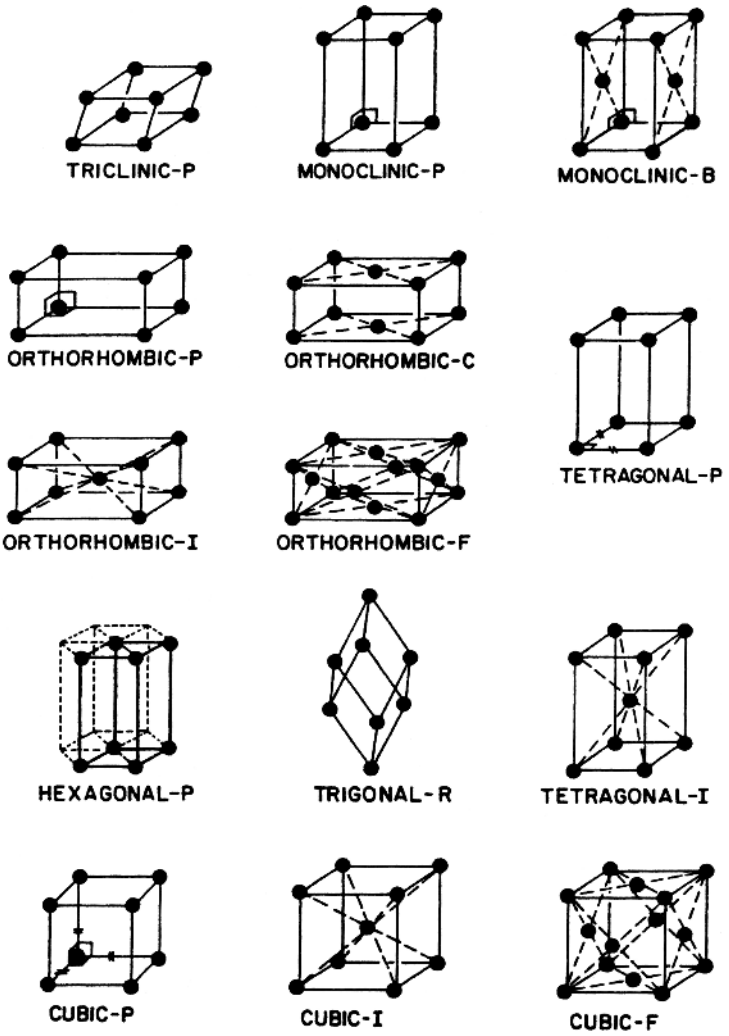

Fig. 1.40. *The 14 Bravais lattices belonging to the seven crystallographic systems [135].*

Bravais lattices are also classified into the seven crystallographic systems mentioned above. Here, the lattice points are regarded as "points" or "small, indentical, perfect spheres," thus representing the highest symmetry possible. In actual crystals, these points are occupied by unsymmetric but identical molecules or ions so that their high symmetry is lowered. In Fig. 1.40 P, C (or A or B), F, I, and R indicate primitive, base-centered, face-centered, body-centered, and rhombohedral lattices, respectively. The number of lattice points (LP) in each cell is summarized in Table 1.18. For crystal structures designated by P, crystallographic unit cells are identical with the Bravais unit cells. For those designated by other letters, crystallographic unit cells contain 2, 3, or 4 Bravais cells. In these cases, the number of molecules in the crystallographic unit

TABLE 1.18. Primitive and Centered Lattices

Type of Crystal Structure	Number of Lattice Points (LP)
Primitive (P)	1
Base-centered (A, B, or C)	2
Body-centered (I)	2
Rhombohedral (R)	3 or 1[a]
Face-centered (F)	4

[a]The crystallographic unit cell may have been divided by 3.

cell must be divided by the corresponding LP since only the consideration of one Bravais cell is sufficient to interpret the vibrational spectra of crystals.

1.27.3. Space Groups

As stated above, the 32 point groups describe the symmetry of the unit cells, and the 14 Bravais lattices describe all possible arrangements of crystal lattices. To describe space symmetry, however, symmetry operations mentioned earlier are not enough. We must add three new symmetry operations:

Translation. A translational operation along one lattice direction gives an identical point.

Screw Axis. Rotation of a lattice point about an axis followed by translation gives an identical point. Namely, rotation by $2\pi/p$ followed by a translation of $q/p(q = 1, 2, \ldots, n-1)$ in the direction of the axis is written as p_q. For example, 2_1 indicates twofold rotation followed by a translation of $\frac{1}{2}a, \frac{1}{2}b$, or $\frac{1}{2}c$, as shown in Fig. 1.41A. If the axis is threefold, the translation must be $\frac{1}{3}$ or $\frac{2}{3}$, and the symbols are 3_1 and 3_2, respectively.

Glide Plane. Reflection in a plane followed by translation by $\frac{1}{2}a, \frac{1}{2}b, \frac{1}{2}c$, as shown in Fig. 1.41B. These planes are indicated by a, b, and c, respectively, n is used for diagonal translation of $(b+c)/2$, $(c+a)/2$, or $(a+b)/2$.

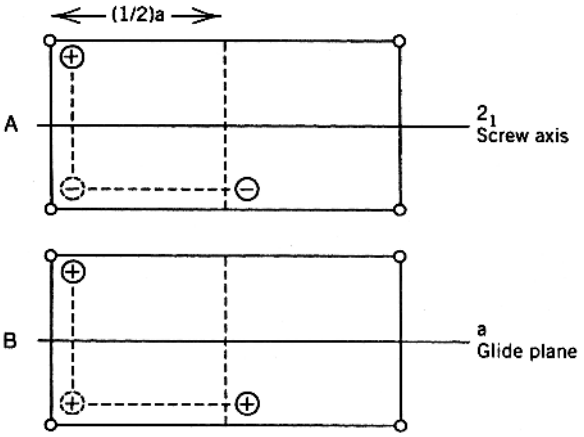

Fig. 1.41. *Screw axis and glide plane.*

Addition of these symmetry operations results in 230 different combinations which are called "space groups." Table 1.19 shows the distribution of space groups among the seven crystal systems [136]. Some of these space groups are rarely found in actual crystals. About half of the crystals belong to 13 space groups of the monoclinic system. Space groups can be described by using either Hermann–Mauguin (HM) or Schönflies (S) notations. For example, P2/m($\equiv C_{2h}^1$) indicates a primitive lattice with m perpendicular to 2. The first symbol (capital letter) refers to the Bravais lattice (P, A, B, C, F, I, and R), and the next symbol indicates fundamental symmetry elements that lie along the special direction in the crystal. In the case of the monoclinic system, it is the twofold axis. Thus, P2_1/m($\equiv C_{2h}^2$) is a primitive cell with m perpendicular to 2_1. These symbols indicate only the minimum symmetry elements that are necessary to distinguish the space groups. The differences among space groups can be found by comparing the "unit cell maps" given in the *International Tables for X-Ray Crystallography* [137] .

1.28. VIBRATIONAL ANALYSIS OF CRYSTALS [48–52]

Because of intermolecular interactions, the symmetry of a molecule is generally lower in the crystalline state than in the gaseous (isolated) state. This change in symmetry may split the degenerate vibrations and activate infrared- (or Raman-) inactive vibrations. Additionally, intermolecular (interionic) interactions in the crystal lattice cause frequency shifts relative to the gaseous state. Finally, the spectra obtained in the crystalline state exhibit *lattice modes*—vibrations due to translatory and rotatory motions of a molecule in the crystalline lattice. Although their frequencies are usually lower than 300 cm^{-1}, they may appear in the high-frequency region as the combination bands with internal modes (see Fig. 2.18, for example). Thus, the vibrational spectra of crystals must be interpreted with caution, especially in the low-frequency region.

To analyze the spectra of crystals, it is necessary to carry out a site group or factor group analysis, as described in the following subsection.

1.28.1. Subgroups and Correlation Tables

For any point group, there are "subgroups" which consist of some, but not all, symmetry elements of the "parent group." For example, the character table of the point group, $\mathbf{C}_{3v}$ (Table 1.6) contains I, C_3, and σ_v as the symmetry elements. Then, the subgroups of $\mathbf{C}_{3v}$ are $\mathbf{C}_3$, consisting of I and C_3, and $\mathbf{C}_s$, consisting of I and σ_v only. The relationship between the symmetry species in the "parent group" and those in "subgroups" is given in a "correlation table." Such correlation tables have already been worked out for all common point groups and are listed in Appendix IX. As an example, the correlation table for $\mathbf{C}_{3v}$ is shown below:

$\mathbf{C}_{3v}$	$\mathbf{C}_3$	$\mathbf{C}_s$
A_1	A	A'
A_2	A	A''
E	E	$A' + A''$

TABLE 1.19. The 230 Space Groups

	Point Groups								
System	S[a]	HM[b]	Space Group						
Triclinic	C_1	1	*P*1						
	C_i	$\bar{1}$	P$\bar{1}$						
Monoclinic	$C_2^{(1-3)}$	2	*P*2	$P2_1$	*C*2				
	$C_S^{(1-4)}$	*m*	*Pm*	*Pc*	*Cm*	*Cc*			
	$C_{2h}^{(1-6)}$	2/*m*	*P*2/*m*	P2_1/*m*	*C*2/*m*	*P*2/*c*	$P2_1/c$	*C*2/*c*	
Orthorhombic	$D_2^{(1-9)}$	222	*P*222	$P222_1$	$P2_12_12$	$P2_12_12_1$	$C222_1$	*C*222	*F*222
			*I*222	$I2_12_12$					
	$C_{2v}^{(1-22)}$	*mm*2	*Pmm*2	$Pmc2_1$	*Pcc*2	*Pma*2	$Pca2_1$	*Pnc*2	$Pmn2_1$
			*Pba*2	$Pna2_1$	*Pnm*2	*Cmm*2	$Cmc2_1$	*Ccc*2	*Amm*2
			*Abm*2	*Ama*2	*Aba*2	*Fmm*2	*Fdd*2	*Imm*2	*Iba*2
			*Ima*2						
	$D_{2h}^{(1-28)}$	*mmm*	*Pmmm*	*Pnnn*	*Pccm*	*Pban*	*Pmma*	*Pnna*	*Pmna*
			Pcca	*Pbam*	*Pccn*	*Pbcm*	*Pnnm*	*Pmmn*	*Pbcn*
			Pbca	*Pnma*	*Cmcm*	*Cmca*	*Cmmm*	*Cccm*	*Cmma*
			Ccca	*Fmmm*	*Fddd*	*Immm*	*Ibam*	*Ibca*	*Imma*
Tetragonal	$C_4^{(1-6)}$	4	*P*4	$P4_1$	$P4_2$	$P4_3$	*I*4	$I4_1$	
	$S_4^{(1-2)}$	$\bar{4}$	P$\bar{4}$	I$\bar{4}$					
	$C_{4h}^{(1-6)}$	4/*m*	*P*4/*m*	$P4_2/m$	*P*4/*n*	$P4_2/n$	*I*4/*m*	$I4_1/a$	
	$D_4^{(1-10)}$	422	*P*422	$P42_12$	$P4_122$	$P4_12_12$	$P4_222$	$P4_22_12$	$P4_322$
			$P4_32_12$	*I*422	$I4_122$				
	$C_{4v}^{(1-12)}$	4*mm*	*P*4*mm*	*P*4*bm*	$P4_2cm$	$P4_2nm$	*P*4*cc*	*P*4*nc*	$P4_2mc$
			$P4_2bc$	*I*4*mm*	*I*4*cm*	$I4_1md$	$I4_1cd$		
	$D_{2d}^{(1-12)}$	$\bar{4}$2m	P$\bar{4}$2m	P$\bar{4}$2c	P$\bar{4}2_1$m	P$\bar{4}2_1$c	P$\bar{4}$m2	P$\bar{4}$c2	P$\bar{4}$b2
			P$\bar{4}$n2	I$\bar{4}$m2	I$\bar{4}$c2	I$\bar{4}$2m	I$\bar{4}$2d		
	$D_{4h}^{(1-20)}$	4/*mmm*	*P*4/*mmm*	*P*4/*mcc*	*P*4/*nbm*	*P*4/*nnc*	*P*4/*mbm*	*P*4/*mnc*	*P*4/*nmm*
			*P*4/*ncc*	$P4_2/mmc$	$P4_2/mcm$	$P4_2/nbc$	$P4_2/nnm$	$P4_2/mbc$	$P4_2/mnm$
			$P4_2/ncm$	$P4_2/ncm$	*I*4/*mmm*	*I*4/*mcm*	$I4_1/amd$	$I4_1/acd$	

Trigonal	$C_3^{(1-4)}$	3	$P3$	$P3_1$	$P3_2$	$R3$			
	$C_{3i}^{(1-2)}$	$\bar{3}$	$P\bar{3}$	$R\bar{3}$					
	$D_3^{(1-7)}$	32	$P312$	$P321$	$P3_112$	$P3_121$	$P3_212$	$P3_221$	$R32$
	$C_{3v}^{(1-6)}$	$3m$	$P3m1$	$P31m$	$P3c1$	$P31c$	$R3m$	$R3c$	
	$D_{3d}^{(1-6)}$	$\bar{3}$m	P$\bar{3}$1m	P$\bar{3}$1c	P$\bar{3}$m1	P$\bar{3}$c1	R$\bar{3}$m	R$\bar{3}$c	
Hexagonal	$C_6^{(1-6)}$	6	$P6$	$P6_1$	$P6_5$	$P6_2$	$P6_4$	$P6_3$	
	$C_{3h}^{(1)}$	$\bar{6}$	P$\bar{6}$						
	$C_{6h}^{(1-2)}$	$6/m$	$P6/m$	$P6_3/m$					
	$D_6^{(1-6)}$	622	$P622$	$P6_122$	$P6_522$	$P6_222$	$P6_422$	$P6_322$	
	$C_{6v}^{(1-4)}$	$6mm$	$P6mm$	$P6cc$	$P6_3cm$	$P6_3mc$			
	$D_{3h}^{(1-4)}$	$\bar{6}$m2	P$\bar{6}$m2	P$\bar{6}$c2	P$\bar{6}$2m	P$\bar{6}$2c			
	$D_{6h}^{(1-4)}$	$6/mmm$	$P6/mmm$	$P6/mcc$	$P6_3/mcm$	$P6_3/mmc$			
Cubic	$T^{(1-5)}$	23	$P23$	$F23$	$I23$	$P2_13$	$I2_13$		
	$T_h^{(1-7)}$	$m3$	$Pm3$	$Pn3$	$Fm3$	$Fd3$	$Im3$	$Pa3$	$Ia3$
	$O^{(1-8)}$	432	$P432$	$P4_232$	$F432$	$F4_132$	$I432$	$P4_332$	$P4_132$
			$I4_132$						
	$T_d^{(1-6)}$	$\bar{4}3m$	P$\bar{4}$3m	F$\bar{4}$3m	I$\bar{4}$3m	P$\bar{4}$3n	F$\bar{4}$3c	I$\bar{4}$3d	
	$O_h^{(1-10)}$	$m3m$	$Pm3m$	$Pn3n$	$Pm3n$		$Fm3m$	$Fm3c$	$Fd3m$
			$Fd3c$	$Im3m$	$Ia3d$	$Ph3m$			

[a] Schönflies.
[b] Hermann–Mauguin.
Source: Ref. [136].

A pyramidal XY_3 molecule such as NH_3 belongs to the point group $\mathbf{C}_{3v}$. If one of the Y atoms is replaced by a Z atom, the resulting XY_2Z molecule belongs to the point group $\mathbf{C}_s$. As a result, the doubly degenerate vibration (E) splits into two vibrations ($A' + A''$). These correlation tables are highly important in predicting the effect of lowering of symmetry on molecular vibrations. Chapter 2 includes a number of examples of symmetry lowering by substitution of an atomic group by another group.

1.28.2. Site Group Analysis

According to Halford [138], the vibrations of a molecule in the crystalline state are governed by a new selection rule derived from *site symmetry*—a local symmetry around the center of gravity of a molecule in a unit cell. The site symmetry can be found by using the following two conditions: (1) the site group must be a subgroup of both the space group of the crystal and the molecular point group of the isolated molecule, and (2) the number of equivalent sites must be equal to the number of molecules in the unit cell. Halford derived a complete table that lists possible site symmetries and the number of equivalent sites for 230 space groups. Suppose that the space group of the crystal, the number of molecules in the unit cell (Z), and the point group of the isolated molecule are known. Then, the site symmetry can be found from the *Table of Site Symmetry for the 230 Space Groups*, which was originally derived by Halford. Appendix X gives its modified version by Ferraro and Ziomek [9]. In general, the site symmetry is lower than the molecular symmetry in an isolated state. In some cases, it may be difficult to make an unambiguous choice of site symmetry by the method cited above. Then, Wyckoff 's tables on crystallographic data [139] must be consulted.

The vibrational spectra of calcite and aragonite crystals are markedly different, although both have the same composition (Sec. 2.4). This result can be explained if we consider the difference in site symmetry of the CO_3^{2-} ion between these crystals. According to X-ray analysis, the space group of calcite is $\mathbf{D}_{3d}^6$ and Z is 2 Appendix X gives

$$\mathbf{D}_3(2), \quad \mathbf{C}_{3i}(2), \quad \mathbf{C}_3(4), \quad \mathbf{C}_i(6), \quad \mathbf{C}_2(6), \quad \mathbf{C}_1(12)$$

as possible site symmetries for space group $\mathbf{D}_{3d}^6$ (the number in front of point group notation indicates the number of distinct sets of sites, and that in parentheses denotes the number of equivalent sites for each distinct set). Rule 2 eliminates all but $\mathbf{D}_3(2)$ and $\mathbf{C}_{3i}(2)$. Rule 1 eliminates the latter since $\mathbf{C}_{3i}$ is not a subgroup of $\mathbf{D}_{3h}$. Thus, the site symmetry of the CO_3^{2-} ion in calcite must be $\mathbf{D}_3$. On the other hand, the space group of aragonite is $\mathbf{D}_{2h}^{16}$ and Z is 4. Appendix X gives

$$2\mathbf{C}_i(4), \quad \mathbf{C}_s(4), \quad \mathbf{C}_1(8)$$

Since $\mathbf{C}_i$ is not a subgroup of $\mathbf{D}_{3h}$, the site symmetry of the CO_3^{2-} ion in aragonite must be $\mathbf{C}_s$. Thus, the $\mathbf{D}_{3h}$, symmetry of the CO_3^{2-} ion in an isolated state is lowered to $\mathbf{D}_3$ in

TABLE 1.20. Correlation Table for D_{3h}, D_3, C_{2v}, and C_s

Point Group	ν_1	ν_2	ν_3	ν_4
D_{3h}	A'_1(R)	A''_2(I)	E'(I, R)	E'(I, R)
D_3	A_1(R)	A_2(I)	E(I, R)	E(I, R)
C_{2v}	A'_1(I, R)	B_1 (I, R)	A_1 (I, R) + B_2 (I, R)	A_1 (I, R) + B_2 (I, R)
C_s	A'(I, R)	A''(I, R)	A'(I, R) + A'(I, R)	A'(I, R) + A'(I, R)

calcite and to C_s in aragonite. Then, the selection rules are changed as shown in Table 1.20.

There is no change in the selection rule in going from the free CO_3^{2-} ion to calcite. In aragonite, however, ν_1 becomes infrared active, and ν_3 and ν_4 each split into two bands. The observed spectra of calcite and aragonite are in good agreement with these predictions (see Table 2.4b).

1.28.3. Factor Group Analysis

A more complete analysis including lattice modes can be made by the method of factor group analysis developed by Bhagavantam and Venkatarayudu [140]. In this method, we consider all the normal vibrations for an entire Bravais cell. Figure 1.42 illustrates the Bravais cell of calcite, which consists of the following symmetry elements:

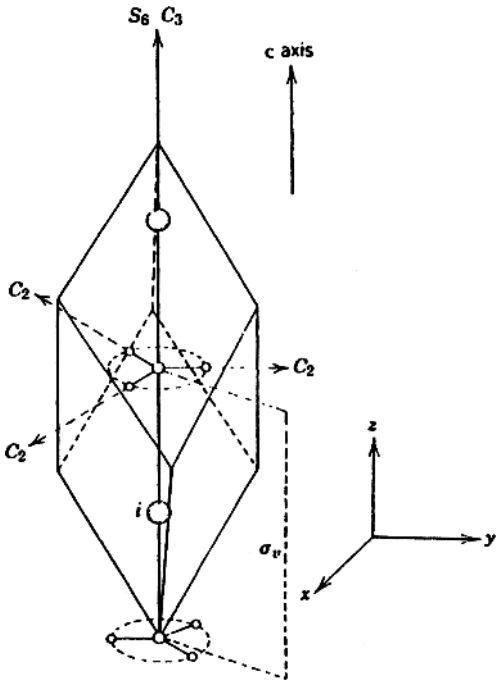

Fig. 1.42. *The Bravais cell of calcite.*

I, $2S_6$, $2S_6^2 \equiv 2C_3$, $S_6^3 \equiv i$, $3C_2$, and $3\sigma_v$ (glide plane). These elements are exactly the same as those of the point group $\mathbf{D}_{3d}$, although the last element is a glide plane rather than a plane of symmetry in a single molecule.

As mentioned in Sec. 1.27, it is possible to derive the 230 space groups by combining operations possessed by the 32 crystallographic point groups with operations such as pure translation, screw rotation (translation + rotation), and glide plane reflection (translation + reflection). If we regard the translations that carry a point in a unit cell into the equivalent point in another cell as identity, we define the 230 factor groups that are the subgroups of the corresponding space groups. In the case of calcite, the factor group consists of the symmetry elements described above, and is denoted by the same notation as that used for the space group ($\mathbf{D}_{3d}^6$). The site group discussed previously is a subgroup of a factor group.

Since the Bravais cell contains 10 atoms, it has $3 \times 10 - 3 = 27$ normal vibrations, excluding three translational motions of the cell as a whole.* These 27 vibrations can be classified into various symmetry species of the factor group $\mathbf{D}_{3d}^6$, using a procedure similar to that described in Sec. 1.8 for internal vibrations. First, we calculate the characters of representations corresponding to the entire freedom possessed by the Bravais cell [$\chi_R(N)$], translational motions of the whole cell [$\chi_R(T)$], translatory lattice modes [$\chi_R(T')$] rotatory lattice modes [$\chi_R(R')$], and internal modes [$\chi_R(n)$], using the equations given in Table 1.21. Then, each of these characters is resolved into the symmetry species of the point group, $\mathbf{D}_{3d}$. The final results show that three internal modes (A_{2u} and two E_u), three translatory modes (A_{2u} and two E_u), and two rotatory modes (A_{2u} and E_u) are infrared-active, and three internal modes (A_{1g} and two E_g) one translatory mode (E_g), and one rotatory mode (E_g) are Raman-active. As will be shown in the following sections, these predictions are in perfect agreement with the observed spectra.

1.29. THE CORRELATION METHOD

In the preceding section, we described the application of factor group analysis to the calcite crystal. However, the correlation method developed largely by Fateley et al. [15] is simpler and gives the same results. In this method, intramolecular and lattice vibrations are classified under point groups of molecular symmetry, site symmetry, and factor group symmetry, and correlations are made using the correlation tables given in Appendix IX. In the following, we demonstrate its utility using calcite as an example. For more detailed discussions and applications, the reader should consult the books by Fateley et al. [15] and Ferraro and Ziomek [9].

1.29.1. The CO_3^{2-} Ion in the Free State

As mentioned in Sec. 1.4, normal vibrations of a molecule can be described in terms of translational motions of the individual atoms along the x, y, and z axes. Thus, the

*These three motions give acoustical modes (Sec. 1.30).

TABLE 1.21. Factor Group Analysis of Calcite Crystal

D_{3d}^6	I	$2S_6$	$2C_3$ $\|\|\|$ $2S_6^2$	i $\|\|\|$ S_6^3	$3C_2$	$3\sigma_v$	Number of Vibrations N	T	T'	R'	n		
A_{1g}	1	1	1	1	1	1	1	0	0	0	1		$\alpha_{xx}+\alpha_{yy},\alpha_{zz}$
A_{1u}	1	−1	1	−1	1	−1	2	0	1	0	1		
A_{2g}	1	1	1	1	−1	−1	3	0	1	1	1		
A_{2u}	1	−1	1	−1	−1	1	4	1	1	1	1	T_z	
E_g	2	−1	−1	2	0	0	4	0	1	1	2		$(\alpha_{xx}-\alpha_{yy},\alpha_{xy}),(\alpha_{xz},\alpha_{yz})$
E_u	2	1	−1	−2	0	0	6	1	2	1	2	(T_x,T_y)	
$N_R(p)$	10	2	4	2	4	0							
$N_R(s)$	4	2	4	2	2	0							
$N_R(s-v)$	2	0	2	0	2	0							
$\chi_R(N)$	30	0	0	−6	−4	0							
$\chi_R(T)$	3	0	0	−3	−1	1							
$\chi_R(T')$	9	0	0	−3	−1	−1							
$\chi_R(R')$	6	0	0	0	−2	0							
$\chi_R(n)$	12	0	0	0	0	0							

Key:

p, total number of atoms in the Bravais cell.

s, total number of molecules (ions) in the Bravais cell.

v, total number of monoatomic molecules (ions) in the Bravais cell.

$N_R(p)$, number of atoms unchanged by symmetry operation R.

$N_R(s)$, number of molecules (ions) whose center of gravity is unchanged by symmetry operation R.

$N_R(s-v)$, $N_R(s)$ minus number of monoatomic molecules (ions) unchanged by symmetry operation R.

$\chi_R(N)=N_R(p)[\pm(1+2\cos\theta)]$, character of representation for entire freedom possessed by the Bravias cell.

$\chi_R(T)=\pm(1+2\cos\theta)$, character of representation for translation motions of the whole Bravais cell.

$\chi_R(T')=\{N_R(s)-1\}\{\pm(1+2\cos\theta)\}$ character of representation for translatory lattice modes.

$\chi_R(R')=N_R(s-v)\{\pm(1+2\cos\theta)\}$, character of representation for rotary lattice modes.

$\chi_R(n)=\chi_R(N)-\chi_R(T)-\chi_R(T')-\chi_R(R')$, character of representation for internal modes.

Note that + and – signs are for proper and improper rotations, respectively. The symbol θ should be taken as defined in Sec. 1.8.

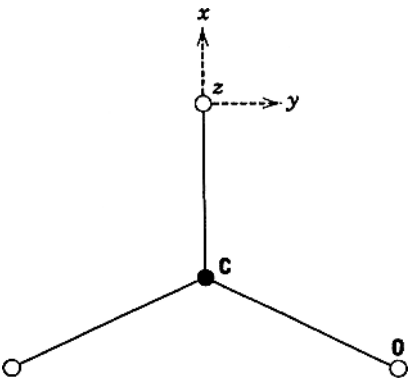

Fig. 1.43. *The x, y,* and *z* axes chosen for planar CO_3^{2-} ion.

normal modes of an *N*-atom molecule can be expressed by using 3*N* translational motions. Furthermore, the symmetry species of these normal modes must correlate with those of the translational motions of an atom located at a particular site within the molecule. Since the latter are known from the molecular structure, the former may be determined directly by using the correlation table.

As an example, consider a planar CO_3^{2-} ion for which the *x*, *y*, and *z* axes are chosen as shown in Fig. 1.43. It is readily seen that the C atom is situated at the $\mathbf{D}_{3h}$ site, whereas the O atom is situated at a site where the local symmetry is only $\mathbf{C}_{2v}$ ($\boldsymbol{I}$, C_2, σ_h, and σ_v). The translational motions of the C atom under $\mathbf{D}_{3h}$ symmetry are: T$z(A''_2)$and $(T_x, T_y)(E')$. The translational motions of the O atom under $\mathbf{C}_{2v}$ symmetry are: $T_x(A_1)$, $T_y(B_2)$ and $T_z(B_1)$. In Table 1.22, the symmetry species of these translational motions are connected by arrows to those of the whole ion using the correlation table. Then, the number of times a particular symmetry species occurs in the total representation is given by the number of arrows that terminate on that species. The number of normal vibrations of the CO_3^{2-} ion in each symmetry species is given by subtracting those of the translational and rotational motions of the whole ion from the total representation. The results are shown at the bottom of Table 1.22.

Thus, the CO_3^{2-} ion exhibits four normal vibrations; v_1 (A'_1 Raman-active), v_2 (A''_2 IR-active), $v_3(E')$, IR- and Raman-active), and v_4 (E', IR- and Raman-active). The normal modes of these four vibrations are shown in Fig. 2.8.

In Sec. 1.8, we derived the general method to classify normal vibrations into symmetry species based on group theory. As seen above, this procedure is greatly simplified if we use the correlation method.

1.29.2. Intramolecular Vibrations in the CO_3^{2-} Ion in Calcite

Applying the same principle as that used above, we can classify the normal vibrations of the CO_3^{2-} ion in the calcite lattice by using the correlation method. As discussed in

TABLE 1.22. Correlation Method for the CO_3^{2-} Ion in the Free State

C Atom D_{3h}	CO_3^{2-} Ion D_{3h}	O Atom C_{2v}
	A_1'	
	$A_2'(R_z)$	$A_1(T_x)$
	A_1''	
$A_2''(T_z)$ →	$A_2''(T_z)$	$B_2(T_y)$
$E'(T_x, T_y)$ →	$E'(T_x, T_y)$	$B_1(T_z)$
	$E''(R_x, R_y)$	

$\chi_{(total)} = A_1' + A_2' + 2A_2'' + 3E' + E''.$

$\chi_{(trans)} = A_2'' + E'.$

$\chi_{(rot)} = A_2' + E''.$

$\chi_{(vib)} = A_1' + A_2'' + 2E'.$

Sec. 1.28, calcite belongs to the space group $\mathbf{D}_{3d}^6$, and Z is 2. From the Bravais cell shown in Fig. 1.42, it is readily seen that the CO_3^{2-} ion is at the $\mathbf{D}_3$ site, whereas the Ca^{2+} ion is at the $\mathbf{C}_{3i}$ ($\equiv\mathbf{S}_6$) site. Table 1.23 shows the correlations among the molecular symmetry ($\mathbf{D}_{3h}$), site symmetry ($\mathbf{D}_3$), and factor group symmetry ($\mathbf{D}_{3d}$). Under the "Vib." column, we list the number of vibrations belonging to each species of $\mathbf{D}_{3h}$ symmetry (Table 1.22). Throughout the present correlations, the number of degrees of vibrational freedom for all the doubly degenerate species must be multiplied by 2 since there are two E' modes (ν_3 and ν_4). Thus, it is 4 for the E' species. The number under "f" indicates "Vib." times Z (=2), which is the number of vibrations of the unit cell. In going from D_{3h} to $\mathbf{D}_3$, no changes occur

TABLE 1.23. Correlation between Molecular Symmetry, Site Symmetry, and Factor Group Symmetry for Intramolecular Vibrations of CO_3^{2-} Ion in Calcite

f	Vib.	Molecular Symmetry ($\mathbf{D}_{3h}$)	Site Symmetry ($\mathbf{D}_3$)	C_{a_m}	Factor Group Symmetry ($\mathbf{D}_{3d}$)	C_{a_ζ}
2	1	A_1' (ν_1) →	A_1	1 × 2	A_{1g}	1 × 1
					A_{1u}	1 × 1
8	4	E' (ν_3, ν_4) →	E	2 × 4	E_g	2 × 2
					E_u	2 × 2
2	1	A_2'' (ν_2) →	A_2	1 × 2	A_{2g}	1 × 1
					A_{2u}	1 × 1

$\chi_{(intra)} = A_{1g} + A_{1u} + A_{2g} + A_{2u} + 2E_g + 2E_u.$

TABLE 1.24. Correlation between Site Symmetry and Factor Group Symmetry for Lattice Vibrations of CO_3^{2-} Ion in Calcite

f	t	Site Symmetry ($\mathbf{D}_3$)	Factor Group Symmetry ($\mathbf{D}_{3d}$)	C	a_ζ
4	2	$E(T_x, T_y)$ (R_x, R_y)	$E_g(R_x, R_y)$	2	1
			$E_u(T_x, T_y)$	2	1
2	1	$A_2(T_z)$ (R_z)	$A_{2g}(R_z)$	1	1
			$A_{2u}(T_z)$	1	1

$\chi(\text{trans}, CO_3^{2-}) = E_g + E_u + A_{2g} + A_{2u}.$
$\chi(\text{rot}, CO_3^{2-}) = E_g + E_u + A_{2g} + A_{2u}.$

except for changes in notations of symmetry species. Column C indicates the degeneracy, and column a_m shows the degree of vibrational freedom contributed by the corresponding molecular symmetry species. Finally, the species under $\mathbf{D}_3$ symmetry are connected to those of the factor group by the arrows using the correlation table. The last column, "a", is the degree of vibrational freedom contributed by the corresponding site symmetry species to the factor group species. It should be noted that the number of degrees of vibrational freedom must be 12 throughout the described correlations above. Such bookkeeping must be carried out for every correlation.

1.29.3. Lattice Vibrations in Calcite

Table 1.24 shows the correlation diagram for lattice vibrations of the CO_3^{2-} ion. The variables "t" and "f" denote the degrees of translational freedom of the CO_3^{2-} ion for each ion and for the Bravais cell, respectively. The same result is obtained for the rotatory lattice vibrations. Table 1.25 shows the correlation diagram for translatory

TABLE 1.25. Correlation between Site Symmetry and Factory Group Symmetry for Lattice Vibrations of the Ca^{2+} Ion in Calcite

f	t	Site Symmetry ($\mathbf{C}_{3i}$)	Factor Group Symmetry ($\mathbf{D}_{3d}$)	C	a_ζ
2	1	$A_u(T_z)$	A_{1u}	1	1
			$A_{2u}(T_z)$	1	1
4	2	$E_u(T_x, T_y)$	$E_u(T_x, T_y)$	2	2

$\chi(\text{trans}, Ca^{2+}) = A_{1u} + A_{2u} + 2E_u.$
$\chi(\text{acoustical}) = A_{2u} + E_u.$
$\chi(\text{trans, total}) = \chi(\text{trans}, CO_3^{2-}) + \chi(\text{trans}, Ca^{2+}) - \chi(\text{acoustical})$
$= A_{1u} + A_{2g} + A_{2u} + E_g + 2E_u.$

TABLE 1.26. Distribution of Normal Vibrations of Calcite as Obtained by Correlation Method

Symmetry Species of Factor Group (D_{3d})	Translatory Lattice	Acoustical	Rotatory Lattice	Intramolecular
A_{1g} (Raman)	0	0	0	1
A_{1u}	1	0	0	1
A_{2g}	1	0	1	1
A_{2u} (IR)	1	1	1	1
E_g (Raman)	1	0	1	2
E_u (IR)	2	1	1	2
Total	9	3	6	12

lattice vibrations of the Ca^{2+} ion. No rotatory lattice vibrations exist for single-atom ions such as the Ca^{2+} ion. The distribution of all the translatory lattice vibrations can be obtained by subtracting χ (acoustical) from χ (*trans*, CO_3^{2-}) + χ (*trans*, Ca^{2+}).

1.29.4. Summary

Table 1.26 summarizes the results obtained in Tables 1.23–1.25. The total number of vibrations including the acoustical modes should be 30 since the Bravais cell contains 10 atoms. These results are in complete agreement with that obtained by factor group analysis (Table 1.21).

1.30. LATTICE VIBRATIONS [48]

Consider a lattice consisting of two alternate layers of atoms; atoms 1 of mass M_1 lie on one set of planes and atoms 2 of mass M_2 lie on another set of planes, as shown in Fig. 1.44. For example, such an arrangement is found in the 111 plane of the

TABLE 1.27. Correlation between Site Symmetry (C_{2v}) and Factor Group Symmetry (D_{2h}) for Orthorhombic form of the 123 Conductor[a]

f	t	Site Symmetry (C_{2v}), $C_2(z)$	Factor Group Symmetry (D_{2h})	a_ζ
2	1	$A_1(T_z)$	A_g	1
			$B_{1u}(T_z)$	1
2	1	$B_1(T_x, R_y)$	$B_{2g}(R_y)$	1
			$B_{3u}(T_x)$	1
2	1	$B_2(T_y, R_x)$	$B_{3g}(R_x)$	1
			$B_{2u}(T_y)$	1

[a]For *f*, *t*, and *a*, see Sec. 1.29. The complete correlation table is found in Appendix IX.

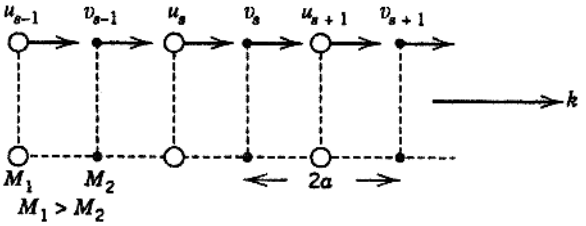

Fig. 1.44. *Displacements of atoms 1 and 2 in a diatomic lattice.*

NaCl crystal. Let a denote the distance between atoms 1 and 2. Then the length of the primitive cell is $2a$. We consider waves that propagate in the direction shown by the arrow, and assume that each plane interacts only with its neighboring planes. If the force constants (f) are identical between all these neighboring planes, we have

$$M_1 \frac{d^2 u_s}{dt^2} = f(v_s + v_{s-1} - 2u_s) \tag{1.233}$$

$$M_2 \frac{d^2 v_s}{dt^2} = f(u_{s+1} + u_s - 2v_s) \tag{1.234}$$

where u_s and v_s denote the displacements of atoms 1 and 2 in the cell indexed by s.

The solutions for these equations take the form of a traveling wave having different amplitudes u and v. Thus, we obtain

$$u_s = u \exp[i(\omega t + 2ska)] \tag{1.235}$$

$$v_s = v \exp[i(\omega t + 2ska)] \tag{1.236}$$

Here ω is angular frequency, $2\pi\nu$ [in reciprocal seconds (s^{-1})]. If these are substituted in Eqs. 1.233 and 1.234, respectively, we obtain

$$[M_1\omega^2 - 2f]u + f[1 + \exp(-2ika)]v = 0 \tag{1.237}$$

$$f[1 + \exp(2ika)]u + [M_2\omega^2 - 2f]v = 0 \tag{1.238}$$

These homogeneous linear equations have a nontrivial solution if the following determinant is zero:

$$\begin{vmatrix} M_1\omega^2 - 2f & f[1 + \exp(-2ika)] \\ f[1 + \exp(2ika)] & M_2\omega^2 - 2f \end{vmatrix} = 0 \tag{1.239}$$

By solving this equation, we obtain

$$\omega^2 = f\left(\frac{1}{M_1} + \frac{1}{M_2}\right) + f\left[\left(\frac{1}{M_1} + \frac{1}{M_2}\right)^2 - \frac{4\sin^2 ka}{M_1 M_2}\right]^{1/2} \tag{1.240}$$

(optical branch)

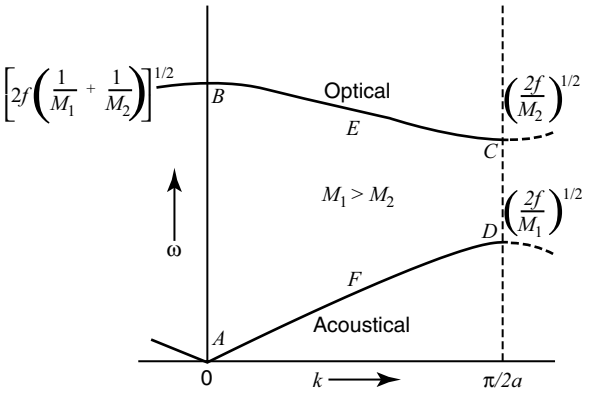

Fig. 1.45. *Dispersion curves for lattice vibrations.*

$$\omega^2 = f\left(\frac{1}{M_1}+\frac{1}{M_2}\right) - f\left[\left(\frac{1}{M_1}+\frac{1}{M_2}\right)^2 - \frac{4\sin^2 ka}{M_1 M_2}\right]^{1/2} \qquad (1.241)$$
(acoustical branch)

The term k in Eqs. 1.235–1.241 is called the *wavevector* and indicates the phase difference between equivalent atoms in each unit cell. In the case of a one-dimensional lattice, $|k| = k$. Thus, we use k rather than $|k|$ in this case, and k can take any value between $-\pi/2a$ and $+\pi/2a$. This region is called the *first Brillouin zone*. Figure 1.45 shows a plot of ω versus k for the positive half of the first Brillouin zone. There are two values for each ω that constitute the "optical" and "acoustical" branches in the dispersion curves.

At the center of the first Brillouin zone ($k = 0$), we have

$$\omega = 0 \quad \text{and} \quad u = v \quad \text{(acoustical)} \qquad (1.242)$$

$$\omega = \sqrt{2f\left(\frac{1}{M_1}+\frac{1}{M_2}\right)} \qquad (1.243)$$

$$\text{and} \quad \frac{u}{v} = -\frac{M_2}{M_1} \quad \text{or} \quad M_1 u + M_2 v = 0 \quad \text{(optical)}$$

At the end of the first Brillouin zone ($k = \pi/2a$), we have

$$\omega = \sqrt{\frac{2f}{M_2}} \quad \text{and} \quad u = 0 \quad \text{(optical)} \qquad (1.244)$$

$$\omega = \sqrt{\frac{2f}{M_1}} \quad \text{and} \quad v = 0 \quad \text{(acoustical)} \qquad (1.245)$$

points A, B, C, and D in Fig. 1.45 correspond to Eqs. 1.242, 1.243, 1.244, and 1.245, respectively.

To observe lattice vibrations in IR spectra, the momentum of the IR photon must be equal to that of the phonon.* The momentum of the photon (P) is given by

$$P = \frac{h}{\lambda} = \frac{h/2\pi}{\lambda/2\pi} = \hbar Q \tag{1.246}$$

where $Q = 2\pi/\lambda$. On the other hand, the momentum of the phonon is given by $\hbar k$ [141]. Thus, the following relationship must hold:

$$\hbar Q = \hbar k \tag{1.247}$$

Since lattice vibrations are observed in the low-frequency region ($\lambda \cong 10^{-3}$ cm), $Q = 2\pi/\lambda \cong 10^{3}$ cm. The k value at the end of the Brillouin zone is $k = \pi/2a \cong 10^{8}$ cm^{-1}. Thus, the k value that corresponds to the IR photon for lattice vibration is much smaller than the k value at the end of the Brillouin zone. This result indicates that the optical transitions we observe in IR spectra occur practically at $k \cong 0$. A similar conclusion can be derived for Raman spectra of lattice vibrations.

Figure 1.46 shows the modes of lattice vibrations corresponding to various points on the dispersion curve shown in Fig. 1.45. At point A (acoustical mode), all atoms move in the same direction (translational motion of the whole lattice) and its frequency is zero. This is seen in Fig. 1.46a. In a three-dimensional lattice, there are three such modes. Thus, we subtract 3 from our calculations in factor group analysis (Sec. 1.28).

On the other hand, at point B (optical branch), the two atoms move in opposite directions, but the center of gravity of the unit cell remains unshifted (Fig. 1.46b). Furthermore, the equivalent atom in each lattice moves in phase. If the two atoms carry opposite electrical charges, such a motion produces an oscillating dipole moment that can interact with incident IR radiation. Thus, it is possible to observe it optically. It should be noted that the frequency of a diatomic molecule in the free state is $\omega = \sqrt{f/\mu}$, whereas that of a diatomic lattice is $\omega = \sqrt{2f/\mu}$ (μ = reduced mass).

At point C (optical branch), the lighter atoms are moving back and forth against each other while the heavier atoms are fixed (Fig. 1.46c). At point D (acoustical branch), the situation is opposite to that of point C. The vibrational modes in the middle of the Brillouin zone (points E and F) are shown in Figs. 1.46e and 1.46f, respectively.

Thus far, we have discussed the lattice vibrations of a one-dimensional chain. The treatment of the three-dimensional lattice is basically the same, although more complicated [48]. If the primitive cell contains σ molecules, each of which consists of N atoms, there are 3 acoustical modes and $3N\sigma - 3$ optical modes. The latter is grouped into $(3N-6)\sigma$ internal modes and $6\sigma - 3$ lattice modes. The general forms of

*The lattice vibration causes elastic waves in crystals. The quantum of die lattice vibrational energy is called "phonon," in analogy with the photon of the electromagnetic wave.

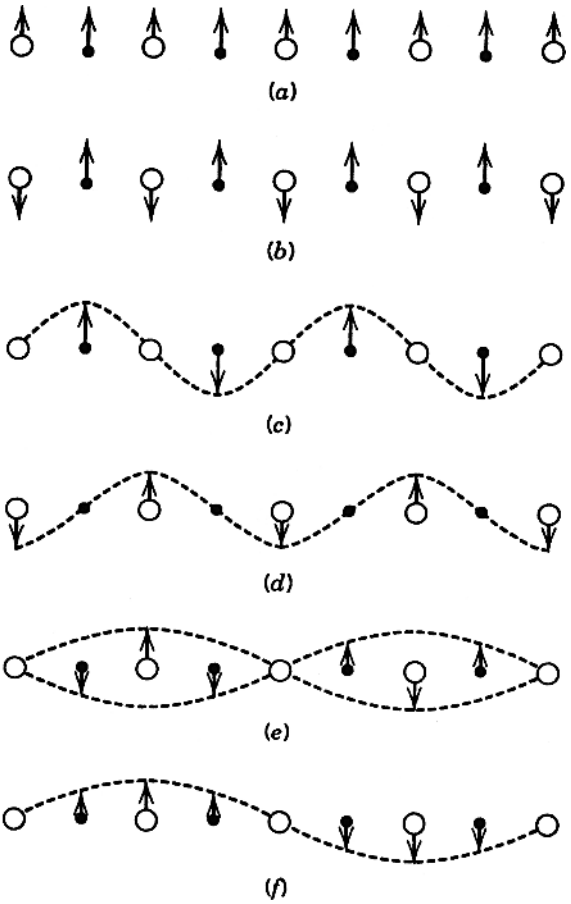

Fig. 1.46. *Wave motions corresponding to various points on the dispersion curves.*

the dispersion curves of such a crystal are shown in Fig. 1.47. In this book, our interest is focused on vibrational analysis of $3N\sigma$–3 optical modes at $k \cong 0$. Examples are found in diamond and graphite (Sec. 2.14.3) and quartz (Sec. 2.15.2).

1.31. POLARIZED SPECTRA OF SINGLE CRYSTALS

In the preceding section, the 30 normal vibrations of the Bravais cell of calcite crystal have been classified into symmetry species of the factor group $\mathbf{D}_{3d}$. The results (Table 1.26) show that three intramolecular $(A_{2u} + 2E_u)$, three translatory lattice $(A_{2u} + 2E_u)$ and two rotatory lattice $(A_{2u} + E_u)$ vibrations are IR-active, whereas three intramolecular $(A_{1g} + 2E_g)$, one translatory lattice (E_g), and one rotatory lattice (E_g) vibrations are Raman-active. In order to classify the observed bands into these symmetry species, it is desirable to measure infrared dichroism and polarized Raman spectra using single crystals of calcite.

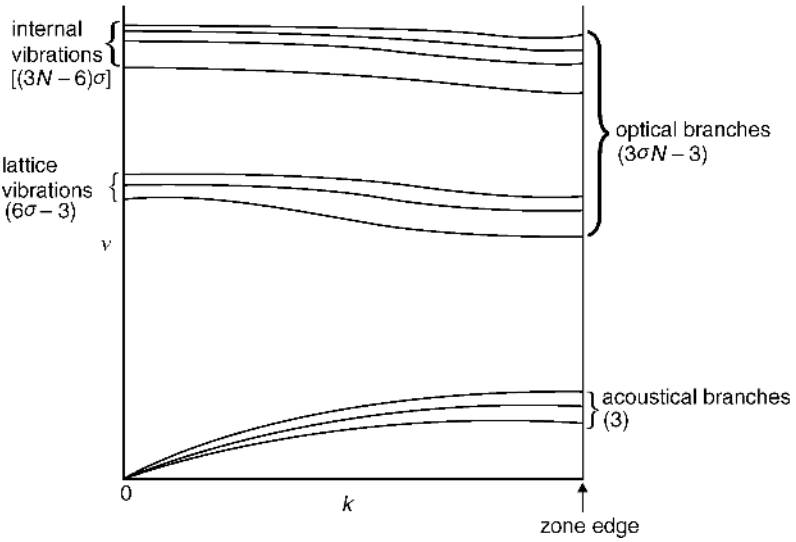

Fig. 1.47. *General form of dispersion curves for a molecular crystal [48].*

1.31.1. Infrared Dichroism

Suppose that we irradiate a single crystal of calcite with polarized infrared radiation whose electric vector vibrates along the c axis (z direction) in Fig. 1.42. Then the infrared spectrum shown by the solid curve of Fig. 1.48 is obtained [142]. According to Table 1.21, only the A_{2u} vibrations are activated under such conditions. Thus, the three bands observed at 885(v), 357(t), and 106(r) cm^{-1} are assigned to the A_{2u} species. The spectrum shown by the dotted curve is obtained if the direction of polarization is perpendicular to the c axis (x,y plane). In this case, only the E_u vibrations should be infrared-active. Therefore the five bands observed at 1484(v), 706(v), 330(t), 182(t), and 106(r) cm^{-1} are assigned to the E_u species. Here, v, t, and r denote intramolecular, translatory lattice, and rotatory lattice modes, respectively.

1.31.2. Polarized Raman Spectra

Polarized Raman spectra provide more information about the symmetry properties of normal vibrations than do polarized infrared spectra [143]. Again consider a single

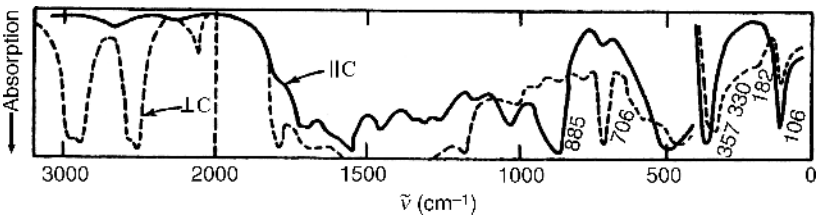

Fig. 1.48. *Infrared dichroism of calcite [142].*

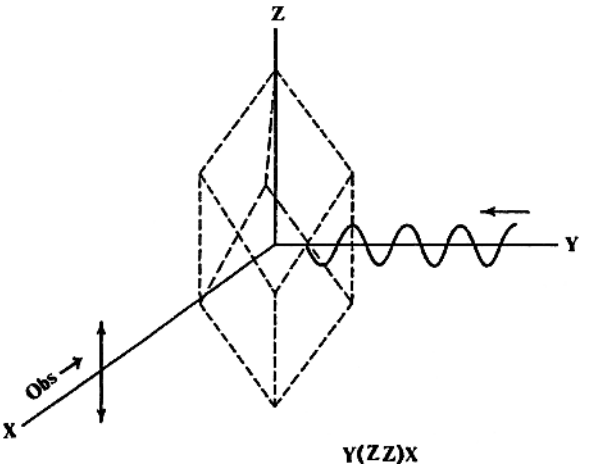

Fig. 1.49. *Schematic representation of experimental condition y(zz)x.*

crystal of calcite. According to Table 1.21, the A_{1g} vibrations become Raman-active if any one of the polarizability components, α_{xx}, α_{yy}, and α_{zz}, is changed. Suppose that we irradiate a calcite crystal from the y direction, using polarized radiation whose electric vector vibrates parallel to the z axis (see Fig. 1.49), and observe the Raman scattering in the x direction with its polarization in the z direction. This condition is abbreviated as $y(zz)x$. In this case, Eq. 1.66 is simplified to $Pz = \alpha_{zz}E_z$ because $E_x = E_y = 0$ and $P_x = P_y = 0$. Since α_{zz} belongs to the A_{1g} species, only the A_{1g} vibrations are observed under this condition. Figure 1.50c illustrates the Raman spectrum obtained with this condition. Thus, the strong Raman line at 1088 cm^{-1} (v) is assigned to the A_{1g} species. Both the A_{1g} and E_g vibrations are observed if the $z(xx)y$ condition is used. The Raman spectrum (Fig. 1.50a) shows that five Raman lines [1088(v), 714(v), 283(r), 156(t), and 1434(v) cm^{-1} (not shown)] are observed under this condition. Since the 1088 cm^{-1} line belongs to the A_{1g} species, the remaining four must belong to the E_g species. These assignments can also be confirmed by measuring Raman spectra using the $y(xy)x$ and $x(zx)y$ conditions (Figs. 1.50b and 1.50d) .

1.31.3. Normal Coordinate Analysis on the Bravais Cell

In the discussion above, we have assigned several bands in the same symmetry species to the v, t, and r types. In general, the intramolecular (v) vibrations appear above 400 cm^{-1}, whereas the lattice vibrations appear below 400 cm^{-1}. However, more complete assignments can be made only via normal coordinate analysis on the entire Bravais cell [144]. Such calculations have been made by Nakagawa and Walter [145] on crystals of alkali–metal nitrates that are isomorphous with calcite. These workers employed four intramolecular and seven intermolecular force constants. The latter are in the range of 0.12–0.00 mdyn/Å. Figure 1.51 illustrates the vibrational modes of the 18 (27 if E modes are counted as 2) optically active vibrations together with the corresponding frequencies of calcite.

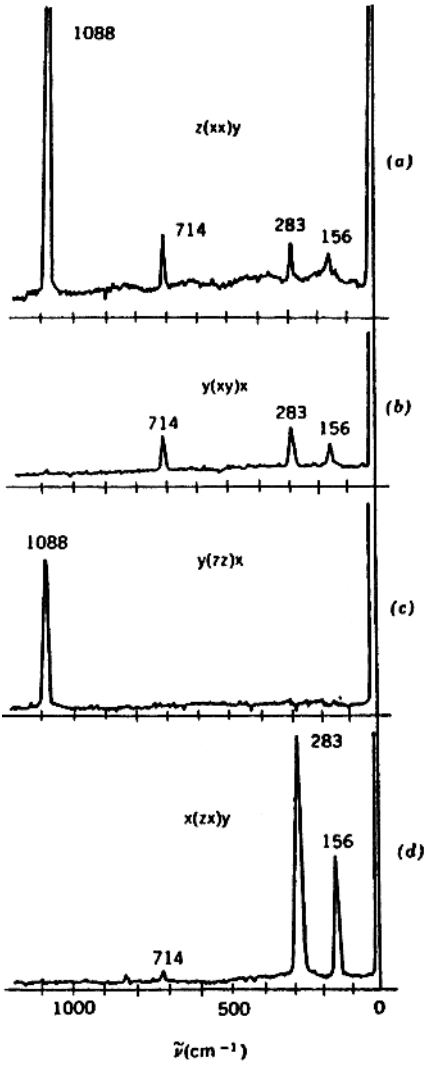

Fig. 1.50. *Polarized Raman spectra of calcite [143].*

1.32. VIBRATIONAL ANALYSIS OF CERAMIC SUPERCONDUCTORS

In 1987, Wu et al. [146] synthesized a ceramic superconductor of the composition, $YBa_2Cu_3O_{7-\delta}$, whose superconducting critical temperature (T_c) was above the boiling point of liquid nitrogen (77 K). Since then, IR and Raman spectra of this and related compounds have been studied extensively, and the results are reviewed by Ferraro and Maroni [147,148]. Here, we limit our discussion to the Raman spectra of the superconductor mentioned above and their significance in studying oxygen deficiency and the structural changes resulting from it.

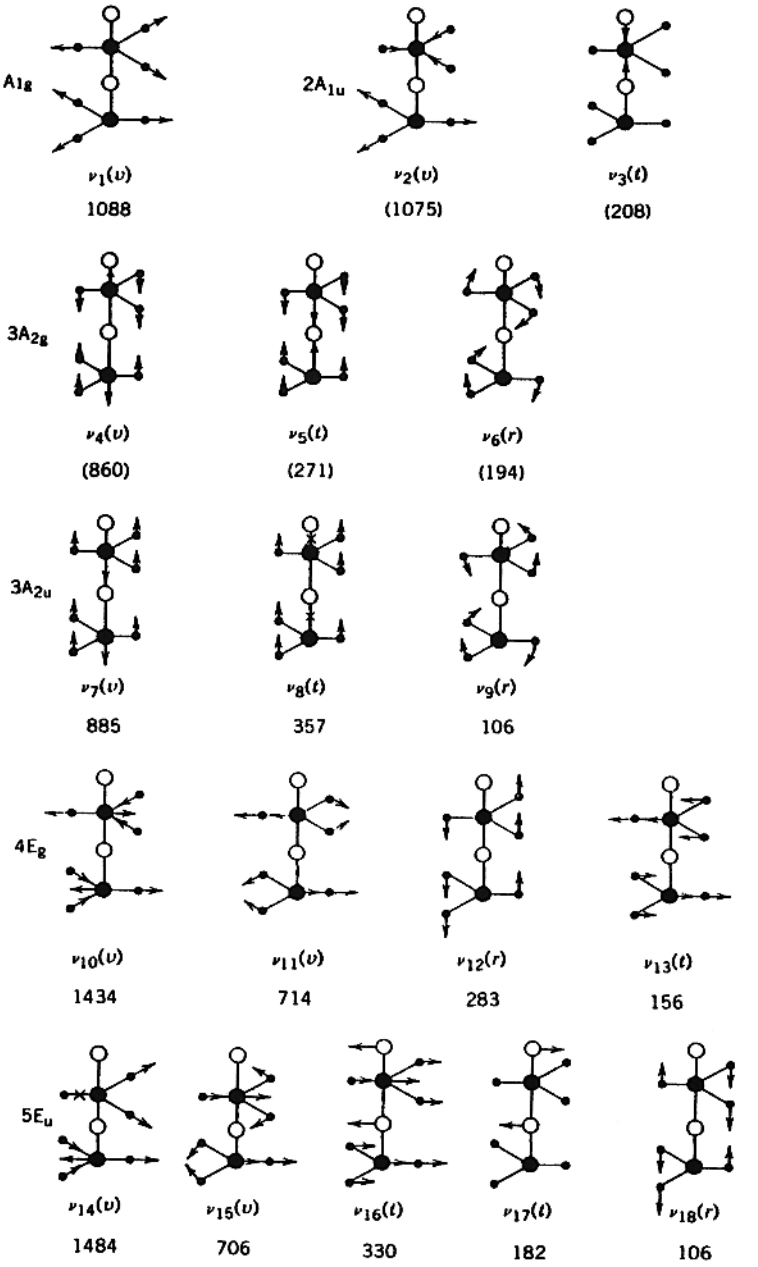

Fig. 1.51. *Vibrational modes of calcite. The observed and calculated (in parentheses) are listed under each mode [145].*

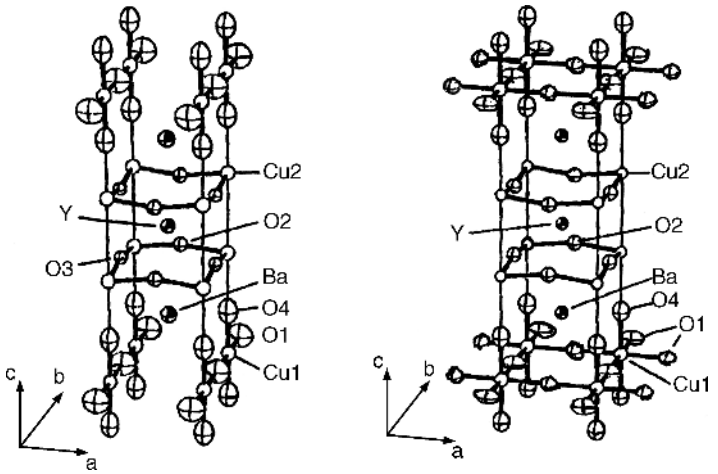

Fig. 1.52. *The Bravais unit cells of the orthorhombic and tetragonal forms of* $YBa_2Cu_3O_{7-\delta}$ *[149].*

The superconductor, $YBa_2Cu_3O_{7-\delta}$ (abbreviated as the 123 conductor), can be obtained by baking a mixture of Y_2O_3, and $BaCO_3$, and CuO in a proper ratio. The product is normally a mixture of an orthorhombic form ($0 < \delta < 1$) which is superconducting and a tetragonal form ($\delta = 1$) that is an insulator. The T_c increases as δ approaches 0.

Figure 1.52 shows the Bravais unit cells of the orthorhombic ($Pmmm = D^1_{2h}$) and tetragonal ($P4/mmm = D^1_{4h}$) forms. The former is a distorted, oxygen-deficient form of perovskite. The orthorhombic unit cell contains 13 atoms, and their possible site symmetries can be found from the tables of site symmetries (Appendix X) as follows:

$$8\mathbf{D}_{2h}(1), \quad 12\mathbf{C}_{2v}(2), \quad 6\mathbf{C}_s(4), \quad \mathbf{C}_1(8)$$

It is seen in Fig. 1.52 that the three atoms, Y, O(1), and Cu(1), are at the $\mathbf{D}_{2h}$ sites. These atoms contribute $3B_{1u} + 3B_{2u} + 3B_{3u}$ vibrations since T_x, T_y, and T_z belong to the B_{3u}, B_{2u}, and B_{1u} species, respectively, in the $\mathbf{D}_{2h}$ point group. On the other hand, the 10 atoms, 2Ba, 2Cu(2), 2O(2), 2O(3), and 2O(4) are at the $\mathbf{C}_{2v}$ sites. As shown in Table 1.27, each pair of these atoms possess six degrees of vibrational freedom ($2A_1 + 2B_1 + 2B_2$), which are split into $A_g + B_{2g} + B_{3g} + B_{1u} + B_{2u} + B_{3u}$ under $\mathbf{D}_{2h}$ symmetry. The number of optical modes at $k \cong 0$ in each species can be obtained by subtracting three acoustical modes ($B_{1u} + B_{2u} + B_{3u}$) from the above counting. Table 1.28 summarizes the results. It is seen that the orthorhombic unit cell has 15 Raman-active modes ($5A_g + 5B_{2g} + 5B_{3g}$) and 21 IR-active modes ($7B_{1u} + 7B_{2u} + 7B_{3u}$). It should be noted that the mutual exclusion rule holds in this case since the $\mathbf{D}_{2h}$ point group has a center of symmetry. Although the same results can be obtained by using factor group analysis [150], the correlation method is simpler and straightforward.

Similar calculations on the tetragonal unit cell ($YBa_2Cu_3O_6$) show that 10 vibrations ($4A_{1g} + B_{1g} + 5E_g$) are Raman-active while 11 vibrations ($5A_{2u} + 6E_u$) are IR-active under $\mathbf{D}_{4h}$ symmetry.

TABLE 1.28. Vibrational Analysis for Orthorhombic Form of $YBa_2Cu_3O_{7-\delta}$ Using the Correlation Method

D_{2h}	D_{2h} Y, O(1), Cu (1)	C_{2v} Ba, Cu(2), O(2), O(3), O(4)	Acoustical Vib.	Total Optical Vib.	Activity
A_g	0	5	0	5	Raman
B_{1g}	0	0	0	0	Raman
B_{2g}	0	5	0	5	Raman
B_{3g}	0	5	0	5	Raman
Au	0	0	0	0	Inactive
B_{1u}	3	5	1	7	IR
B_{2u}	3	5	1	7	IR
B_{3u}	3	5	1	7	IR
Total	9	30	3	36	

Figure 1.53 shows the Raman spectrum of a polished sintered pellet of the 123 conductor ($\delta = 0.3$) obtained by Ferraro et al. [151]. The five A_g modes appear strongly, and the most probable assignments for these bands are [152,153].

$492\,cm^{-1}$	Axial motion of the O(4) atoms
$445\,cm^{-1}$	O(2)−Cu(2)−O(3) bending with the two O atoms moving in phase
$336\,cm^{-1}$	O(2)−Cu(2)−O(3) bending with the two O atoms moving out of phase
$145\,cm^{-1}$	Axial motion of the Cu(2) atoms
$116\,cm^{-1}$	Axial motion of the Ba atoms

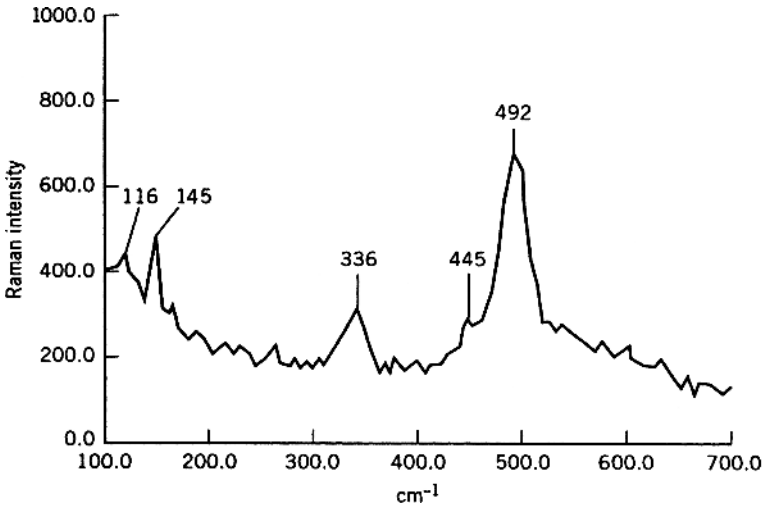

Fig. 1.53. *Backscattered Raman spectrum of a polished sintered pellet of $YBa_2Cu_3O_{7-\delta}$ [151].*

These values fluctuate within $\pm 10\,\mathrm{cm}^{-1}$ depending on variations in oxygen stoichiometry and crystalline disorder. The results of normal coordinate analysis [154] indicate considerable mixing among the vibrations represented by the Cartesian coordinates of individual atoms.

If the 123 conductor is prepared in pure oxygen and the oxygen is removed quantitatively by heating the sample in argon, a series of samples having $\delta = 0$, 0.2, 0.5, and 0.7 can be obtained. The T_c values of these samples were found to be 94, 77, 50, and 20 K, respectively. Thomsen et al. [155] prepared a series of such samples, and measured their Raman spectra. Figure 1.54 shows a plot of vibrational frequencies of the four A_g modes mentioned above against δ values. It is seen that the two modes at 502 and $154\,\mathrm{cm}^{-1}$ are softened and the two modes at 438 and $334\,\mathrm{cm}^{-1}$ are hardened as the oxygen is removed from the sample. These results

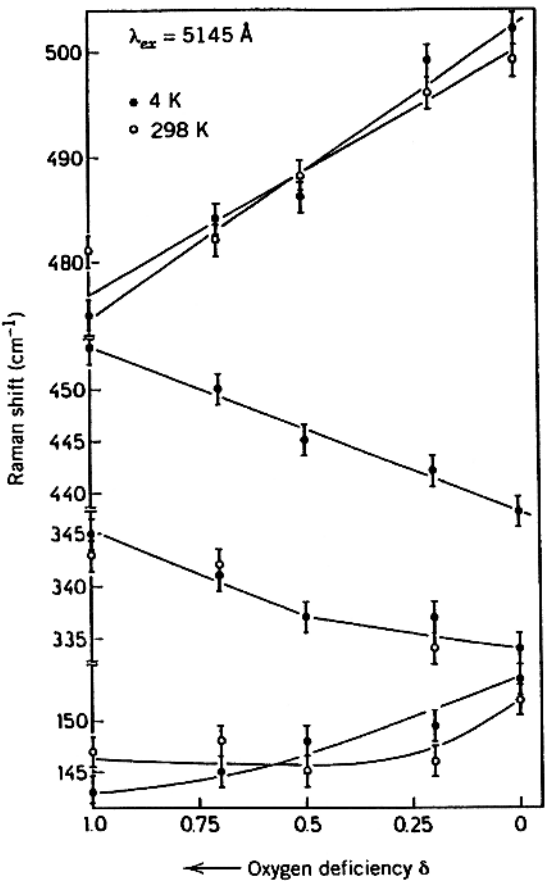

Fig. 1.54. *Dependence of four Raman frequencies on oxygen concentration at 4 K and 298 K [155].*

seem to suggest that the T_c of the 123 conductor is related to oxygen deficiency in the O(2)−Cu(2)−O(3) layer. The effect of changing the size of the cation (Y) [156] and isotopic substitution ($^{16}O/^{18}O$) [157] on these Raman bands has also been studied.

Thus far, IR studies on the 123 conductor have been hindered by the difficulties in obtaining IR spectra from highly opaque samples and in making reliableb and assignments [147,148].

REFERENCES

Theory of Molecular Vibrations

1. G. Herzberg, *Molecular Spectra and Molecular Structure, Vol. II: Infrared and Raman Spectra of Polyatomic Molecules*, Van Nostrand, Princeton, NJ, 1945.
2. G. Herzberg, *Molecular Spectra and Molecular Structure, Vol. I: Spectra of Diatomic Molecules*, Van Nostrand, Princeton, NJ, 1950.
3. E. B. Wilson, J. C. Decius, and P. C. Cross, *Molecular Vibrations*, McGraw-Hill, New York, 1955.
4. C. J. H. Schutte, *The Theory of Molecular Spectroscopy, Vol. I: The Quantum Mechanics and Group Theory of Vibrating and Rotating Molecules*, North Holland, Amsterdam, 1976.
5. L. A. Woodward, *Introduction to the Theory of Molecular Vibrations and Vibrational Spectroscopy*, Oxford University Press, London, 1972.
6. J. D. Craybeal, *Molecular Spectroscopy*, McGraw-Hill, New York, 1988.
7. J. M. Hollas, *Modern Spectroscopy*, 2nd ed., Wiley, New York, 1992.
8. M. Diem, *Introduction to Modern Vibrational Spectroscopy*, Wiley, New York, 1993.

Symmetry and Group Theory

9. J. R. Ferraro and J. S. Ziomek, *Introductory Group Theory and Its Application to Molecular Structure*, 2nd ed., Plenum Press, New York, 1975.
10. D. C. Harris and M. D. Bertolucci, *Symmetry and Spectroscopy*, Oxford University Press, London, 1978.
11. P. R. Bunker, *Molecular Symmetry and Spectroscopy*, Academic Press, New York, 1979.
12. F. A. Cotton, *Chemical Application of Group Theory*, 3rd ed., Wiley-Interscience, New York, 1990.
13. R. L. Carter, *Molecular Symmetry and Group Theory*, Wiley, New York, 1992.
14. S. F. A. Kettle, *Symmetry and Structure*, 2nd ed., Wiley, New York, 2000.

Correlation Method

15. W. G. Fateley, F. R. Dollish, N. T. McDevitt, and F. F. Bentley, *Infrared and Raman Selection Rules for Molecular and Lattice Vibrations: The Correlation Method*, Wiley-Interscience, New York, 1972.

Vibrational Intensities

16. W. B. Person and G. Zerbi, eds., *Vibrational Intensities in Infrared and Raman Spectroscopy*, Elsevier, Amsterdam, 1982.

Fourier Transform Infrared Spectroscopy

17. J. R. Ferraro and L. J. Basile, eds., *Fourier Transform Infrared Spectroscopy*, Vol. I, Academic Press, New York, 1978 to present.
18. P. G. Griffiths, and J. A. de Haseth, *Fourier Transform Infrared Spectrometry*, Wiley, New York, 1986.
19. J. R. Ferraro and K. Krishnan, eds., *Practical Fourier Transform Infrared Spectroscopy*, Academic Press, San Diego, CA, 1990.
20. H. C. Smith, *Fundamentals of Fourier Transform Infrared Spectroscopy*, CRC Press, Boca Raton, FL, 1996.

Raman Spectroscopy

21. D. P. Strommen and K. Nakamoto, *Laboratory Raman Spectroscopy*, Wiley, New York, 1984.
22. J. G. Grasselli and B. J. Bulkin, eds., *Analytical Raman Spectroscopy*, Wiley, New York, 1991.
23. H. A. Szymanski, eds., *Raman Spectroscopy: Theory and Practice*, Vol. 1, Plenum Press, New York, 1967; Vol. 2 1970.
24. J. A. Koningstein, *Introduction to the Theory of the Raman Effect*, D. Reidel, Dordrecht (Holland), 1973.
25. D. A. Long, *Raman Spectroscopy*, McGraw-Hill, New York, 1977.
26. J. R. Ferraro, K. Nakamoto, and C. W. Brown, *Introductory Raman Specctroscopy*, 2nd ed., Academic Press, San Diego, CA, 2003.
27. E. Smith, *Modern Raman Spectroscopy*, Wiley, New York, 2004.

Low-Temperature and Matrix Isolation Spectroscopy

28. B. Meyer, *Low-Temperature Spectroscopy*, Elsevier, Amsterdam, 1971.
29. H. E. Hallarn, ed., *Vibrational Spectroscopy of Trapped Species*, Wiley, New York, 1973.
30. M. Moskovits and G. A. Ozin, eds., *Cryochemistry*, Wiley, New York, 1976.

Time-Resolved Spectroscopy

31. G. H. Atkinson, *Time-Resolved Vibrational Spectroscopy*, Academic Press, New York, 1983.
32. M. D. Fayer, ed., *Ultrafast Infrared and Raman Spectroscopy*, Marcel Dekker, New York, 2001.

High-Pressure Spectroscopy

33. J. R. Ferraro, *Vibrational Spectroscopy at High External Pressures—the Diamond Anvil Cell*, Academic Press, New York, 1984.

Vibrational Spectra of Inorganic, Coordination, and Organometallic Compounds

34. J. R. Ferraro, *Low-Frequency Vibrations of Inorganic and Coordination Compounds*, Plenum Press, New York, 1971.
35. L. H. Jones, *Inorganic Spectroscopy*, Vol. I, Marcel Dekker, New York, 1971.
36. R. A. Nyquist and R. O. Kagel, *Infrared Spectra of Inorganic Compounds*, Academic Press, New York, 1971.
37. S. D. Ross, *Inorganic Infrared and Raman Spectra*, McGraw-Hill, New York, 1972.
38. E. Maslowsky, Jr., *Vibrational Spectra of Organometallic Compounds*, Wiley, New York, 1977.

Vibrational Spectra of Organic Compounds

39. N. B. Colthup, L. H. Daly, and S. E. Wiberley, *Introduction to Infrared and Raman Spectroscopy*, 3rd ed., Academic Press, San Diego, CA, 1990.
40. D. Lin-Vien, N. B. Colthup, W. G. Fateley, and J. G. Grasselli, *The Handbook of Infrared and Raman Characteristic Frequencies of Organic Molecules*, Academic Press, San Diego, CA, 1991.

Vibrational Spectra of Biological Compounds

41. A. T. Tu, *Raman Spectroscopy in Biology*, Wiley, New York, 1982.
42. P. R. Carey, *Biochemical Applications of Raman and Resonance Raman Spectroscopies*, Academic Press, New York, 1982.
43. F. S. Parker, *Application of Infrared, Raman and Resonance Raman Spectroscopy in Biochemistry*, Plenum Press, New York, 1983.
44. T. G. Spiro, ed., *Biological Applications of Raman Spectroscopy*, Vols. 1–3, Wiley, New York, 1987–1988.
45. H.-U. Gremlich and B. Yan, eds., *Infrared and Raman Spectroscopy of Biological Materials*, Marcel Dekker, New York, 2001.

Vibrational Spectra of Adsorbed Species

46. A. T. Bell and M. L. Hair, eds., *Vibrational Spectroscopies for Adsorbed Species*, American Chemical Society, Washington, DC, 1980.
47. J. T. Yates, Jr. and T. E. Madey, eds., *Vibrational Spectroscopy of Molecules on Surfaces*, Plenum Press, New York, 1987.

Vibrational Spectra of Crystals and Minerals

48. G. Turrell, *Infrared and Raman Spectra of Crystals*, Academic Press, New York, 1972.
49. V. C. Farmer, *The Infrared Spectra of Minerals*, Mineralogical Society, London, 1974.
50. J. A. Gadsden, *Infrared Spectra of Minerals and Related Inorganic Compounds*, Butterworth, London, 1975.
51. C. Karr, ed., *Infrared and Raman Spectroscopy of Lunar and Terrestrial Minerals*, Academic Press, New York, 1975.

52. J. C. Decius and R. M. Hexter, *Molecular Vibrations in Crystals*, McGraw-Hill, New York, 1977.

Advances Series

53. *Spectroscopic Properties of Inorganic and Organometallic Compounds*, Vol. 1 to present, The Chemical Society, London.
54. *Molecular Spectroscopy—Specialist Periodical Reports*, Vol. 1 to present, The Chemical Society, London.
55. R. J. H. Clark and R. E. Hester, eds., *Advances in Infrared and Raman Spectroscopy*, Vol. 1 to present, Heyden, London.
56. J. Durig, ed., *Vibrational Spectra and Structure*, Vol. 1 to present, Elsevier, Amsterdam.
57. C. B. Moore, ed., *Chemical and Biochemical Applications of Lasers*, Vol. 1 to present, Academic Press, New York.
58. *Structure and Bonding*, Vol. 1 to present, Springer-Verlag, New York.

Index and Collection of Spectral Data

59. N. N. Greenwood, E. J. F. Ross, and B. P. Straughan, *Index of Vibrational Spectra of Inorganic and Organometallic Compounds*, Vols. 1–3, Butterworth, London, 1972–1977.
60. B. Schrader, *Raman/IR Atlas of Organic Compounds*, VCH, New York, 1989.
61. *Sadtler's IR Handbook of Inorganic Chemicals*, Bio-Rad Laboratories, Sadtler Division, Philadelphia, PA, 1996.

Handbooks and Encyclopedia

62. R. A. Ayquist, R. O. Kagel, C. I. Putzig, and M. A. Leugers, *The Handbook of Infrared and Raman Spectra of Inorganic Compounds and Organic Salts*, Vols. 1–4, Academic Press, San Diego, CA, 1996.
63. *Encyclopedia of Spectroscopy and Spectrometry*, 3-vol. set with online version Academic Press, San Diego, CA, 2000.
64. I. R. Lewis and H. G. M. Edwards, eds., *Handbook of Raman Spectroscopy*, Marcel Dekker, New York, 2001.
65. J. M. Chalmers and P. R. Griffiths, eds., *Handbook of Vibrational Spectroscopy*, Vols. 1–5, Wiley, Chichester, UK, 2002.

General

66. W. Holzer, W. F. Murphy, and H. J. Bernstein, *J. Chem. Phys.* **52**, 399 (1970).
67. C. F. Shaw, III, *J. Chem. Educ.* **58**, 343 (1981).
68. R. M. Badger, *J. Chem. Phys.* **2**, 128 (1934).
69. W. Gordy, *J. Chem. Phys.* **14**, 305 (1946).
70. D. R. Herschbach and V. W. Laurie, *J. Chem. Phys.* **35**, 458 (1961).
71. K. Nakamoto, M. Margoshes, and R. E. Rundle, *J. Am. Chem. Soc.* **77**, 6480 (1955).
72. E. M. Layton, Jr., R. D. Cross, and V. A. Fassel, *J. Chem. Phys.* **25**, 135 (1956).

73. F. D. Hardcastle and I. E. Wachs, *J. Raman Spectrosc.* **21**, 683 (1990).
74. F. D. Hardcastle and I. E. Wachs, *J. Phys. Chem.* **95**, 5031 (1991).
75. D. P. Strommen and E. R. Lippincott, *J. Chem. Educ.* **49**, 341 (1972).
76. G. C. Lie, *J. Chem. Educ.* **56**, 636 (1979).
77. H. Eyring, J. Walter, and G. E. Kimball, *Quantum Chemistry*, 5th ed., Wiley, New York, 1949, p. 121.
78. E. B. Wilson, *J. Chem, Phys.* **7**, 1047 (1939); **9**, 76 (1941).
79. J. C. Decius, *J. Chem. Phys.* **16**, 1025 (1948).
80. T. Shimanouchi, *J. Chem. Phys.* **25**, 660 (1956).
81. T. Shimanouchi, "The Molecular Force Field," in D. Henderson,ed., *Physical Chemistry: An Advanced Treatise*, Vol. 4, Academic Press, New York, 1970.
82. T. Shimanouchi, *J. Chem. Phys.* **17**, 245, 734, 848 (1949).
83. D. F. Heath and J. W. Linnett, *Trans. Faraday Soc.* **44**, 556, 873, 878, 884 (1948); **45**, 264 (1949).
84. J. Overend and J. R. Scherer, *J. Chem. Phys.* **32**, 1289, 1296, 1720 (1960); **33**, 446 (1960); **34**, 547 (1961); **36**, 3308 (1962).
85. T. Shimanouchi, *Pure Appl. Chem.* **7**, 131 (1963).
86. J. H. Schachtschneider, "Vibrational Analysis of Polyatomic Molecules," Pts. V and VI, Tech. Rept. 231-64 and 53-65, Shell Development Co., Emeryville, CA, 1964 and 1965.
87. K. Nakamoto, *Angew. Chem.* **11**, 666 (1972).
88. N. Mohan, K. Nakamoto, and A. Müller, "The Metal Isotope Effect on Molecular Vibrations," in R. J. H. Clark and R. E. Hester,eds., Advances in Infrared and Raman Spectroscopy, Vol. 1, Heyden, London, 1976.
89. K. Nakamoto, K. Shobatake, and B. Hutchinson, *Chem. Commun.* 1451 (1969).
90. J. Takemoto and K. Nakamoto, *Chem. Commun.* 1017 (1970).
91. J. R. Kincaid and K. Nakamoto, *Spectrochim. Acta.* **32A**, 277 (1976).
92. P. M. Champion, B. R. Stallard, G. C. Wagner, and I. C. Gunsalus, *J. Am. Chem. Soc.* **104**, 5469 (1982).
93. Y. Morino and K. Kuchitsu, *J. Chem. Phys.* **20**, 1809 (1952).
94. B. L. Crawford and W. H. Fletcher, *J. Chem. Phys.* **19**, 141 (1951).
95. P. LaBonville and J. M. Williams, *Appl. Spectrosc.* **25**, 672 (1971).
96. D. A. Ramsey, *J. Am. Chem. Soc.* **74**, 72 (1952).
97. D. P. Strommen and K. Nakamoto, *Appl. Spectrosc.* **37**, 436 (1983).
98. T. G. Spiro and T. C. Strekas, *Proc. Natl Acad. Sci. USA.* **69**, 2622 (1972).
99. W. M. McClain, *J. Chem. Phys.* **55**, 2789 (1971).
100. D. P. Strommen, *J. Chem. Educ.* **69**, 803 (1992).
101. W. Kiefer, *Appl. Spectrosc.* **28**, 115 (1974).
102. M. Mingardi and W. Siebrand, *J. Chem. Phys.* **62**, 1074 (1975).
103. A. C. Albrecht, *J. Chem. Phys.* **34**, 1476 (1961).
104. S. A. Asher, *Anal. Chem.* **65**, 59A, 201A (1993).
105. W. Kiefer and H. J. Bernstein, *J. Raman Spectrosc.* **1**, 417 (1973).
106. R. J. H. Clark and P. D. Mitchell, *J. Am. Chem. Soc.* **95**, 8300 (1973).

107. L. A. Nafie, P. Stein, and W. L. Peticolas, *Chem. Phys. Lett.* **12**, 131 (1971).
108. Y. Hirakawa and M. Tsuboi, *Science* **188**, 359 (1975).
109. T. G. Spiro, R. S. Czernuszewicz, and X.-Y. Li, *Coord. Chem. Rev.* **100**, 541 (1990).
110. X.-Y. Li, R. S. Czernuszewicz, J. R. Kincaid, P. Stein, and T. G. Spiro, *J. Phys. Chem.* **94**, 47 (1990).
110a. Y. Mizutani, Y. Uesugi, and T. Kitagawa, *J. Chem. Phys.* **111**, 8950 (1999).
111. H. Hamaguchi, I. Harada, and T. Shimanouchi, *Chem. Phys. Lett.* **32**, 103 (1975).
112. H. Hamaguchi, *J. Chem. Phys.* **69**, 569 (1978).
113. F. Inagaki, M. Tasunai, and T. Miyazawa, *J. Mol. Spectrosc.* **50**, 286 (1974).
114. P. Pulay, *Mol. Phys.* **17**, 192 (1969); **18**, 473 (1970); P. Pulay and W. Meyer, *J. Mol. Spectrosc.* **40**, 59 (1971).
115. R. G. Parr and W. Yang, *Density Functional Theory of Atoms and Molecules*, Oxford University Press, Oxford, 1989; J. K. Labanowski and J. W. Andzelm, eds., *Density Functional Methods in Chemistry*, Springer, Berlin, 1990. S. M. Clark, R. L. Gabriel, and D. Ben-Amotz, *J. Chem. Educ.* **27**, 654 (2000).
116. J. B. Foresman and A. Fisch, *Exploring Chemistry with Electronic Structure Method*, 2nd ed., Gaussian Inc., Pittsburgh, PA, 1996.
116a B. G. Johnson and M. J. Fisch, *J. Chem. Phys.* **100**, 7429 (1994).
117. H. D. Stidham, A. C. Vlaservich, D. Y. Hsu, G. A. Guirgis, and J. R. Durig, *J. Raman Spectrosc.* **25**, 751 (1994).
118. W. B. Collier, *J. Chem. Phys.* **88**, 7295 (1988).
119. J. A. Boatz and M. S. Gordon, *J. Phys. Chem.* **93**, 1819 (1989).
120. P. Pulay, *J. Mol. Struct.* **147**, 293 (1995).
121. M. W. Wong, *Chem. Phys. Lett.* **256**, 391 (1996).
122. G. A. Ozin, "Single Crystal and Gas Phase Raman Spectroscopy in Inorganic Chemistry," in S. J. Lippard,ed., *Progress in Inorganic Chemistry*, Vol. 14, Wiley-Interscience, New York, 1971.
123. R. J. H. Clark and D. M. Rippon, *J. Mol. Spectrosc.* **44**, 479 (1972).
124. E. Whittle, D. A. Dows, and G. C. Pimentel, *J. Chem. Phys.* **22**, 1943 (1954).
125. M. J. Linevsky, *J. Chem. Phys.* **34**, 587 (1961).
126. D. E. Milligan and M. E. Jacox, *J. Chem. Phys.* **38**, 2627 (1963).
127. D. Tevault and K. Nakamoto, *Inorg. Chem.* **14**, 2371 (1975).
128. S. P. Willson and L. Andrews, "Matrix Isolation Infrared Spectroscopy," in J. M. Chalmers and P. R. Griffiths, eds., *Handbook of Vibrational Spectroscopy*, Vol.2, Wiley, London, 2002, p. 1342 .
129. B. Liang, L. Andrews, N. Ismail, and C. J. Marsden, *Inorg. Chem.* **41**, 2811 (2002).
130. M. Zhou and L. Andrews, *J. Phys. Chem. A* **103**, 2964 (1999).
131. D. Tevault and K. Nakamoto, *Inorg. Chem.* **15**, 1282 (1976).
132. B. S. Ault, *J. Phys. Chem.* **85**, 3083 (1981).
133. T. Watanabe, T. Ama, and K. Nakamoto, *J. Phys. Chem.* **88**, 440 (1984).
134. K. Bajdor and K. Nakamoto, *J. Am. Chem. Soc.* **106**, 3045 (1984).
135. G. Burns and A. M. Glazer, *Space Groups for Solid State Scientists*, Academic Press, New York, 1978, p. 81.

136. J. M. Robertson, *Organic Crystals and Molecules*, Cornell University Press, Ithaca, NY, 1953, p. 44.
137. *International Tables for X-Ray Crystallography*, Knoch Press, Birmingham, UK, 1952.
138. R. S. Halford, *J. Chem. Phys.* **14**, 8 (1946).
139. R. W. C. Wyckoff, *Crystal Structures*, Vols. I and II, Wiley-Interscience, New York, 1964.
140. S. Bhagavantam and T. Venkatarayudu, *Proc. Indian Acad. Sci.* **9A**, 224 (1939).*Theory of Groups and Its Application to Physical Problems*, Andhra University, Waltair, India, 1951.
141. C. Kittel, *Introduction to Solid State Physics*, 5th ed., Wiley, New York, 1976, p. 118.
142. M. Tsuboi, *Infrared Absorption Spectra*, Vol. 6, Nankodo, Tokyo, 1958, p. 41.
143. S. P. Porto, J. A. Giordmaine, and T. C. Damen, *Phys. Rev.* **147**, 608 (1966).
144. T. Shimanouchi, M. Tsuboi, and T. Miyazawa, *J. Chem. Phys.* **35**, 1597 (1961).
145. I. Nakagawa and J. L. Walter, *J. Chem. Phys.* **51**, 1389 (1969).
146. M. K. Wu, J. R. Ashburn, C. J. Torng, P. H. Hor, R. L. Meng, L. Gao, Z. J. Huang, Y. Q. Wang, and C. W. Chu, *Phys. Rev. Lett.* **55**, 908 (1987).
147. J. R. Ferraro and V. A. Maroni, *Appl Spectrosc*. **44**, 351 (1990).
148. V. A. Maroni and J. R. Ferraro, *Practical Fourier Transform Infrared Spectrocopy*, Academic Press, San Diego, CA, 1990, p. 1.
149. I. K. Schuller and J. D. Jorgensen, *Mater. Res. Soc. Bull.* **14**(1), 27 (1989).
150. J. Hanuza, J. Klamut, R. Horyń, and B. Jeżowska-Trzebiatowska, *J. Mol Struct.* **193**, 57 (1989).
151. J. R. Ferraro and V. A. Maroni, private communication.
152. M. Stavola, D. M. Krol, L. F. Schneemeyer, S. A. Sunshine, J. V. Waszczak, and S. G. Kosinski, *Phys. Rev. B: Condens. Matter [3]* **39**, 287 (1989).
153. Y. Morioka, A. Tokiwa, M. Kikuchi, and Y. Syono, *Solid State Commun*. **67**, 267 (1988).
154. F. E. Bates and J. E. Eldridge, *Solid State Commun*. **64**, 1435 (1987). F. E. Bates, *Phys. Rev.* **B39**, 322 (1989).
155. C. Thomsen, R. Liu, M. Bauer, A. Wittlin, L. Genzel, M. Cardona, E. Schönherr, W. Bauhofer, and W. König, *Solid State Commun*. **65**, 55 (1988).
156. M. Cardona, R. Liu, C. Thomsen, M. Bauer, L. Genzel, W. König, A. Wittlin, U. Amador, M. Barahona, F. Fernandez, C. Otero, and R. Saez, *Solid State Commun*. **65**, 71 (1988).
157. B. Batlogg, R. J. Cava, A. Jarayaman, R. B. van Dover, G. A. Kourouklis, S. Sunshine, D. W. Murphy, L. W. Rupp, H. S. Chen, A. White, K. T. Short, A. M. Mujsce, and E. A. Rietman, *Phys. Rev. Lett.* **58**, 2333 (1987).